

*Performance Analysis of TH-PPM and DS-BPSK
in AWGN Channels for UWB Communication*

A Thesis

Submitted in the partial fulfillment of requirement for the award of the degree of

*Master of Engineering
in
Electronics and Communication Engineering*

by

*Parveen Singh
Regn. No. 8034112*

Under the guidance of

Mr. Kulbir Singh



**Department of Electronics and Communication Engineering
THAPAR INSTITUTE OF ENGINEERING AND
TECHNOLOGY
(DEEMED UNIVERSITY)
PATIALA (PUNJAB)-147004**

CERTIFICATE

I, Parveen Singh, hereby certify that the work which is being presented in this thesis entitled "**Performance Analysis of TH-PPM and DS-BPSK in AWGN Channels for UWB Communication**" by me in partial fulfillment of the requirements for the award of degree of Master of Engineering in Electronics and Communication from Thapar Institute of Engineering and Technology (Deemed University), Patiala, is an authentic record of my own work carried out under the supervision of Mr. Kulbir Singh.

The matter presented in this thesis has not been submitted in any other University / Institute for the award of Master of Engineering.



(Parveen Singh)
Signature of the Student

Date...17/06/2005

This is certified that the above statement made by the candidate is correct to the best of my knowledge



(Mr. Kulbir Singh)
Supervisor

Date...17/06/2005



Head of Department
ECED,

T.I.E.T, Patiala

Date...17.6.05



(Dr D.S Bawa)

Dean of Academic Affairs

T.I.E.T, Patiala

Date.....

Acknowledgement

Throughout my life I have found there are several constants, which I feel should be acknowledged first and foremost because without these things, I would not be writing this thesis. The most significant comes in the form of my Almighty Savior, Waheguru, who has not only given me the strength and ability to achieve my goals, but has surrounded me with the greatest family, well wishers, friends, and professional colleagues. If there is one thing I have learned in my adult life, it is that “for with God all things are possible”.

The next constant in my life has been my family to which I am forever grateful. My family has been my backbone from the start, to provide love and support. Mom, there are no words to describe how much I love, even now sitting in heaven, you always guide me to achieve my goal by coming in my dreams. I also thank my wife Sarbjeet, as she has allowed me to improve my qualification and hope in future also she will extend the same cooperation. It has truly been an honor to have you by my side and I hope to continue our relationship for the whole life. I certainly need to thank my daughters, Riptapan and Sahaj Jappan, who means the world to me, as they miss me, at the time, they need me the most.

The other constant in my life has been my well wishers, who have provided me with the encouragement necessary for me to succeed; I would also like to express gratitude towards his holiness **Shriman Mahant Manjeet Singh Ji**, the Sole trustee of my college and management committee of Mahant Bactitter Singh college of engineering and technology who provided me the opportunity to improve my technical qualification by sponsoring me for Masters in Engineering degree.

Last but definitely not least, my professional thanks to my Guide, **Mr. Kulbir Singh**, of Electronics and Communication department for giving me this research opportunity and offering his guidance along the way. I have learned a great deal from him and am very appreciative of the commitment he has not only shown to me, but to every student who walks through his door despite his busy schedule. I would also like to thank **Dr. R S Kaler**, Head of Department for all support to me for completing my this thesis by allowing me to use M E lab even after college hours whenever I needed it. I also wish to express my deepest gratitude to **Mr Sunil Singla**, of Electrical and Instrumentation

department for the interest he showed in my thesis and encouraging me to complete this thesis on time and all the teaching and non teaching staff members of electronics and communication department for their undue help to me to complete this thesis.

Place: T.I.E.T, Patiala



(Parveen Singh)

INDEX

<i>Chapter No.</i>	<i>Title</i>	<i>Page No.</i>
	<i>Certificate</i>	<i>i</i>
	<i>Acknowledgement</i>	<i>ii- iii</i>
	<i>Contents</i>	<i>iv- vi</i>
	<i>List of Tables</i>	<i>vii</i>
	<i>List of Figures</i>	<i>viii- ix</i>
	<i>List of Abbreviations</i>	<i>x</i>
	<i>Abstract</i>	<i>xi</i>
1.	Introduction	1-6
1.1	Introduction	1
1.2	Objective of Thesis	5
1.3	Methodology	5
1.4	Organization of Thesis	5
2.	Ultra wideband communication	7-28
2.1	Introduction	7
2.1.1	The Basics of Radio	7
2.2	Definition	11
2.3	History of UWB	12
2.4	Basic Properties of UWB	12
2.4.1	Higher Bit Rate	13
2.4.2	High Resolution	13
2.4.3	Extremely Low Signal Power Spectrum Density	14
2.4.4	High Multipath Resistance	15
2.4.5	Good Penetration Properties	16
2.4.6	Covert Radio LPI/LPD	16
2.4.7	Crowded Spectrum	16
2.4.8	Implementation Cost	16
2.5	Regulation of UWB Technology	17
2.6	Pulse Spectrum	20

2.6.1 Gaussian monocycle	20
2.6.1.1 Gaussian Pulse Satisfying FCC Mask	23
2.6.2 Raised Cosine Pulse	26
2.6.3 Pulse Shape Selection	27
3. Ultra Wideband Modulation Techniques	29-46
3.1 Introduction	29
3.2 Spreading Approaches	29
3.2.1 Time Hopping	29
3.2.2 Direct Sequence	31
3.3 Modulation Techniques	32
3.3.1 Pulse Amplitude Modulation (PAM)	33
3.3.2 Pulse Position Modulation (PPM)	33
3.3.2.1 TH-PPM	35
3.3.2.2 DS-PPM	38
3.3.3 Bi-phase Shift Keying	38
3.3.3.1 TH-PSK	39
3.3.3.2 DS-PSK	40
3.3.4 OOK	41
3.3.4.1 DS-OOK	42
3.3.4.2 TH-OOK	42
3.3.5 Other modulation schemes	42
3.3.6 Selected modulation scheme	43
3.4 Power analysis	44
3.5 Transmission effects on UWB signals	45
3.5.1 Multipath affects	45
3.5.2 Effects caused by related moving between Tx and Rx	46
3.5.3 Relocking on the most resolvable path(s)	46
4. Rake Receiver:	47-57
4.1 Introduction	47
4.2 Conventional Rake receiver	48
4.3 Types of Rake Receivers for UWB	49
4.3.1 Flex Rake receiver	49
4.3.2 Post Buffer Rake Receiver	50
4.4 RAKE Receiver Performance Analysis	51

4.4.1 Desired term	53
4.4.2 Noise term	54
4.4.3 Interference term	54
4.4.4 RAKE Receiver Output	55
4.4.5 Average Bit Error Probability	56
5. Results and Discussion	58-92
6. Conclusion	93
References	94-96

List of Tables

<i>Table No.</i>	<i>Title</i>	<i>Page No.</i>
2.1	FCC part 15 rules for class A and B energy level	18
3.1	Power budget of UWB system	45
5.1	Design parameters for TH-PPM/DS-BPSK	58

List of Figures

<i>Figure No.</i>	<i>Title</i>	<i>Page No.</i>
1.1	Coexistence and FCC limit.	2
1.2	FCC Spectral Mask for ultra wideband indoor communication systems.	3
2.1	A basic radio link includes a transmitter, propagating waves, filling space and a receiver	7
2.2	Radio services occupy unique locations in the electromagnetic spectrum.	8
2.3	Sines and cosines of different wavelengths occupy unique spots in the spectrum.	9
2.4.	A finite length signal in time occupies a definite spectrum width in frequency, for that finite time.	10
2.5	Shorter a time signal is, the wider its bandwidth.	10
2.6	Multiple users each occupy the entire spectrum for .1 sliver of time	11
2.7	Unity amplitude Gaussian monopulse with center frequency 2 GHz sampled at a rate of 100 GHz	14
2.8	Bandwidth-limit regime (conventional wireless system) vs. Power limit regime (Ultra wideband radio system).	15
2.9	Power spectral density limits in current NPRM	18
2.10	Power spectral density for the first-derivative Gaussian pulse for various values of the pulse width. The FCC spectral mask for indoor systems is shown for comparison.	22
2.11	The pulse shape for the fifth derivative of the Gaussian pulse.	25
2.12	PSD of the higher-order derivatives of the Gaussian pulse for UWB indoor systems.	25
2.13	PSD of the higher-order derivatives of the Gaussian pulse for UWB outdoor systems.	26
2.14	Raised Cosine pulse and its energy spectrum	27
2.15	Second (received) derivative Gaussian pulse and its spectrum	28
3.1	Typical behavior of a TH-UWB signal.	31
3.2	Typical behavior of a DS-UWB signal.	32
3.3	Pulse amplitude modulation	33

3.4	Pulse Position Modulation	34
3.5	Time references structure in the analyzed UWB systems.	34
3.6	Bi-phase Shift keying modulation	39
3.7	On Off Keying modulation	41
3.8	OOK with DS spreading.	42
4.1	A rake	47
4.2	Conventional Rake Receiver	48
4.3	Block diagram of Flex Rake Receiver	49
4.4	Sample Buffer read and write accesses	50
4.5	Block diagram of Post Buffering Rake Receiver.	51
4.6	Frequency domain representation of UWB impulse used to evaluate effect of narrowband interference on UWB performance.	55

List of Abbreviations

UWB	Ultra Wideband
FCC	Federal Communication Commission
IF	Intermediate Frequency
PAN	Personal Area Network
LAN	Local Area Network
OFDM	Orthogonal Frequency Division Multiplexing
PHY	Physical Layer
BER	Bit Error Rate
SNR	Signal to Noise Ratio
TDMA	Time Division Multiple Access
MMIC	Monolithic Microwave Integrated Circuit
NRPM	Notice of Rule Making
NTIA	National Telecommunication and Information Administration
PRF	Pulse Repetition Frequency
PSD	Power Spectral Density
PAM	Pulse Amplitude Modulation
PPM	Pulse Position Modulation
OOK	On Off Keying
BPSK	Bi-phase Shift Keying
TH	Time Hopping
DS	Direct Sequence
PR	Pseudo Random
TX	Transmitter
RX	Receiver
AGWN	Additive White Gaussian Noise
FIFO	First In First Out
MRC	Maximum Ratio Combiner
WCDMA	Wideband Code Division Multiple Access
SF	Spreading Factor

Abstract

Recent increasing demands on high data rate, wide bandwidth, low power and low cost for short-range wireless communication systems, lead the scientist to search a technology that meets these demands. Ultra wideband (UWB) technology has attracted recent interest, because of its remarkable features, to answer these demands.

Some of the important features of UWB technology are.

- High data rate (typically > 100 Mbps)
- Low power consumption
- Low cost
- High channel capacity
- Fading robustness and
- Position location capability

With these advantageous researchers are examining fundamental questions about UWB communication systems.

In this thesis, the UWB communication systems will be examined paying particular attention to shape of pulses used to transmit information and their spectrum, the very high data rate capabilities of UWB (100 Mbps). The study of modulation techniques which can be employed in UWB and the performance of these modulation techniques for AGWN and multipath in term of BER Vs SNR. The modulation techniques are also analyzed for their performance in multi-user UWB systems.

One of the remarkable features of UWB transmission is its ability to resolve individual multipath components. This feature motivates the use of RAKE multipath combining techniques to provide diversity and capture as much energy as possible at UWB receiver. Indoor UWB transmission is a dense multipath fading environment. Therefore, the received number of paths is on the order of hundreds. Trade-offs between UWB RAKE receiver complexity and performance are studied.

Chapter 1

INTRODUCTION

**Performance Analysis of TH-PPM and DS-BPSK
in AGWN Channels for UWB Communication**

1.1 Introduction

Ultra-Wideband (UWB) technology is in use since 1960s, but it was been mainly applicable to radar-based applications until now [1] because of the wideband nature of the signal that results in very accurate timing information. However, due to recent developments in the silicon process and digital signal processing techniques make it possible to apply this technology to high-speed short-range wireless communication applications. Some of the remarkable features of this flexible technology [2] are:

- High data rate (typically > 100 Mbps)
- Low power consumption
- Low cost
- High channel capacity
- Fading robustness and
- Position location capability

Federal communication commission (FCC) defines a UWB as a system with the fractional bandwidth (η) greater than 0.2, or with a -10 dB bandwidth (B_f) greater than 500 MHz. The fractional bandwidth and -10 dB bandwidth are defined as:

$$\eta = 2 \frac{f_H - f_L}{f_H + f_L} \quad (1.1)$$

$$B_f = f_H - f_L \quad (1.2)$$

where f_H and f_L are the upper and lower frequencies of the -10 dB emission point respectively. The main concern regarding UWB is that it occupies a portion of spectrum where other narrowband systems already operate. So a regulation is necessary in order to avoid co-existence problems. Therefore FCC fixed strict limitations in the maximum emission for unlicensed UWB signals thus guaranteeing protection to the already existing

and planned radio services (figure 1.1). The UWB transmission, following the FCC rules, is having a power spectral density below the thermal noise level.

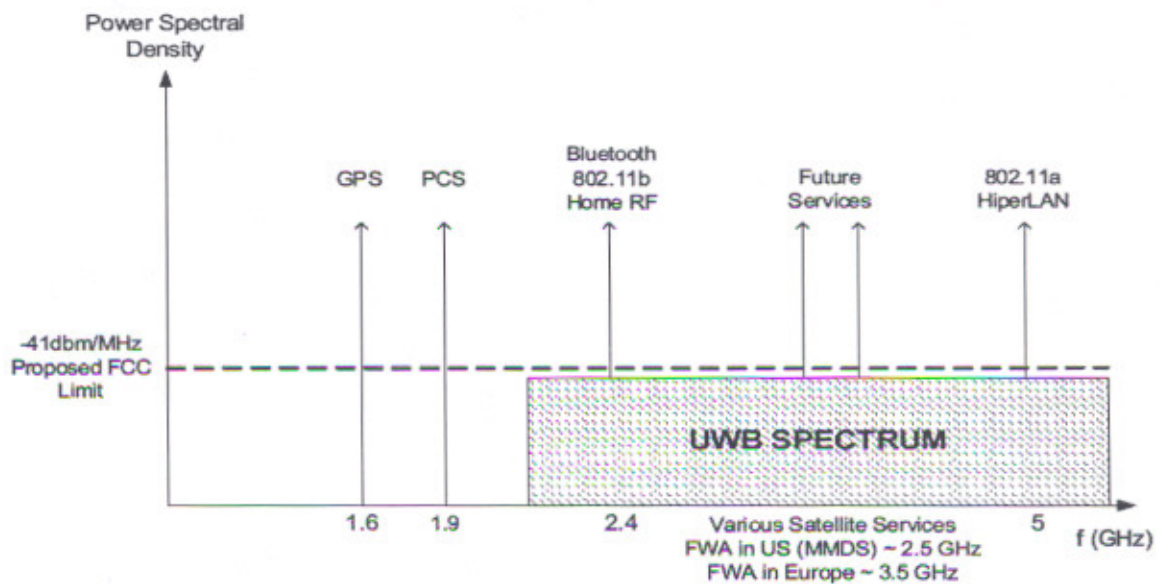


Figure 1.1 Coexistence and FCC limit

Therefore to avoid UWB interference on narrowband systems in the band below 3.1 GHz. FCC permits Ultra wideband communication transmitters to operate in the band between 3.1 and 10.6GHz and use below specified power levels. For indoor systems, the average output power spectral density is limited to $-41.3 \text{ dBm per MHz} = .56 \text{ milliwatts}$. It complies with the long standing Part 15 general emission limits to successfully control radio interference, as shown in figure 1.2 [3].

The great interest residing in this new technology is due to the unique features of UWB signals. First of all the co-existence mentioned above represents a big advantage, which is a better use of the available bandwidth thus representing a sort of spectral reuse. Moreover the huge bandwidth available for UWB systems leads, according to the Shannon theorem, to a very high capacity [4]:

$$C = B \log_2(1 + \gamma) \quad (1.3)$$

In fact the capacity has a linear increase with increasing bandwidth (B) and a logarithm increase as a function of γ (signal to noise ratio): this gives a lot of interest around systems occupying a huge portion of spectrum. Moreover such a big bandwidth, wider than the coherence bandwidth of the multipath channel, gives the system a fine time resolution. This makes the receiver able to resolve and combine individual multipath components and robust against multipath fading problems. Fine time resolution allows

also having an accurate delay estimate and this is a very nice feature for ranging and locating applications.

Other important features that make UWB a very promising technology are related to the low implementation cost and low power consumption. In fact the transmitter can be simply realized as a single transistor which can operate in a digital mode ('0' and '1' state), which produce a step waveform that can be easily filtered to get a monocycle pulse. Therefore there is no necessity for a linear power amplifier and this reduces costs and power consumption. The receiver is also simpler than a narrowband receiver because it does not require intermediate frequency (IF) stages and also because the control loop operates at low frequencies thus saving cost.

Anyway some problems still need to be addressed before the UWB technology can be fully developed and exploited. First of all an appropriate channel model that describes the UWB signal propagation, taking into account the existence of multipath components and should be simple enough for tractable analysis and computer simulation is needed.

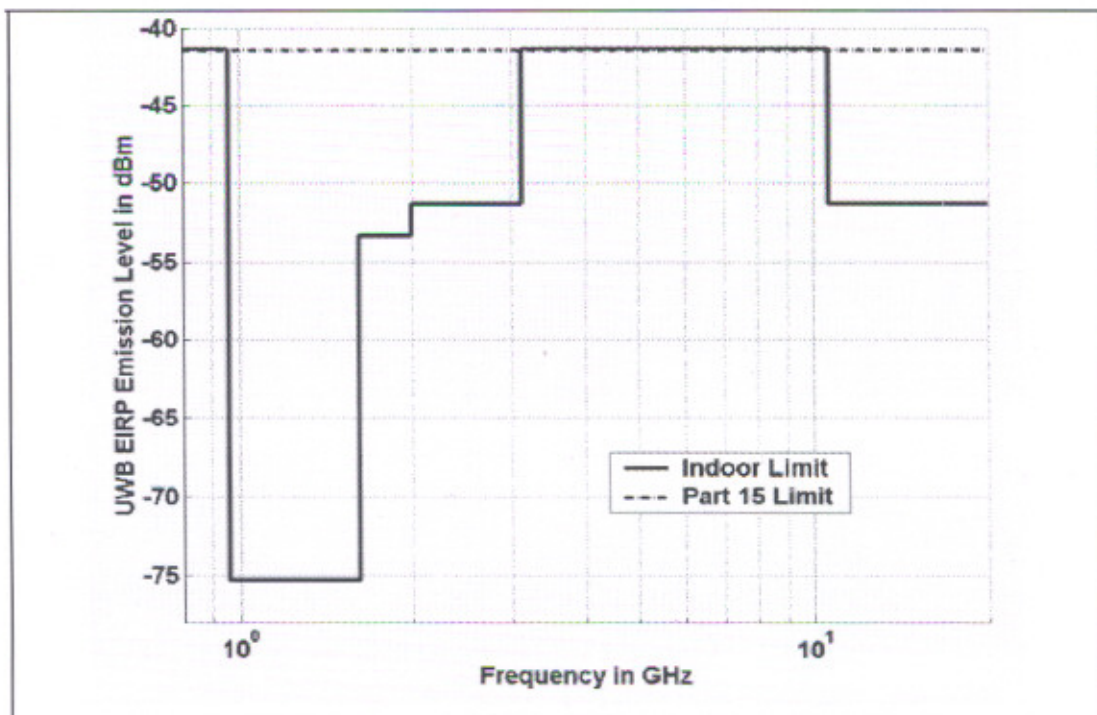


Figure 1.2 FCC Spectral Mask for ultra wideband indoor communication systems

In addition the system design is a central topic as it deeply influences the performance. In particular a receiver able to capture adequate signal energy from the multipath (such as the correlator or Rake receiver) with antennas. Such that a wideband system able to avoid dispersion at the receiver is achieved

Due to the fine time resolution, sync acquisition time increases and the synchronization is no longer be a trivial task. Moreover the limited emitted power makes UWB systems most likely to suffer from narrowband interference. Therefore interference suppression techniques may be required. So the design of effective modulation schemes with multiple access capability together with appropriate techniques to reduce interference caused by other users is a very challenging topic for using UWB technology in wireless communications.

The realization of low cost RF component with several gigahertz of bandwidth represents a central and decisive aim. The main applications taking advantages of UWB technology are as:

The UWB technology features perfectly suite the requirements of high speed multi-user wireless networks, with central regard on wireless PAN and LAN.

For indoor video/data/voice distribution could also take advantage of the promising possibilities of it.

In military applications it is possible to use for tactical hand-held and network radios and also in non-line of sight ground wave communications systems.

The other big reason of interest for UWB technology is related to RADAR applications. The fine time resolution opens the way to the realization of high precision measurements device, while a strong wall penetration capability allows through wall imaging. Important technologies like vehicular radar for collision detection/avoidance and for road conditioning sensing are also closely related to UWB technology development.

This technology can also be used for tracking applications such as intelligent transportation systems, in-building and aviation ground tracking, fire and rescue teams.

The UWB systems design includes the design of signal models, modulation and demodulation techniques. The design can be mainly categorized into two groups: time domain and frequency domain. In the past few years there were proposed frequency domain UWB systems basically based on orthogonal frequency-division multiplexing OFDM which has been widely used for wireless broadband communications. But now time domain UWB systems represent the most interesting and challenging topic, in time domain perspective, the UWB signal comprise short duration pulses, generally in the order of nanoseconds, formed using a single basic pulse shape. This pulse train is called impulse radio (IR). The data bits are modulated using these short pulses with repetition period larger than the time delay spread of the multipath channel. At the receiver, the resolvable multipath components are combined in such a way that the information is recovered with least probability of error.

1.2 Objective of Thesis

The current thesis work is carried out to meet the following objectives:

- To study the basic flexible features of ultra wideband communications system which make this technology very useful for short range, indoor and outdoor wireless communication?
- To analyze the very data rate capabilities of ultra wideband systems.
- To compare the performance of TH-PPM and DS_BPSK modulation techniques used for ultra wideband communication.
- To study RAKE receivers for ultra wideband systems.

1.3 Methodology

PC Configuration: Intel (R),
Pentium 4 (R), 1.70 GHz,
256 Mb, RAM.

Operating System: Windows XP Professional, Version 2002 (Service pack 2).

Software: MATLAB.
DSP Toolbox, communication Toolbox.

1.4 Organization of Thesis

The thesis is organized in six chapters.

In Chapter one an introduction to Ultra wideband communication, its proposed areas of applications are discussed. Fundamental concept of ultra wideband communication, its Historical background, basic features, FCC regulations for ultra wide band communication, and pulse shapes used in this technology are discussed in chapter two.

The various modulation and multi-access techniques, the limitation of these techniques for ultra wide band communication and the modulation and multi-access techniques commonly used for UWB are discussed in chapter three. Receivers used for ultra wideband communication i.e. RAKE receivers and their performance for various numbers of fingers is discussed in chapter in four. Chapter five provides the simulated results for, different data rate for time-hopping pulse position modulation technique and direct-sequence bi-phase shift keying. Performance of these techniques under AGWN, multipath and multi-user environment in term of bit error rate verses signal to noise ratio. Simulation results of RAKE receivers for different values of RAKE fingers. The thesis is concluded with chapter six

Chapter 2

ULTRA WIDEBAND COMMUNICATION

**Performance Analysis of TH-PPM and DS-BPSK
in AGWN Channels for UWB Communication**

ULTRA WIDEBAND COMMUNICATION

2.1 Introduction

The Ultra-wideband is an unconventional type of radio. So to understand variation on the convention one must grasp the basics of traditional radio. When most people hear the word 'radio' they think of the small device that brings music and news into their homes and automobiles. That is true but radio has many forms. In fact, many common devices that perform some function in a wireless mode are called radio, such as the wireless baby monitors, Wireless internet connections, garage door openers and mobile cell phones.

2.1.1 The Basics of Radio

Radio is the art of sending and receiving electromagnetic signal between transmitter and receiver without wires as shown in figure 2.1. Radio require transmitter for generating signal, and receiver to translate the received information. Both use antennas for sending and collecting the signals as electromagnetic energy. Information, such as voice into a microphone is supplied to transmitters, which then encode or modulate this information in some form on the signal. This information could be someone's voice, music, data, or other information. Receivers recover that information of the received signal by decoding or demodulating and present it as received information.

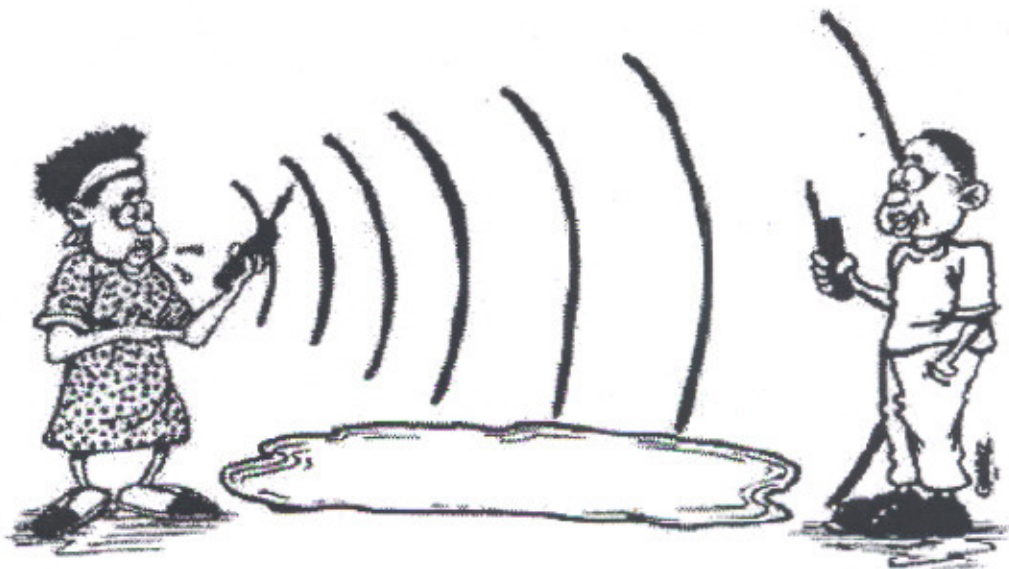


Figure 2.1 A basic radio link includes a transmitter, waves propagating and filling space, and a receiver

All signals regardless of their origin, simultaneously share the same transmission medium such as the near vacuum of space or the air enveloping the earth or the materials' surrounding us. Yet the signal can be selectively choose for a particular radio station to which one wish to listen, the television program one want to watch, or the call intended for a mobile telephone. Radio signals in the electromagnetic spectrum keep us informed and entertained as shown in Figure 2.2.

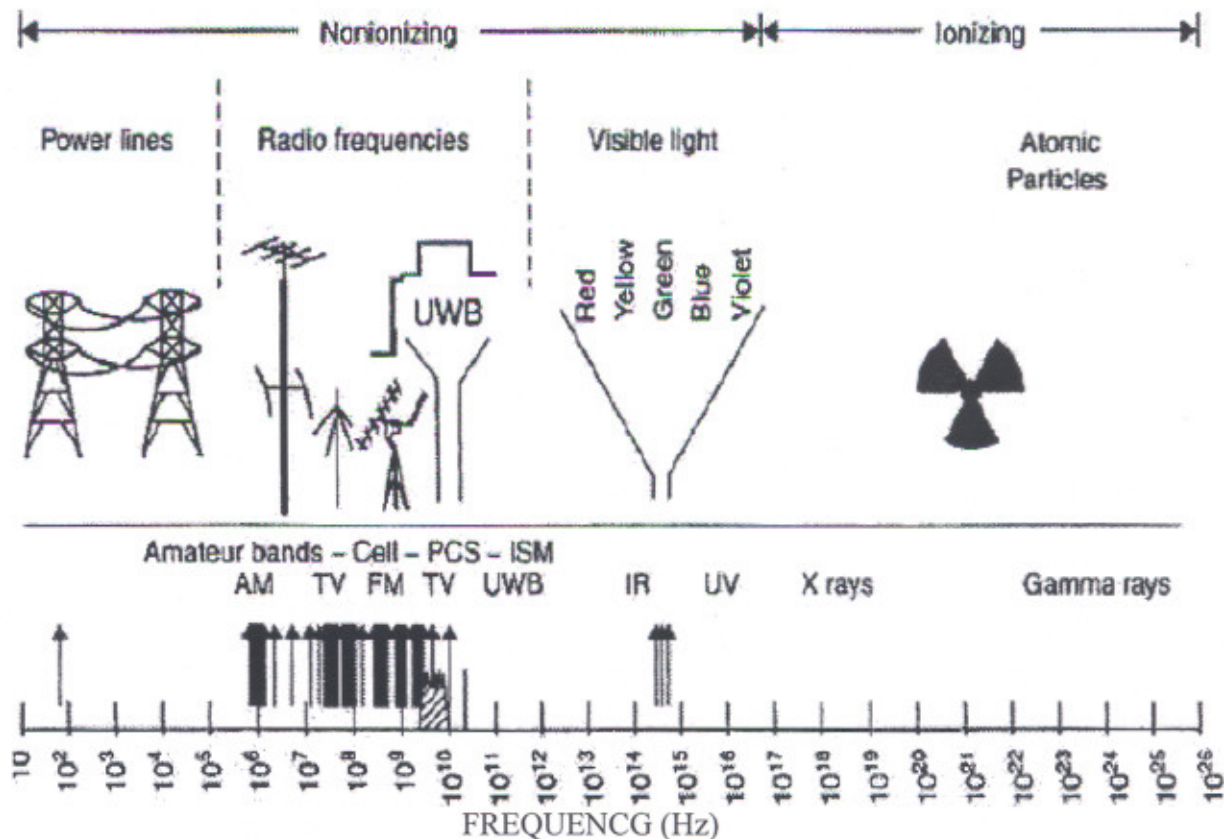


Figure 2.2 Radio services occupy unique locations in the electromagnetic spectrum.

Conventional radio signals can be discerned one from the other because they occupy unique locations in the radio spectrum as shown in figure 2.3, for instance, unique audio tones or discrete colors in the rainbow spectrum. Similarly they are distinct, narrowband places on a radio dial indicated by channel numbers. Radio signals share the limited spectrum by occupying slivers of spectrum that are as narrow as possible. A signal without information has zero bandwidth. Modulating information on that signal spreads its bandwidth in proportion to the information bandwidth. For example a music signal with tonal content up to 15 kHz requires at least 15 kHz of information bandwidth. The "ideal" in radio spectrum usage is to use the smallest bandwidth compared to the bandwidth of the signal information. Narrowband signals

are often represented by their zero bandwidth ideals, the sine and cosine functions, also known as circular functions or harmonic waves. They are the narrowest possible representation of signals in the spectrum at distinct frequencies. Tuning radios to a particular frequency allows us to select the desired narrow band signal. So, the dogma of the circular functions, sines and cosines, [4] began to dominate radio development.

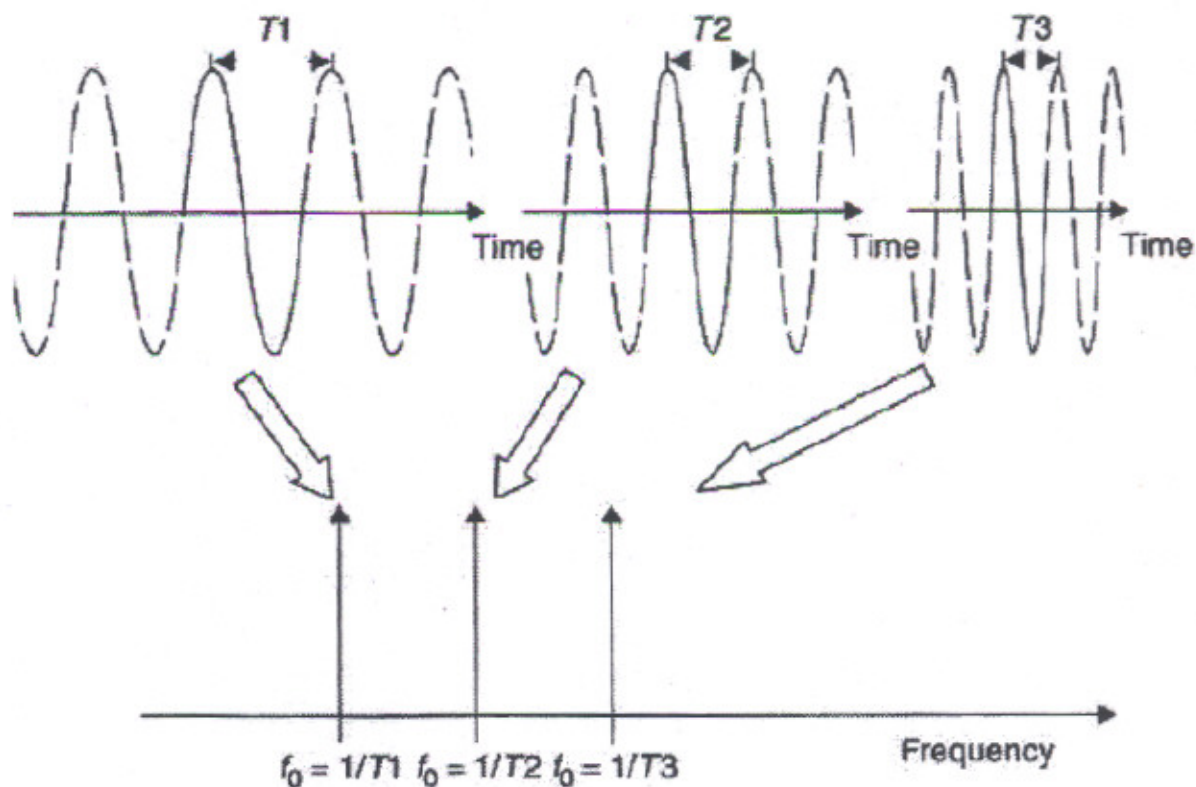


Figure 2.3 Sines and cosines of different wavelengths occupy unique spots in the spectrum.

Separation of signals by bands, by channels, and by frequencies is not the only way the share the radio spectrum. Information bearing signals can also separated in time, especially in tiny slivers of time. These signals occupy wide bandwidths, ultra wide bandwidths but short and ultra short slivers of time as shown in figure 2.4.

The tinier the sliver of time, the wider is the bandwidth of the signal in the radio spectrum as shown in Figure 2.5. When confined to just four cycles of a sine wave, the signal occupies significant bandwidth, of the order of 50%. Clever coding, modulation, and packing of short signals in time, rather than in frequency, allows us to separate these desired short signals to distinguish one user from another. This variety of radio signaling is called UWB

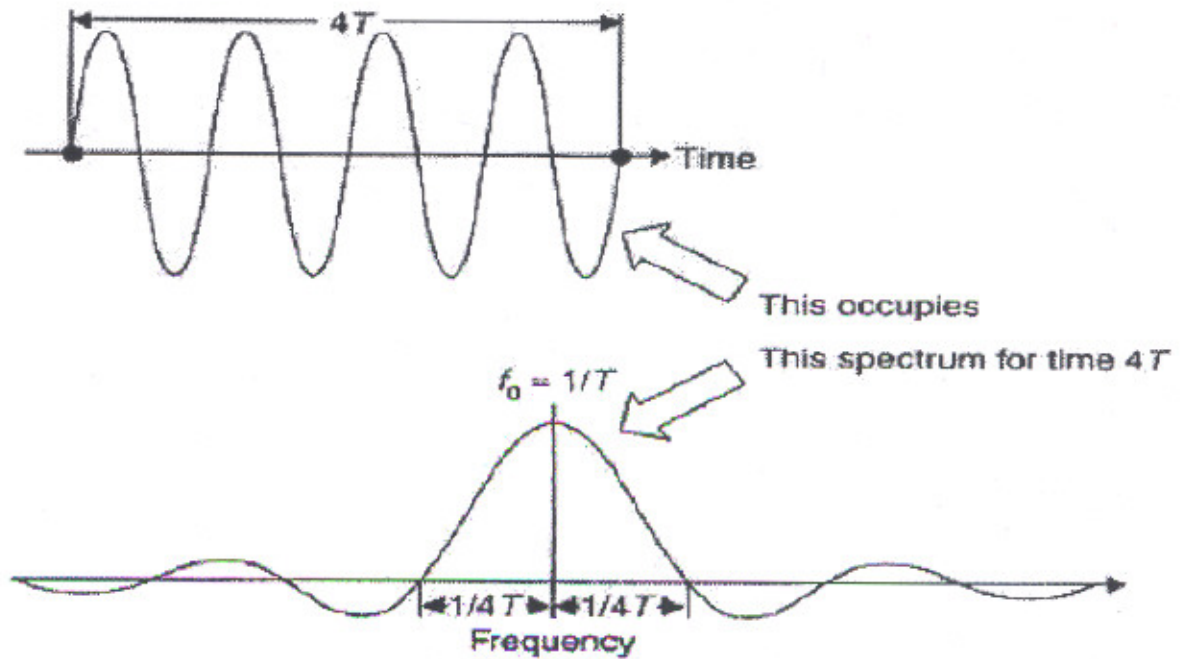


Figure 2.4 A finite length signal in time occupies a definite spectrum width in frequency, for that finite time.

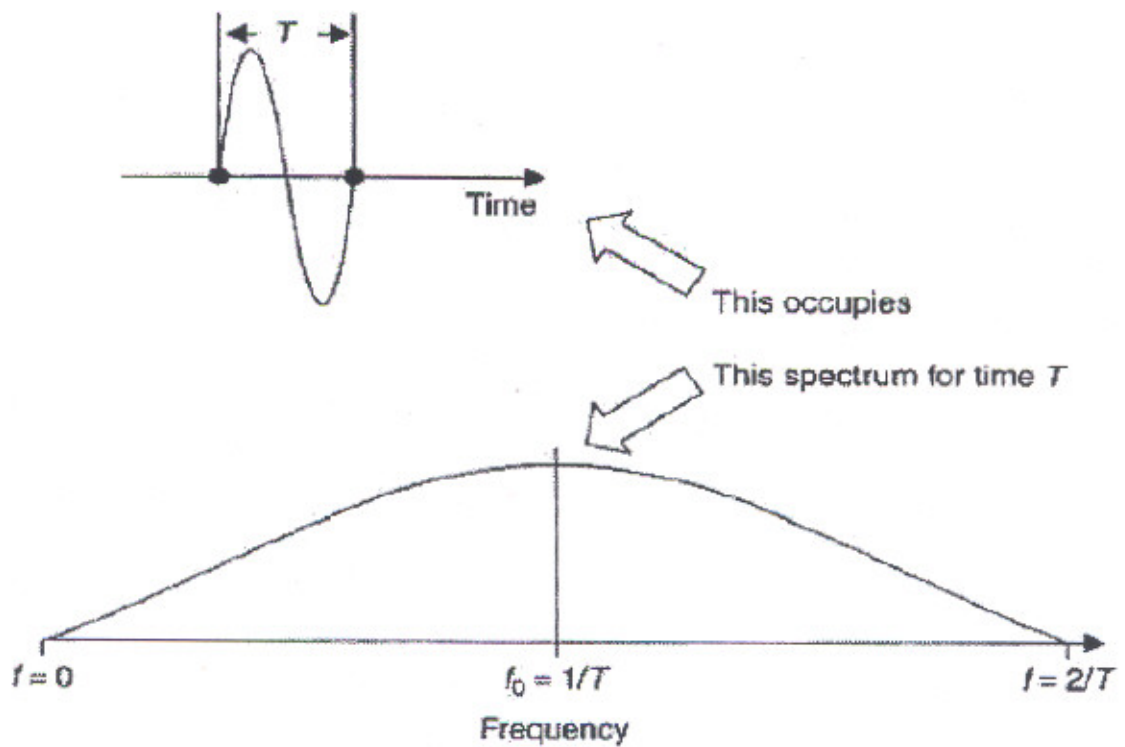


Figure 2.5 Shorter a time signal is, the wider its bandwidth.

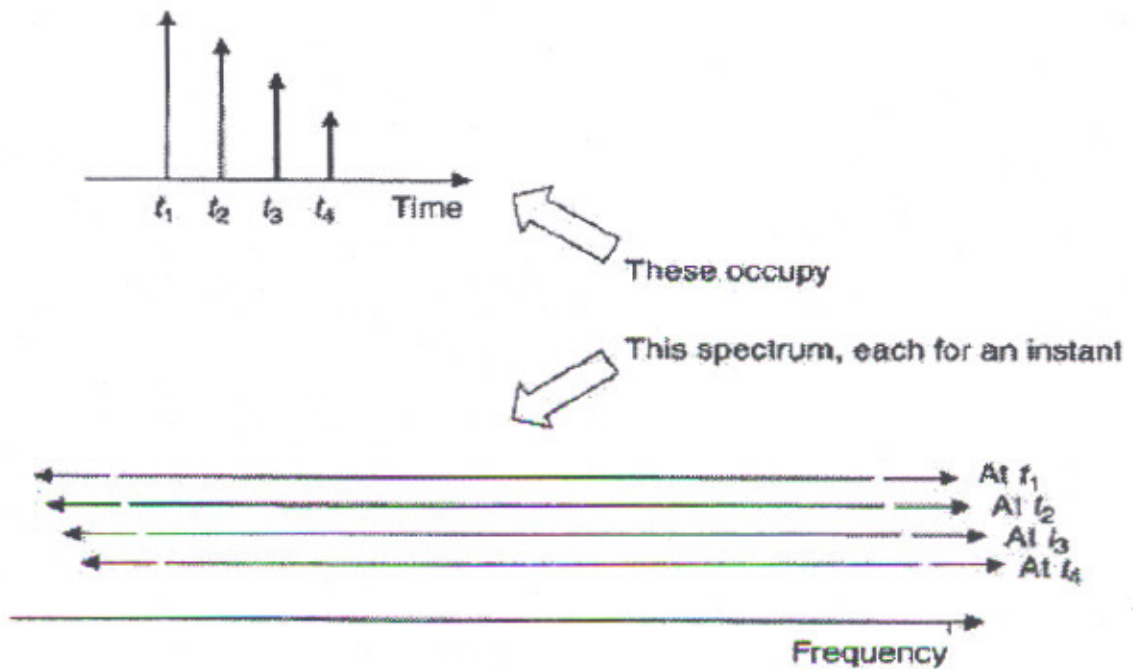


Figure 2.6 Multiple users each occupy the entire spectrum for a sliver of time.

In figure 2.6 it is seen that the entire frequency spectrum can be occupied by multiple users. The users in this case are separated in time rather than in frequency. This is the direct analog of the separation in frequency depicted in Figure 2.3; UWB radio tends to the extreme of separating users in time, while simultaneously occupying large segments of the electromagnetic spectrum. There are two ways of sharing the electromagnetic spectrum among many users. The spectrum can be divided in frequency and each user can be assigned a small sliver of the spectrum: a channel. Alternatively, the many users can each occupy the whole spectrum, but for a short sliver of time each. There is of course, a wide range of intermediate possibilities of separating signals by combinations of time and frequency.

2.2 Definition

The Ultra Wideband signals can be defined as signals with the fractional bandwidth (η) greater than 0.2 or with a -10 dB bandwidth (B_{-10}) greater than 500 MHz. The fractional bandwidth and -10dB bandwidth are defined as [5]:

$$\eta = 2 \frac{f_H - f_L}{f_H + f_L} \quad (2.1a)$$

$$B_f = f_H - f_L \quad (2.1b)$$

Where f_H and f_L are the upper and lower frequencies of the -10 dB frequency point of the signal spectrum respectively.

2.3 History of UWB

The history of interest in UWB dates back to the 1960's. Terms used for the concept were "nonsinusoidal," "baseband," "impulse radio," and "carrier free signals." Dr. Gerald F. Ross first demonstrated the feasibility of utilizing UWB waveforms for radar and communications applications in the late 1960's and early 1970's. In the early 1960's Ross developed time-domain electromagnetics. The work was a result of trying to find better tools to analyze the general microwave 2-N port [6]. The term "UWB" was not adopted until approximately 1989. Harmuth conducted other revolutionary work in the late 1960's [4]. Eventually, hardware like the avalanche transistor and tunnel diode made implementations possible. The advent of the sampling oscilloscope further aided in system development. During the 1970's, evolution and research into UWB often focused towards radar systems, which needed to be enhanced with better resolution [8]. This demand required wider bandwidth. At this time extensive research was conducted in the former Soviet Union by researchers like Astanin, and in China as well. Taylor has published some public material based on research in the United States from this period. In 1978, Bennett and Ross wrote a summary of time-domain electromagnetics [9]. At about this time, efforts using carrier-free radio for communication purposes were started. During the last decade, the military has begun to support initiatives for developing commercial applications. These commercial applications, and the evolution of increasingly faster digital circuits, have led to the development of inexpensive hardware. The possibility of producing low cost units, and unlicensed use, has recently boosted the interest in UWB.

2.4 Basic Properties of UWB

There are several favorable properties associated with UWB techniques. Depending on the type of applications considered, different objectives can be identified.

2.4.1 Higher Bit Rate

The demand for broadband services is rapidly increasing. Most of the evolving new services require high data rates. To transmit higher data rates, more bandwidth is required and the need for increased information bandwidth is expected to grow exponentially. Depending on practical considerations, the carrier frequency must be chosen relatively high to accommodate the bandwidth expansion. Narrowband systems can be defined as systems having less than 1% (0.01) fractional bandwidth [1]. In addition, associated antennas, resonators, and other components operate over relatively small bandwidths. Using sinusoidal carrier frequencies eventually forces the carrier into spectral regions where atmospheric absorption is considerably high. As an example, consider a digital radio system designed for a data rate of 100 Mbps. Depending on the modulation used, the required transmission bandwidth may be as high as 200 MHz. To keep the relative bandwidth under 0.01 of the center frequency, the carrier frequency would have to be more than 2 GHz. For a 100 times higher data rate, using the same requirement on relative bandwidth, the required carrier frequency would exceed 200 GHz. With the use of UWB, the low relative bandwidth constraint is removed and higher bit rates may be achieved without moving to higher frequency regions.

2.4.2 High Resolution

Achieving high resolution is of primary importance in radar and geolocation applications. Distance can be determined by measuring the time delay of a pulse as it traverses the channel. The uncertainty of the measurement is proportional to the pulse rise time, which is inversely proportional to the pulse bandwidth. Figure 2.7 shows unity amplitude Gaussian monopulse with center frequency 2 GHz sampled at a rate of 100 GHz.

$$\Delta t \cong \frac{1}{W} = t_r \quad (2.2)$$

where Δt = Measurement the uncertainty (Sec)
 t_r = Rise Time (Sec), W = Signal Bandwidth (Hertz)

The larger the bandwidth, the more precisely one can measure range. As seen from Equation (2.2), it is obvious that a narrow time-domain pulse results in a wide spectrum in the frequency-domain. Additionally, the inverse of the bandwidth is proportional to achieved resolution.

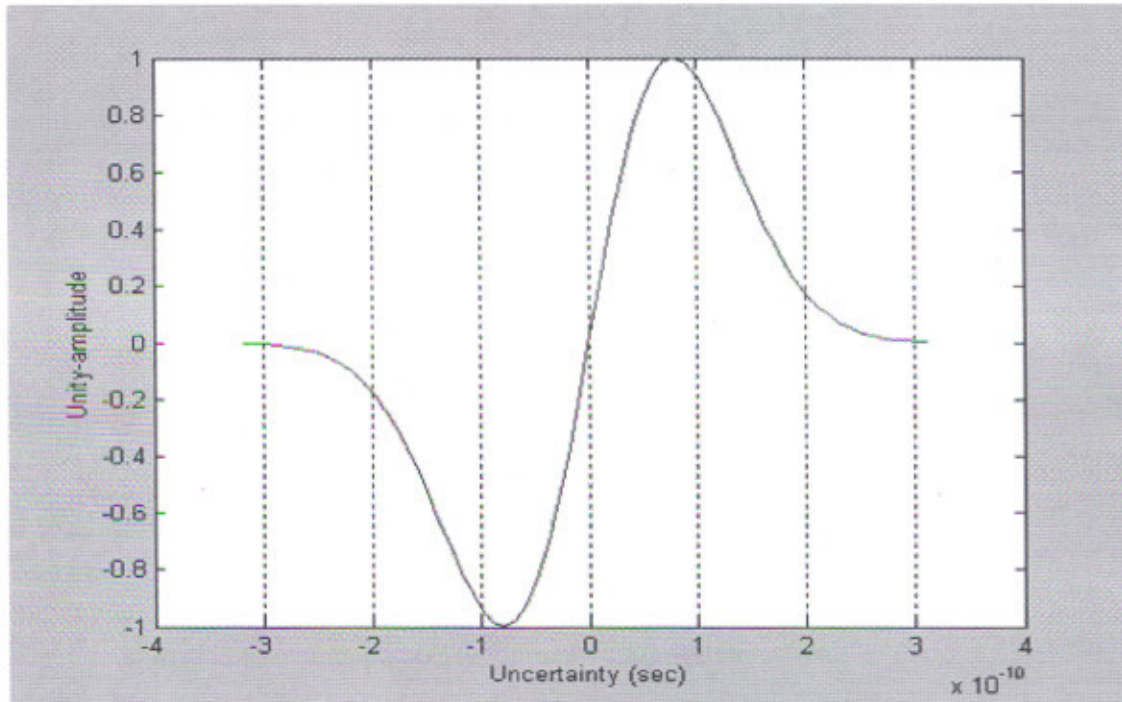


Figure 2.7 Unity amplitude Gaussian monopulse with center frequency 2 GHz sampled at a rate of 100 GHz

2.4.3 Extremely Low Signal Power Spectral Density

Since the bandwidth of UWB signals is much wider than that of conventional wireless systems, a higher channel capacity can be achieved even in a low SNR environment. According to Shannon's theorem:

$$C = B \log_2 \left(1 + \frac{S}{N} \right) \quad (2.3)$$

where C is the channel capacity, B is channel bandwidth, and S/N is the signal to noise power ratio at the input to the receiver. For example, a UWB system that utilizes a 2 GHz spectrum operating in 0dB SNR, its channel capacity can be calculated as $C = 2 \log_2(1 + 1) = 2 \text{ Gbps}$. Based on this result, we can observe that a UWB system with low signal power may still maintain a high data rate, and this feature will allow UWB to

be a good PHY layer solution for PAN equipments. Because of the low signal power and the available large bandwidths, UWB systems perform like spread spectrum systems. However compared to the more common forms of spread spectrum like frequency hopping and direct sequence systems, UWB does not rely on a spreading sequence and a hopping sequence to generate the wide bandwidth signals. Instead, it is the extremely short duration of the UWB basic pulse that gives the system its ultra wide bandwidth. Compared to other narrow band communication systems, which operate in the bandwidth-limit regime, UWB works in the power-limit regime as shown in figure 2.8. Therefore UWB signal power in any single narrow frequency channel is very small and the interference to any other existing products can be ignored in principle.

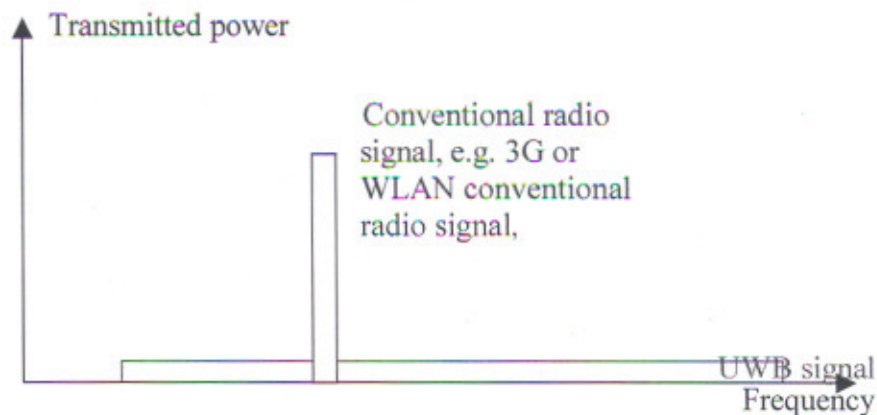


Figure 2.8 Bandwidth-limit regime (conventional wireless system) vs. Power-limit regime (Ultra wideband radio system)

2.4.4 High Multipath Resistance

Ultra wideband systems are particularly well suited for high-speed, mobile wireless applications. Also, because of the extremely short duration waveforms, packet burst and time division multiple access (TDMA) protocols for multi-user communications are readily implemented [6]. In addition, UWB waveforms are relatively immune to multipath cancellation effects as observed in mobile and in-building environments. Multipath cancellation occurs when a strong reflected wave, e.g., off a wall, ceiling, vehicle, building, etc., arrives partially or totally out-of-phase with the direct path signal, causing a reduced amplitude response in the receiver.

Multipath cancellation is a key-limiting factor in the performance of

wireless systems in enclosed spaces. Metallic enclosures and objects accentuate the multipath problems [10]. Received signals can be severely attenuated due to out-of-phase reflections from the surrounding surfaces and other objects interfering with the direct path. Because of its extremely fast response time, the UWB detector responds to this return and ignores or gates out the residue. For a spread spectrum waveform, these inappropriate returns fall directly on top of successive chips, thereby severely limiting system performance.

2.4.5 Good Penetration Properties

Electromagnetic theory suggests that lower frequencies have better penetrating properties. The possibility of using a large spectrum in combination with lower frequencies results in desirable properties. UWB has thus been studied and is being used for applications like ground penetrating radar, foliage penetrating radar [11] and short-range radar to detect hidden objects behind walls. This penetration property is also of great importance for indoor geolocation systems.

2.4.6 Covert Radio LPI/LPD

UWB effectively spreads the energy over a large spectral region and has a low power spectral density (*watts/hertz*). This results in LPD and LPI waveforms. Thus, UWB is highly useful for military applications requiring covert communication in hostile environments. Also, it is relatively insensitive to intentional jamming [12].

2.4.7 Crowded Spectrum

The low energy density implies possible use on an unlicensed basis. The Federal Communications Commission (FCC), which decides regulatory issues in the US market, is now considering this issue. The transmitted signal appears noise-like, and overlay schemes could be used without interfering with existing narrowband radio systems [6].

2.4.8 Implementation Cost

Since the UWB technique can be carrier-free, its transceivers can be inexpensively produced using Complementary Metal Oxide Semiconductor

(CMOS) technology, instead of the more expensive GaAs Monolithic Microwave Integrated Circuit (MMIC) technology. Automotive collision avoidance systems, sensor airbags and liquid level are only some examples of proposed implementations. UWB advocates claim the corresponding cost for UWB circuits will be less than \$1 [6].

2.5 Regulation of UWB Technology

FCC is in the process of determining the legality of UWB transmissions [13]. Due to the wideband nature of UWB emissions, it could potentially interfere with other licensed bands in the frequency domain if left unregulated [14]. The FCC's responsibility is to satisfy the need for more efficient methods of utilizing the available spectrum, as represented by UWB, without causing interference to those currently occupying the spectrum. The FCC is currently working on setting emissions limits that would allow UWB communication systems to be deployed on an unlicensed basis following the Part 15.209 rules for radiated emission of intentional radiators, the same rules governing radiated emissions from home computers, for example. This rule change would allow UWB-enabled devices to overlay with existing narrowband systems, which is currently not allowed, and result in a much more efficient use of the available spectrum. The FCC has studied the topic of UWB and released, in August 1998, a Notice of Inquiry (NOI) [16] to "investigate the possibility of permitting the operation of ultra wideband radio systems on an unlicensed basis under part 15 of its rules." Part 15 regulates the emission from unlicensed intentional radiators and unlicensed unintentional radiators like PCs and other digital devices. It is divided in two classes, A and B, depending on the environment. Class A explains the limits related to digital devices that are marketed for use in commercial and industrial environments. The more restrictive class B explains the limits related to devices used in residential environments, as well as, commercial and industrial environments. These emission limits are defined in terms of microvolt per meter ($\mu V/m$), representing the electric field strength of the radiator. To express this in terms of radiated power the following formula can be used. The radiated power ' P ' from an emitter is given by [2]:

$$P = E_0^2 4\pi R^2 / \eta \quad (2.4)$$

Where E_0 = Electric field strength (V/m)

- R = Radius of the sphere (meters)
 η = Characteristic impedance of vacuum (377Ω)

The FCC Part 15.209 rules limit the emissions for intentional radiators to $500 \mu V/m$ measured at a distance of 3 meters in a 1 MHz bandwidth for frequencies greater than 960MHz. This corresponds to an emitted power spectral density of -41.3 dB m / MHz . Levels for class A and B under part 15 are given in Table 2.1.

Table 2.1 Part 15 Class A and B Limits

CLASS	LIMITS (mV/m)
A	300@10m
B	500@3m

For example, consider a UWB system having 1 W peak power, a 2ns pulse width and 128 kbps data rate. With an obtained bandwidth of 500 MHz, the peak power density is only 2 nW / Hz , with an average power density of 0.5 pW / Hz [35]. Figure 2.9 shows how the current Notice of Rule Making (NPRM) rules would limit UWB transmitted power spectral density for frequencies greater than 2 GHz.

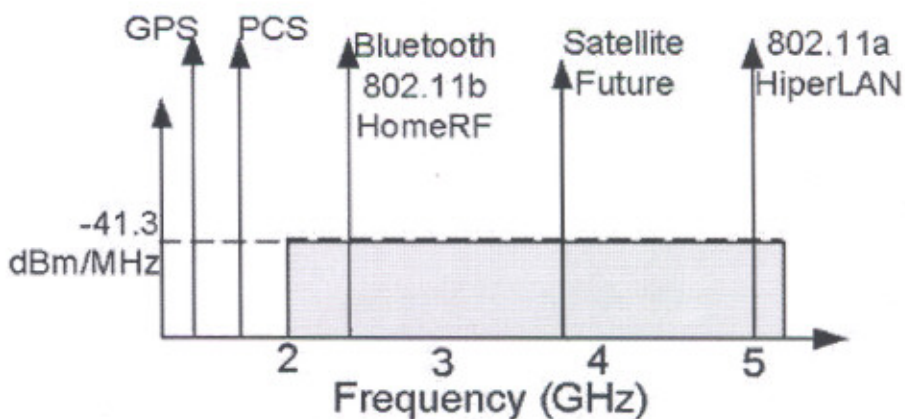


Figure 2.9 Power spectral density limits in current NPRM [6]

The FCC is considering even lower spectral density limits below 2 GHz in order to protect the critical GPS signal even more, but currently no upper boundary has been defined. Results of a National Telecommunications and Information

Administration (NTIA) report analyzing the impact of UWB emissions on GPS, which operate at 1.2 and 1.5GHz, was recently published and suggests that an additional 20-35dB greater attenuation, beyond the power limits described in the FCC Part 15.209, may be needed to protect the GPS band [15].

There are many factors affecting how UWB impacts other "narrowband" systems, including spatial separation between devices, channel propagation losses, modulation techniques, the UWB Pulse Repetition Frequency (PRF), and the "narrowband" receiver antenna gain in the direction of the UWB transmitter [14-16]. For example, a UWB system that sends impulses at a constant rate (PRF) with no modulation causes spikes in the frequency domain that are separated by the PRF. Adding either amplitude modulation or time dithering (i.e., slightly changing the time the impulses are transmitted) results in spreading the spectrum of the UWB emission to look more flat. As a result, the interference caused by a UWB transmitter can be viewed as a wideband interferer, and it has the effect of raising the noise floor of a "narrowband" receiver.

There are three main points to consider when looking at wideband interference [2, 16]. First, if UWB complies with the Part 15 power spectral density requirements, its emissions are no worse than other devices regulated by this same standard, including computers and other electronic devices. Second, interference studies need to consider "typical usage scenarios" for the interaction between UWB and other devices. Third, FCC restrictions are only a beginning. Further coordination through standards participation may be necessary to come up with coexistence methods for operational scenarios that are important for the industry. For example, if UWB is to be used as Personal Area Network (PAN) technology in close proximity to an 802.11a Local Area Network (LAN), then the UWB system must be designed in such a manner as to peacefully coexist with the LAN. This can be achieved through industry involvement and standards participation, as well as, by careful design.

Figure 2.9 illustrates two other important considerations for UWB systems. First, UWB emissions will be allowed only at a much lower transmit power spectral density compared to other "narrowband" services. This low power can be seen as both a

limitation and a benefit. It restricts UWB emissions to relatively short distances, but results in a very power-efficient and low-cost implementation, which preserves battery life. Second, it also shows that UWB systems will most likely suffer from interference from other "narrowband" users. These interferers should be suppressed by using some form of adaptive interference suppression technique.

The first FCC report and order permitting the marketing and operation of certain types of new products incorporating UWB technology come on 14 February 2002 [12]. Under the new rules, UWB communications devices will be restricted to intentional operation only between 3.1 and 10.6 GHz; through-wall imaging and surveillance systems restricted between 1.99 and 10.6 GHz (and used only for law enforcement, fire and rescue, and other designated organizations) and automotive radars restricted to frequencies above 24.075 GHz.

2.6 Pulse Spectrum

In order to comply with the FCC specification, two kinds of pulse shapes are investigated: the Gaussian pulse and the Raised Cosine pulse. The derivation and the comparison of these two pulse shapes is discussed here:

2.6.1 Gaussian monocycle

A Gaussian monocycle is a wide-bandwidth signal, with its center frequency and its bandwidth related and dependent on the monocycle's width. In the time domain, the Gaussian monocycle is mathematically similar to the first derivative of the Gaussian function. But it is seen that Gaussian first derivative does not fall within the spectrum mask allowed by FCC for UWB, Gaussian fifth derivative satisfy the FCC spectral mask for indoor systems and Gaussian seventh derivative for outdoor systems. This is shown in this section. Therefore a general Gaussian pulse is given [17] by:

$$x(t) = \frac{A}{\sqrt{2\pi\sigma^2}} \exp\left(-\frac{t^2}{2\sigma^2}\right) \quad (2.5)$$

then the output of the transmitter antenna will be

$$x^{(1)}(t) = -\frac{At}{\sqrt{2\pi\sigma^3}} \exp\left(-\frac{t^2}{2\sigma^2}\right) \quad (2.6)$$

where the subscript $^{(n)}$ denotes the n^{th} derivative. The pulse at the output of the receiver antenna is then given by

$$x^{(2)}(t) = A\left(\frac{t^2}{\sqrt{2\pi\sigma^5}} - \frac{1}{\sqrt{2\pi\sigma^3}}\right) \exp\left(-\frac{t^2}{2\sigma^2}\right) \quad (2.7)$$

A UWB transmitted signal, using PAM, with uniformly spaced pulses in time can be represented as:

$$s(t) = \sum_{k=-\infty}^{\infty} a_k x^{(n)}(t - KT) \quad (2.8)$$

where T is the pulse-spacing interval and the sequence a_k represents the information symbol. The PSD of the transmitted signal, P_f [18] is:

$$P_f = \frac{\sigma_a^2}{T} |X_n(f)|^2 + \frac{\mu_a^2}{T^2} \sum_{k=-\infty}^{\infty} \left| X_n\left(\frac{k}{T}\right) \right|^2 \delta\left(f - \frac{k}{T}\right) \quad (2.9)$$

where $X_n(f)$ is the Fourier transform of the n^{th} derivative of a Gaussian pulse, σ_a^2 and μ_a are the variance and mean, respectively, of the symbol sequence $\{a_k\}$, and $\delta(\cdot)$ is the Dirac delta function. The second term in equation (2.9) composed of discrete spectral lines, will vanish if the information symbols have zero mean. Let assume this is true and also assume that $\sigma_a^2 = 1$. Here the pulse width ' T_p ' is defined as the interval in which 99.99% of the energy of the pulse is contained. Using this definition, [19] it can be shown that $T_p \approx 7\sigma$ for the first derivative of the Gaussian pulse.

The FCC has issued UWB emission limits in the form of a spectral mask for indoor and outdoor systems [14]. In the band from 3.1 GHz to 10.6 GHz, UWB can use the FCC Part 15 rules with a peak value of -41 dBm/MHz. Outside of this band, the PSD

must be decreased. From 0.96 GHz to 1.61 GHz, the reduction in transmitted power is necessary to protect GPS transmissions. To protect PCS transmission for outdoor systems in the band from 1.99 GHz to 3.1 GHz, the required backoff is 20 dB, rather than the 10 dB for indoor systems.

The figure 2.10 shows the normalized PSD for the first derivative ($n = 1$) of the Gaussian pulse for several values of the pulse width, T_p . The normalization factor is the peak value allowed by the FCC, -41dBm/MHz . It is clear that the PSD of the first derivative pulse does not meet the FCC requirement no matter what value of the pulse width is used. Therefore, a new pulse shape must be found that satisfies the FCC emission requirements. One possibility is to shift the center frequency and adjust the bandwidth so that the requirements are met. This could be done by modulating the monocycle with a sinusoid to shift the center frequency and by varying the values of σ . For example, for a pulse width $T_p = 0.3$ ns, by shifting the center frequency of the monocycles by 3 GHz, the PSD will fall completely within the spectral mask. Impulse UWB, however, is a carrierless system; modulation will increase the cost and complexity. Therefore, alternative approaches are required for obtaining a pulse shape which satisfies the FCC mask.

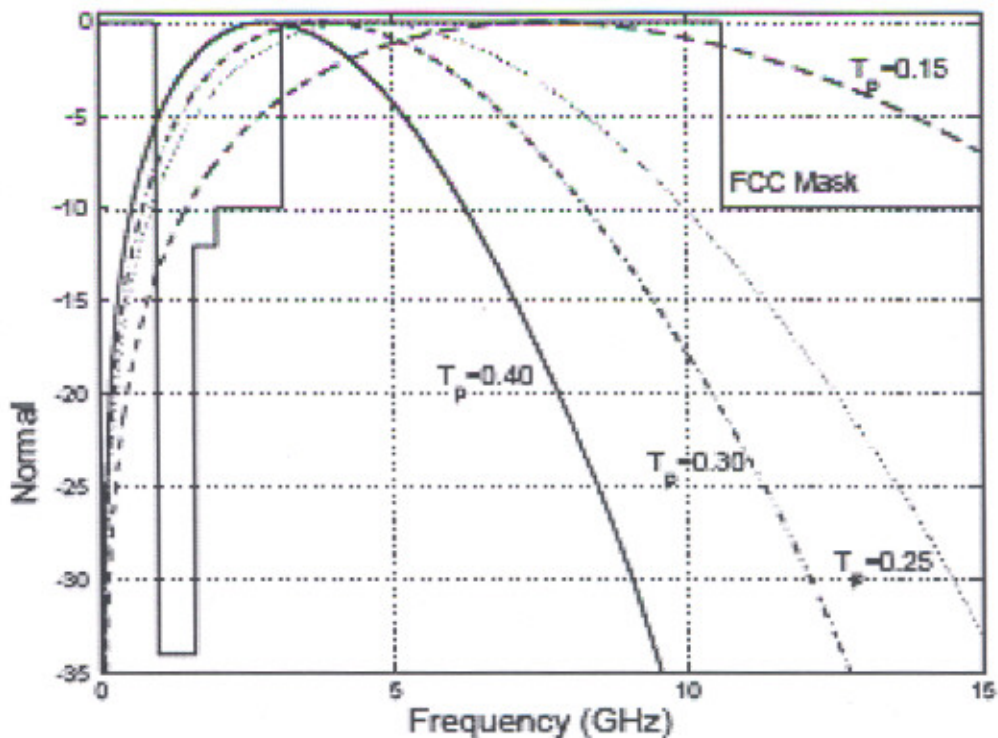


Figure 2.10 Power spectral density for the first-derivative Gaussian pulse for various values of the pulse width. The FCC spectral mask for indoor systems is shown for comparison.

2.6.1.1: Gaussian Pulse Satisfying FCC Mask

It is seen as the order of the derivative increases, the number of zero crossings in time also increases; more zero crossings in the same pulse width correspond to a higher “carrier” frequency modulated by an equivalent Gaussian envelope. These observations lead to considering higher-order derivatives of the Gaussian pulse as candidates for UWB transmission. So by choosing the higher order of the derivative and a suitable pulse width, a pulse that satisfies the FCC’s mask can be obtained [20].

Using the general Gaussian pulse in equation (2.5), its n^{th} derivative can be written [21] as:

$$x^{(n)}(t) = -\frac{n-1}{\sigma^2} x^{(n-2)}(t) - \frac{t}{\sigma^2} x^{(n-1)}(t) \quad (2.10)$$

The Fourier transform of the n^{th} order derivative pulse is

$$X_n(f) = A(j2\pi f)^n \exp\left\{-\frac{(2\pi f\sigma)^2}{2}\right\} \quad (2.11)$$

Consider the amplitude spectrum of the n^{th} derivative

$$|X_n(f)| = A(2\pi f)^n \exp\left\{-\frac{(2\pi f\sigma)^2}{2}\right\} \quad (2.12)$$

The frequency at which the maximum value of amplitude spectrum of the n^{th} derivative is attained, the peak emission frequency, fM can be found by differentiating this equation and setting it equal to zero. Differentiating equation (2.12) gives:

$$\frac{d|X_n(f)|}{df} = A(2\pi f)^{n-1} 2\pi \exp\left\{-\frac{(2\pi f\sigma)^2}{2}\right\} [n - (2\pi f\sigma)^2] \quad (2.13)$$

The peak emission frequency then must satisfy $2\pi fM\sigma = \sqrt{n}$, and the maximum value of the amplitude spectrum is:

$$|X_n(f_M)| = A \left(\frac{\sqrt{n}}{\sigma} \right)^n \exp\left(-\frac{n}{2}\right) \quad (2.14)$$

The normalized PSD $|P_n(f)|$ is:

$$|P_n(f)| \triangleq \frac{|X_n(f)|^2}{|X_n(f_M)|^2} = \frac{(2\pi f\sigma)^{2n} \exp\{-(2\pi f\sigma)^2\}}{n^n \exp(-n)} \quad (2.15)$$

which has a peak value of 1 (0 dB). If n^{th} derivative of the Gaussian pulse is considered as the UWB transmitted pulse, then the PSD of the transmitted signal is given by:

$$|P_t(f)| \triangleq A_{\max} |P_n(f)| = \frac{A_{\max} (2\pi f\sigma)^{2n} \exp\{-(2\pi f\sigma)^2\}}{n^n \exp(-n)} \quad (2.16)$$

Where A_{\max} is the peak value of PSD that FCC permit. The parameters ' n ' and ' σ ' can now be chosen to satisfy the FCC mask. Then the appropriate pulse shape is given by:

$$20n \log_{10}(2\pi f\sigma) - \frac{10(2\pi f\sigma)^2}{\ln 10} - 10n \log_{10} n + \frac{10n}{\ln 10} - R_{db} = 0 \quad (2.17)$$

where $R_{db} \triangleq 10 \log_{10} |P_n(f)|$ is the backoff value of the FCC mask at the chosen corner point (96, 1.61, 1.99, 3.1 and 10.6 GHz). Now taking different values of ' n ' and calculating the value of ' σ ' for each value of ' n ', and solving equation 2.15 for each pair of ' n ' and ' σ ' gives the order of the derivatives of the Gaussian pulse for indoor and outdoor systems satisfying FCC mask spectrum, shown in figure 2.12 and 2.13 respectively. For indoor system fifth order derivative is used, while for outdoor systems seventh or higher order derivative should be used.

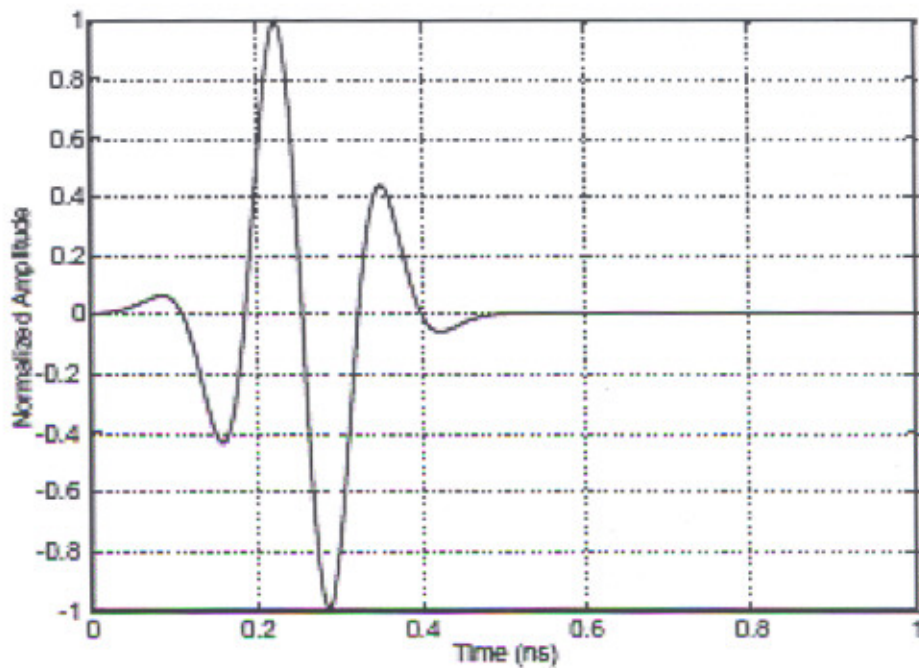


Figure 2.11 The pulse shape for the fifth derivative of the Gaussian pulse.

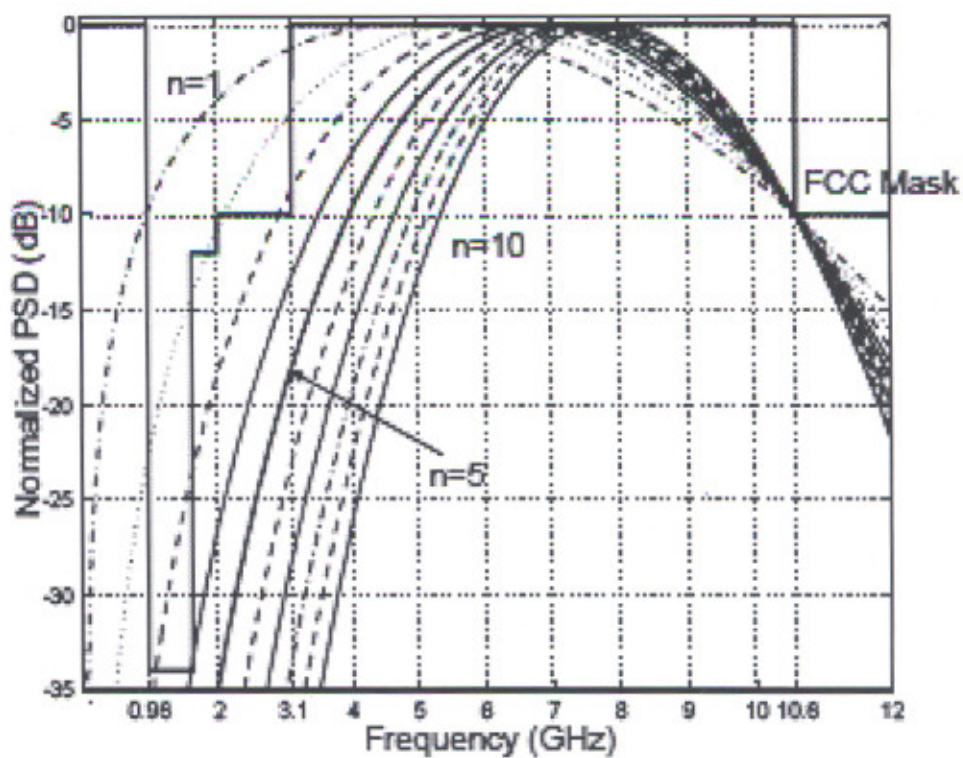


Figure 2.12 PSD of the higher-order derivatives of the Gaussian pulse for UWB indoor systems.

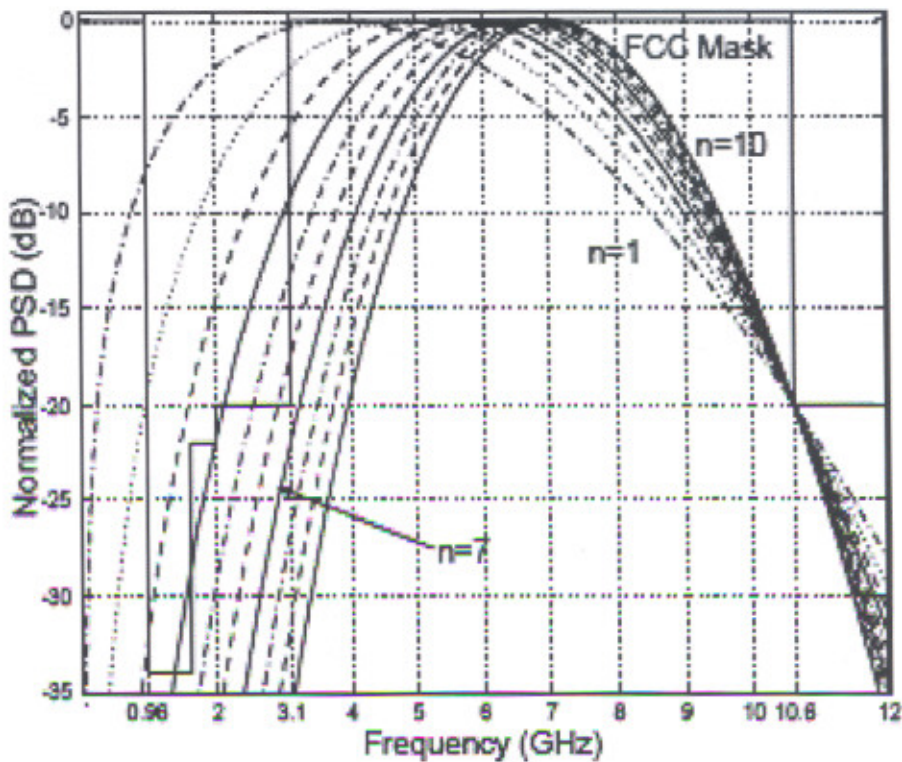


Figure 2.13 PSD of the higher-order derivatives of the Gaussian pulse for UWB outdoor systems.

2.6.2: Raised Cosine Pulse

In the FCC specification, the allowed PSD mask for UWB signal is a rectangular shape. It is obvious that the Gaussian shape pulses do not match with this rule perfectly. Therefore, the Raised Cosine pulse is introduced to provide a better matching with the FCC mask, which is as shown in figure 2.14, [22]. The Raised Cosine pulse can be described in the frequency domain as:

$$H(f) = \begin{cases} 1 & |f| < f_1 \\ \frac{1}{2} \left\{ 1 + \cos \left[\frac{\pi(|f| - f_1)}{2f_\Delta} \right] \right\} & f_1 < |f| < B \\ 0 & |f| > B \end{cases} \quad (2.18)$$

where B is the absolute bandwidth. f_1 and f_Δ are given as:

$$f_\Delta = B - f_{6dB}$$

$$f_1 = f_{6dB} - f_\Delta$$

Where f_{6dB} is the $-6dB$ frequency of the raised cosine pulse. For the aim of utilizing the whole 7.5 GHz FCC approved bandwidth, the value of f_{6dB} is set to 3.75 GHz .

Its corresponding time domain waveform is calculated as:

$$h(t) = F^{-1}[H(f)] = 2f_{6dB} \left(\frac{\sin 2\pi f_{6dB} t}{2\pi f_{6dB} t} \right) \left[\frac{\cos 2\pi f_{\Delta} t}{1 - (4f_{\Delta} t)^2} \right] \quad (2.19)$$

Since $h(t)$ is the low frequency band signal $(-f_{6dB}, +f_{6dB})$, it needs to be shifted to the desired frequency band. For example, if the Raised Cosine pulse spectrum utilizes the whole FCC approved frequency band, the baseband pulse should be up converted to the central frequency f_c (6.85GHz). Therefore, the transmitted pulse will be:

$$rc(t) = h(t) \cdot \cos(2\pi f_c t) \quad (2.20)$$

$rc(t)$ and its energy spectrum $RC(f)$ are shown in Figure 2.14

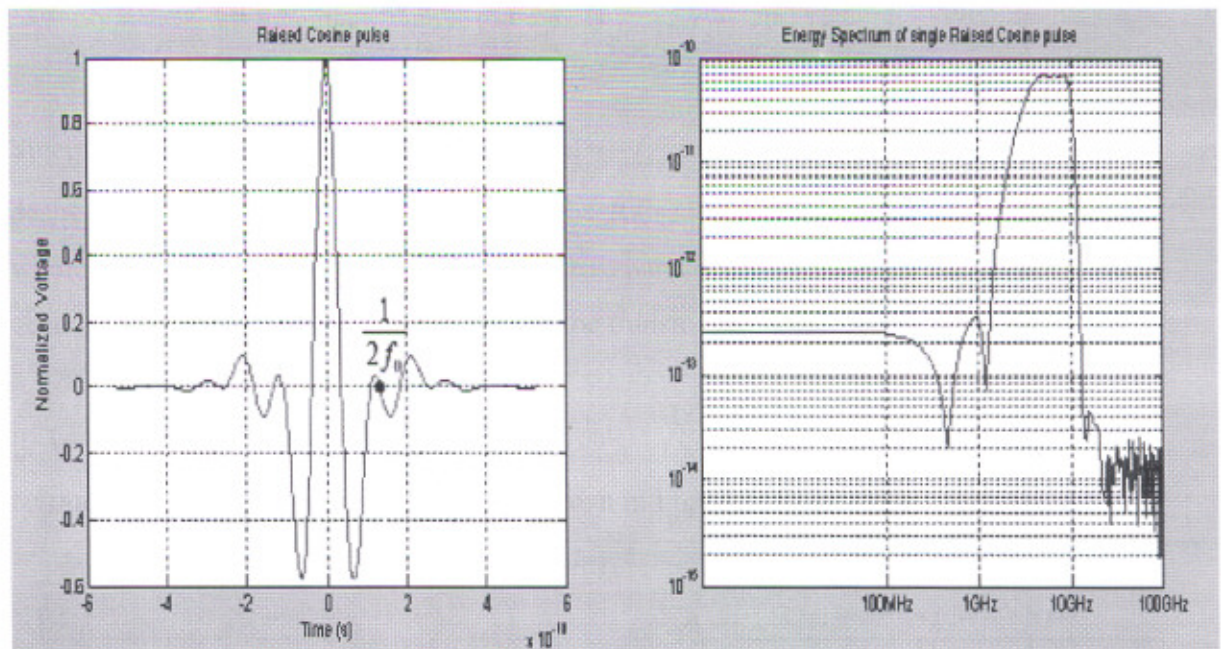


Figure 2.14 Raised Cosine pulse and its energy spectrum

2.6.3: Pulse Shape Selection

By comparing the two proposed pulse shapes, we need to select one to be used for the UWB system. It is seen that although the Raised Cosine pulse might have nice spectral properties, which fits FCC approved rectangular mask very well, but they are hard to

generate by a simple circuit. Because in the time domain, Raised Cosine pulses have a non-realistic side lobe and building such a pulse is too difficult for the circuits. On the other hand, the Gaussian monocycle is relatively simpler to generate, and therefore it is used as the pulse for UWB communication systems.

At the receiver's end, pulse shaping caused by an antenna that can be considered as a filter with impulse response matched to the transmitted pulse. If the transmitted pulse is the Gaussian monocycle (1st derivative Gaussian pulse), then 2nd derivative Gaussian pulse is expected to be received as ideal pulse at receiver end, as shown in figure 2.15.

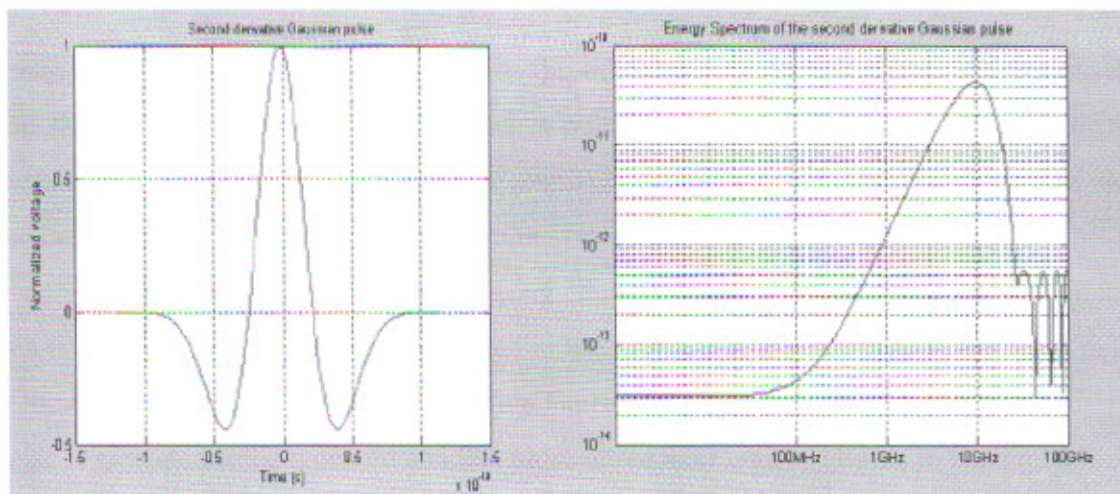


Figure2 .15 Second (received) derivative Gaussian pulse and its spectrum

Chapter 3

ULTRA WIDEBAND MODULATION TECHNIQUES

**Performance Analysis of TH-PPM and DS-BPSK
in AGWN Channels for UWB Communication**

ULTRA WIDEBAND MODULATION TECHNIQUES

3.1 Introduction

For efficient transmission of information, additional processing is needed. This process is called modulation. In ultra wide band communication monocycle pulse are modulated.

The desired modulation technique needs to provide the best error performance (BER) for a given energy per bit. In this chapter different modulation schemes are examined for power efficiency, the effect of the modulation on the PSD and also its robustness against interference of wireless links. Specifically, some modulation approaches produce spectral lines, thus further limiting total transmit power to stay within FCC limits on signal PSD, leading to a lower average power solution. Some of the most popular methods to create UWB pulse streams using mono-phase techniques are:

Pulse Amplitude Modulation (PAM)

Pulse Position Modulation (PPM)

On-Off Keying (OOK)

Antipodal Modulation (BPSK)

In these techniques, a '1' is differentiated from a '0' either by the amplitude of the signal or its time of arrival, but all the pulses have the same shape.

3.2 Spreading Approaches

UWB transmission systems are planned to work with different kinds of spreading approaches, based on time repetition of single pulses. One data bit is spread over multiple pulses to achieve a processing gain due to the pulse repetition. The processing gain is hereby defined as the ratio between the data bit length ' T_b ' and the chip length ' T_c '

3.2.1 Time Hopping

In the time hopping (TH) approach the instant of pulse transmission is defined by the pseudo random time hopping code $c_j^{(k)}$. In this case the processing gain is also increased

by the low transmission duty cycle. The pseudo random time hopping code is used to separate the users according to the code division multiple access (CDMA), and to smooth the spectrum. However, if the pulse repetition interval (PIR) is fixed, lines will appear in the spectrum. The separation between consecutive spectral lines is inversely proportional to the pulse repetition interval [23]. A general equation UWB signal representing data transmission flow in the time domain is given by

$$s(t) = \sum_{k=-\infty}^{+\infty} \sum_{j=1}^{N_f} w_{b[k]}(t - kT_b - jT_f - c_j T_c - \tau_\delta b[k])(c_p)_j \quad (3.1)$$

Where

- k is the data bit index
- T_b is the time duration of the data bit.
- T_c is the chip length.
- T_f is the time duration of each of the N_f frames composing the data bit. That is:

$$T_f = \frac{T_b}{N_f}$$

- c_j is a pseudo-random time hopping code that gives the time location of the pulse transmitted in the j^{th} frame,
- $(c_p)_j$ is a pseudo-random (PR) time hopping code that gives the polarity of the pulse transmitted in the j^{th} frame. It can assume values $\{+1, -1\}$.
- N_f is the number of frames each single data bit is divided into,
- $b[k]$ is the value of the k^{th} data bit. It can assume values $\{0, 1\}$,
- $w_{b[k]}$ is the UWB pulse waveform used to transmit the bit $b[k]$.
- τ_δ is the time shift that can be assigned to the pulse used to transmit data bit '1' (used as a modulation index for pulse position modulation).

From equation (3.1), the expression characterizing the TH- spreading approach can be obtained by imposing $(c_p)_j = 1, \forall j$, leading to

$$s(t) = \sum_{k=-\infty}^{+\infty} \sum_{j=1}^{N_f} w_{b[k]}(t - kT_b - jT_f - c_j T_c - \tau_\delta b[k]) \quad (3.2)$$

where PR code is represented by c_j . If N_f is the chosen number of frames the data bit has been divided into, c_j will then assume a positive value between 0 and $\left\lfloor \frac{T_f}{T_c} - 1 \right\rfloor$, where the floor function $[x]$ gives the largest integer less than or equal to x . Figure 3.1 shows the temporal behavior of a TH-UWB data bit.

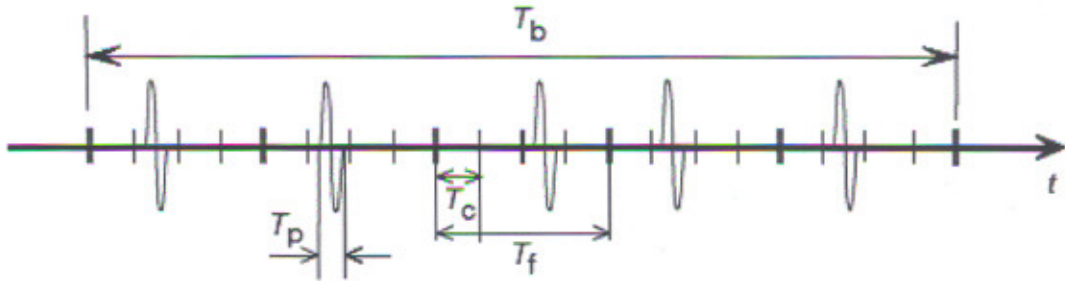


Figure 3.1 Typical behavior of a TH-UWB signal.

3.2.2 Direct Sequence

The direct sequence (DS) spreading approach is based on continuous transmission of pulses composing a single data bit. A PR code c_p is used to spread the data bit into multiple chips, like in conventional DS spread-spectrum systems still having a chip waveform with an UWB spectrum. The resulting signal will then be a continuous transmission of UWB pulses whose number depends on the length of the pulse itself and on the bit rate defined by the system. From equation 3.1, the expression characterizing the DS spreading approach can be obtained by imposing $c_j = 0, \forall j$. Thus, we have

$$s(t) = \sum_{k=-\infty}^{+\infty} \sum_{j=1}^{N_f} w_{b[k]}(t - kT_b - jT_f - \tau_s b[k])(c_p)_j \quad (3.3)$$

where $(c_p)_j$ represents the PR code. In the DS case we have a continuous transmission of pulses within the duration T_b of the data bit. This means the time duration of the frame equals the time chip, that is $T_f = T_c$. The number of frames is then equal to the number of chips N_c transmitted, that is

$$N_f = N_c \quad (3.4)$$

Furthermore, the PR code $(c_p)_j, j = 1, \dots, N_c$, assuming values $\{0, 1\}$, identifies the polarity of each of the N_c pulses the data bit is composed of. Figure 3.2 shows the temporal behavior of a DS-UWB data bit. The PR codes are used for user separation and to provide a “processing gain” against the low signal-to-noise ratio (SNR). Different codes can be used as user separation codes. The selection of the code reflects, e.g., on the sensitivity against multiple access interference. Depending on the UWB system concept, the effect of the channel code is different. In time hopping systems the code is used to generate a pseudo random pattern for the instant of transmission. During the different time hopping patterns the actual instant of transmission changes in consecutive frames. In the DS-UWB systems, the effect of the pseudo random code is similar to that in conventional direct sequence spread-spectrum systems. The code is used to change the pulse polarities within one bit, which improves the randomness of the signal. Using pure repetition coding, N_f replicas of one single pulse are transmitted over the bit period. The processing gain requirement sets the amount of pulses N_f needed for the transmission, and it can be defined as $10 \log_{10}(N_f)$.

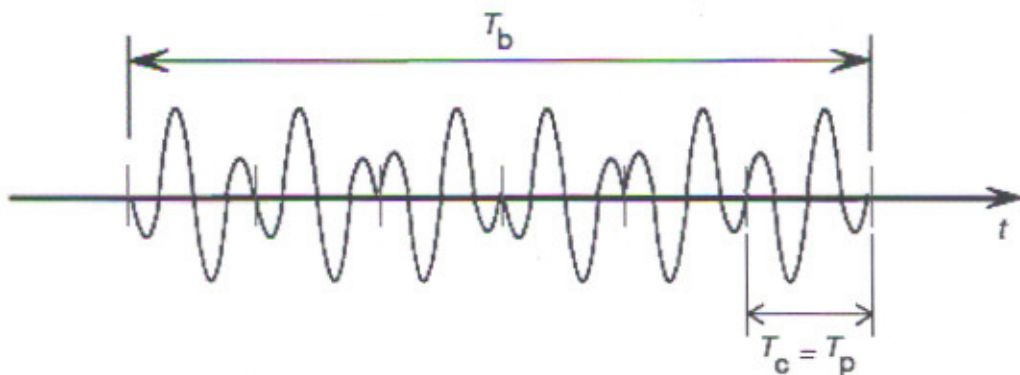


Figure 3.2 Typical behavior of a DS-UWB signal.

3.3 Modulation Techniques

Various modulation techniques used for ultra wideband communication are as follow.

- Pulse Amplitude Modulation (PAM)
- Pulse Position Modulation (PPM)
- On-Off Keying (OOK)
- Antipodal Modulation (BPSK)

3.3.1 Pulse Amplitude Modulation (PAM)

Pulse amplitude modulation works by separating the “large” and the “small” amplitude pulses. By varying the amplitude the receiver can tell the difference between ‘1’ and ‘0’ as shown in figure 3.3 and thereby decode the data from the received signal. But in the wireless channel, attenuation is a significant problem. Due to that, the receiver will need the attenuation gain control. Therefore, this modulation is not very popular for implementation [24].

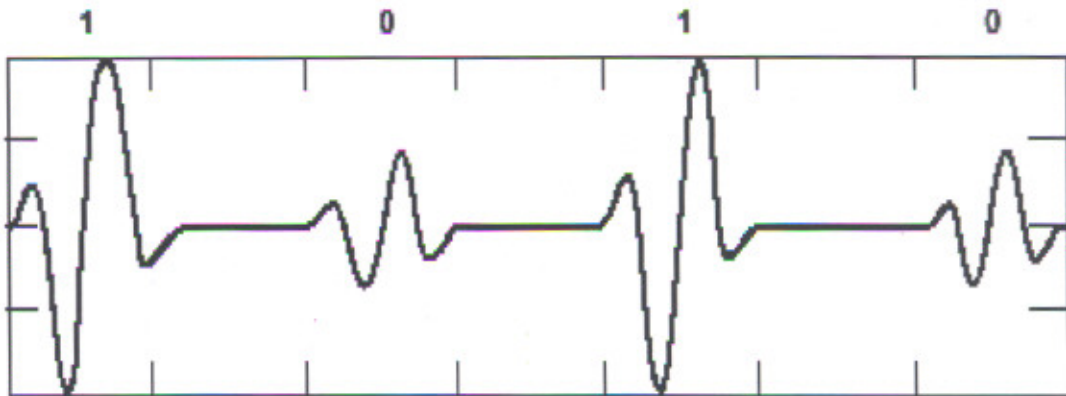


Figure 3.3 Pulse amplitude modulation.

3.3.2 Pulse Position Modulation (PPM)

In PPM, all pulses (both ‘1’s and ‘0’s) are of the same amplitude. The receiver distinguishes between a ‘1’ or a ‘0’ by its time of arrival or the time lag between pulses. In this case, a positive time lag could mean a ‘1’ and a negative time lag a ‘0’ as shown in figure 3.4. Since the multipath channel is causal in time, the difference in time lags is kept by such integrality. PPM modulation will also smooth the spectrum of the signal, thus making the system less likely to interfere with conventional radio systems. PPM allows the use of an optimal matched filter receiving technique. The receiver uses a correlator to find the signal well below the ambient noise level.

Compared to OOK and PAM, PPM has its advantages on synchronization and good ability against attenuation effects. But because the transmitted information is contained in the time lag, a higher timing accuracy is required for the system.



Figure 3.4 Pulse Position Modulation

To derive analytical expressions of the error probability for different kind of UWB modulation techniques and multiaccess schemes some assumptions are considered. The time axis is divided into number of frames each of length (T_f), each corresponding to one bit interval (if no channel coding is present). Each frame is further subdivided into K chips of length T_c shown in figure 3.5.

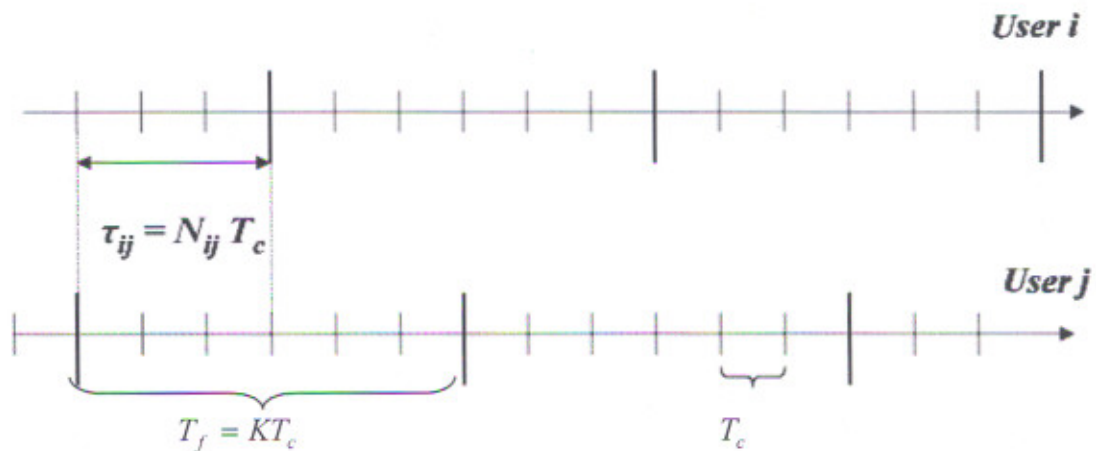


Figure 3.5 Time references structure in the analyzed UWB systems.

It is assumed that the transmitted waveform (and its delayed replica, if PPM is adopted) fits into the chip interval without causing interchip interference. The number of waveforms transmitted in each frame depends on the multiuser scheme (1 with time hopping, K with direct sequence). We will consider an asynchronous multiaccess system with random delays between users that are integer multiples of the chip time. This assumption, generally called chip-synchronous, leads to a worst case analysis [25]. The obtained expressions can then be used as bounds for asynchronous systems performance, even though they are not guaranteed to be tight. In the analysis we will assume an AWGN channel and absence of distortion phenomena due to radiation and propagation [26].

3.3.2.1 TH-PPM

A typical UWB TH-PPM signal can be modeled as follows [27]:

$$s^{(k)}(t) = \sum_{j=-\infty}^{+\infty} \sqrt{E_x} x(t - jT_f - c_j^{(k)}T_c - \delta\alpha_{\lfloor j/N_0 \rfloor}^{(k)}) \quad (3.5)$$

Where $x^{(k)}(t)$ is the random process describing the signal transmitted by the k^{th} user, and $x(t)$ is the signal pulse, normalized so that $\int_{-\infty}^{+\infty} [x(t)]^2 dt = 1$ and with autocorrelation function $\gamma(t)$. The energy of the transmitted waveform is then E_x . The pseudo random time hopping code $\{c_j^{(k)}\}, 0 \leq c_j^{(k)} < K$, for all k , provides an additional shift in order to reduce collisions effects in multiple access.

The binary information stream $\{\alpha_j^k\}$ is transmitted using a PPM modulation format, introducing an additional shift (δ), used to distinguish between pulses carrying bit '0' and '1'. Each information bit is transmitted using N_s consecutive pulses, leading to an $(N_s, 1)$ repetition code. The resulting information bit rate is thus $R_b = (N_s T_f)^{-1}$.

Assuming ideal free-space propagation, AWGN channel and perfect power control, the received signal in the presence of N_u users is:

$$\begin{aligned} y(t) &= \sum_{k=1}^{N_u} s^{(k)}(t - \tau_k) + n(t) \\ &= s^{(1)}(t - \tau_1) + \sum_{k=2}^{N_u} s^{(k)}(t - \tau_k) + n(t) \end{aligned} \quad (3.6)$$

Where τ_k for $k = 1, \dots, N_u$, is the delay associated to each user in an asynchronous multiple access system, and $n(t)$ is a white Gaussian noise process with two-sided power spectral density $N_0/2$. In order to simplify the notation we will further assume $\tau_1 = 0$.

The receiver is a single-user optimum correlator that adopts $v(t) = x(t) - x(t - \delta)$ as correlation waveform. User 1 is the “useful” user that we want to receive, and a perfect knowledge of its time hopping pattern $\{c_j^{(1)}\}$ is assumed. The repetition decoder output, when $\alpha_0^{(1)}$ is transmitted, can be written as:

$$\begin{aligned} \lambda_0^{(1)} &= \sum_{m=0}^{N_s-1} \int_{mT_f}^{(m+1)T_f} y(t)v(t - mT_f - c_m^{(1)}T_c)dt \\ &= s_0^{(1)} + n_{MUI,0} + n_{G,0} \end{aligned} \quad (3.7)$$

where

$$\begin{aligned} s_0^{(1)} &= N_s \int_{-\infty}^{+\infty} \sqrt{E_x} x(t - \delta\alpha_0^{(1)})v(t)dt = \\ &= \begin{cases} N_s \sqrt{E_x} [1 - \gamma(\delta)], & \text{if } \alpha_0^{(1)} = 0 \\ -N_s \sqrt{E_x} [1 - \gamma(\delta)], & \text{if } \alpha_0^{(1)} = 1 \end{cases} \end{aligned} \quad (3.8)$$

$$n_{G,0} = \sum_{m=0}^{N_s-1} \int_{mT_f}^{(m+1)T_f} n(t)v(t - mT_f - c_m^{(1)}T_c)dt \quad (3.9)$$

and

$$n_{MUI,0} = \sum_{m=0}^{N_s-1} \sum_{k=2}^K n_m^{(k)} \quad (3.10)$$

where

$$\begin{aligned} n_m^{(k)} &= \sqrt{E_x} \int_{mT_f}^{(m+1)T_f} v(t - mT_f - c_m^{(1)}T_c) \\ &\quad \cdot \sum_{j=-\infty}^{+\infty} x(t - jT_f - c_j^{(k)}T_c - \delta\alpha_{[j/N_s]}^{(k)} - \tau_k)dt \end{aligned} \quad (3.11)$$

In order to obtain a closed-form expression for the probability of error of this system, the pdf of $n_{MUI,0}$ needs to be calculated. The exact evaluation is cumbersome when the system is asynchronous [28], but an analytical approach is feasible if chip synchronism is assumed and random hopping codes are considered.

In fact, if $\tau_k = N_k T_c$ with $N_k \in \{0, 1, 2, \dots, K-1\}$, then $n_m^{(k)}$ can only assume three values

$$n_m^{(k)} = \begin{cases} \sqrt{E_x} (1 - \gamma(\delta)), & P = 1/(2K) \\ 0, & P = (K-1)/K \\ -\sqrt{E_x} (1 - \gamma(\delta)), & P = 1/(2K) \end{cases} \quad (3.12)$$

Therefore

$$f_{n_m^{(k)}}(x) = f_n(x) = \left(1 - \frac{1}{K}\right) \delta_D(x) + \frac{1}{2K} [\delta_D(x - x_M) + \delta_D(x + x_M)] \quad (3.13)$$

with $f_{n_m^{(k)}}(x)$ being the pdf of $n_m^{(k)}$, $x_M = \sqrt{E_x} (1 - \gamma(\delta))$ and $\delta_D^{(x)}$ the Dirac delta function.

Using equation (3.10) and assuming $n_m^{(k)}$ independent variables for $k=2, \dots, N_u$ and $m=0, \dots, N_s-1$, then:

$$f_{n_{MU,0}}(x) = \underbrace{f_n(x) * f_n(x) * \dots * f_n(x)}_{N_s(N_u-1), \text{times}} \quad (3.14)$$

The n^{th} order convolution of $f_n(x)$ can be derived as follow:

$$f_{n_{MU,0}}(x) = \sum_{i=0}^n \binom{n}{i} (1-c)^{n-i} \left(\frac{c}{2}\right)^i * \sum_{j=0}^i \binom{i}{j} \delta_D(x + x_M(i-2j)) \quad (3.15)$$

where $n = N_s/(N_u-1)n$ and $c = 1/K$.

Knowing that $n_{G,0}$ is a zero mean Gaussian random variable, it is possible to evaluate the probability of error of the system by first conditioning on the multiuser interference, and then averaging. The final result becomes:

$$P(e) = \frac{1}{2} \sum_{i=0}^n \binom{n}{i} (1-c)^{n-i} \left(\frac{c}{2}\right)^i \sum_{j=0}^i \binom{i}{j}$$

$$\cdot \operatorname{erfc} \left[\sqrt{\frac{N_s E_s}{N_0}} \sqrt{\frac{1 - \gamma(\delta)}{2}} \left(1 - \frac{i - 2j}{N_s} \right) \right] \quad (3.16)$$

It is worth pointing out that the relationship between N_u , and K are governed by the following bound :

$$N_u \leq \frac{K - 1}{k(k - 1)} \quad (3.17)$$

Therefore long code words are needed to guarantee good performance (high values of k are in fact required) in a dense multi-user environment.

3.3.2.2 DS-PPM

The choice of using DS spreading was not been taken into account. PPM is time position modulation, having the pulse characterizing bit '0' and '1' placed in different time intervals. The construction of a data bit using DS spreading would lead to continuous transmission during the data bit interval, which is not possible when using a time modulated approach.

3.3.3 Bi-phase Shift Keying

Antipodal modulation is that a binary '1' is represented by a positive pulse and binary '0' is represented by a negative pulse. There is a 180 degrees polarity shift between pulses of '0' and '1' as shown in figure.3.6, [29]. A BPSK is an antipodal signaling technique and has the greatest distance for equal bit energy. This difference leads to a 3dB benefit in efficiency to achieve the same bit error rate, PPM or OOK must use double bit energy, or a 3dB higher E_b .

In the multipath scenario, some of the pulses arrive at the receiver with reflections in the channel. Therefore, they may have a polarity shift of 180 degrees compared to the original transmitted pulses. Thus, the transmitted data '0' could be detected as '1' and vice versa. If the transmission environment contains too many reflections, the communication can only work with precise channel estimation, which is complicated for a high speed UWB signal.

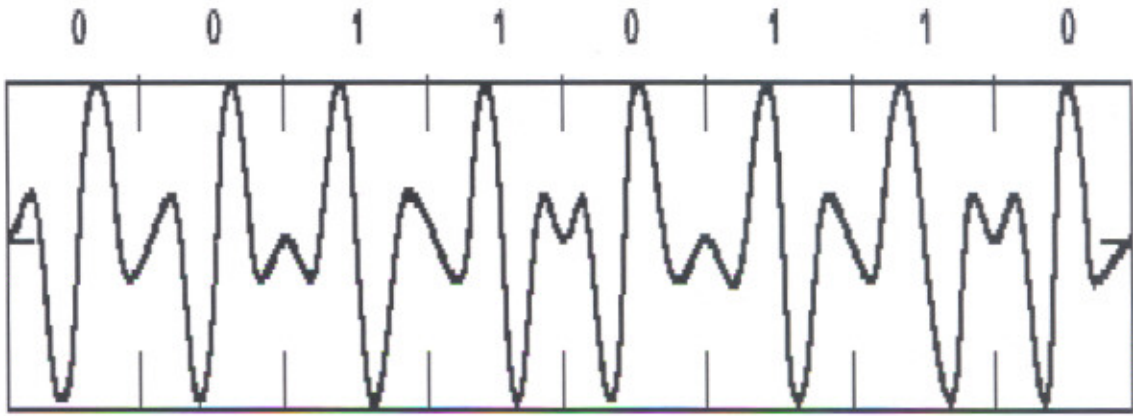


Figure 3.6 Bi-phase Shift keying modulation

3.3.3.1 TH-PSK

Using the same method as in the previous section, it is straightforward to derive a closed-form expression for error probability when 2PSK, instead of 2PPM, is employed. The transmitted signal is

$$s^{(k)}(t) = \sum_{j=-\infty}^{+\infty} \sqrt{E_x} \beta_{[j/N_s]}^{(k)} x(t - jT_f - c_j^{(k)}T_c) \quad (3.18)$$

Where $\beta_j^{(k)} = 1 - 2\alpha_j^{(k)}$. This time $x(t)$ is adopted as correlation waveform at the receiver and the multiuser interference pdf is given by:

$$f_{n_{MUT},0}(x) = \sum_{i=0}^n \binom{n}{i} (1-c)^{n-i} \left(\frac{c}{2}\right)^i * \sum_{j=0}^i \binom{i}{j} \delta_D(x + \sqrt{E_x}(i-2j)) \quad (3.19)$$

Finally

$$P(e) = \frac{1}{2} \sum_{i=0}^n \binom{n}{i} (1-c)^{n-i} \left(\frac{c}{2}\right)^i * \sum_{j=0}^i \binom{i}{j} \operatorname{erfc} \left[\sqrt{\frac{N_s E_x}{N_0}} \left(1 - \frac{i-2j}{N_s}\right) \right] \quad (3.20)$$

3.3.3.2 DS-PSK

Assuming the spreading sequence for the k^{th} user, it is possible to characterize the signal transmitted in a DS-PSK system as follows:

$$s^{(k)}(t) = \sqrt{E_x} \sum_{j=-\infty}^{+\infty} \beta_j^{(k)} \sum_{i=0}^{K-1} A_i^{(k)} x(t - jT_f - iT_c) \quad (3.21)$$

Therefore

$$s_0^{(1)} = K\sqrt{E_x} \beta_0^{(1)} \quad (3.22)$$

Following the same steps as in PPM system, four cases are possible. If $\beta_{-1} = \beta_0 = \pm 1$, then

$$n_{MUI,0}^{(k)} = \pm \sqrt{E_x} \sum_{l=0}^{K-1} A_l^{(1)} A_{l-N_k}^{(k)} \quad (3.23)$$

while, if $\beta_{-1} = -\beta_0$, then

$$n_{MUI,0}^{(k)} = \pm \sqrt{E_x} \left[\sum_{l=0}^{N_k-1} A_l^{(1)} A_{K-N_k+l}^{(k)} - \sum_{l=N_k}^{K-1} A_l^{(1)} A_{l-N_k}^{(k)} \right] \quad (3.24)$$

For simplicity, and in order to obtain a code-independent analysis, we will model the interference value in each chip as a random discrete variable c_i , assuming the values $\pm \sqrt{E_x}$ with the same probability. The following equation describes the pdf [30] of c_i

$$f_c(x) = \frac{1}{2} \left[\delta_D(x - \sqrt{E_x}) + \delta_D(x + \sqrt{E_x}) \right] \quad (3.25)$$

As $n_{MUI,0}^{(k)} = \sum_{i=0}^{K-1} c_i$, if the interference contributes are assumed independent, then $n_{MUI,0}^{(k)}$ pdf is given by:

$$f_n(x) = \underbrace{f_c(x) * f_c(x) * \dots * f_c(x)}_{K, \text{times}} \quad (3.26)$$

And

$$\begin{aligned}
 f_{n_{MUI,0}}(x) &= \underbrace{f_n(x) * \dots * f_n(x)}_{N_u - 1, \text{times}} \\
 &= \underbrace{f_c(x) * f_c(x) * \dots * f_c(x)}_{K(N_u - 1), \text{Times}} \\
 &= \frac{1}{2} \sum_{i=0}^n \delta_D(x + \sqrt{E_x}(n - 2i))
 \end{aligned} \tag{3.27}$$

Where $n = K(N_u - 1)$. Finally:

$$P(e) = \sum_{i=0}^n \frac{1}{2^{n+1}} \operatorname{erfc} \left(\sqrt{\frac{N_b E_x}{N_0}} \left(1 - \frac{n - 2i}{N_c} \right) \right) \tag{3.28}$$

3.3.4 OOK

In On Off Keying, (OOK) '1' is a pulse and an absence of a pulse is a '0'. Actually, it is a special case of PAM where the amplitude of zero represents a '0's' as shown in figure 3.7.

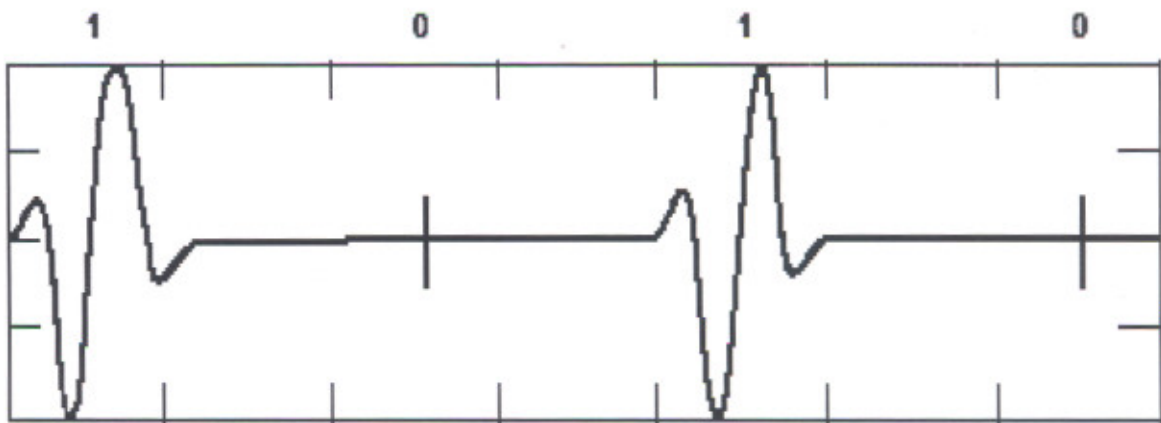


Figure 3.7 On Off Keying modulation

3.3.4.1 DS-OOK

Figure 3.8 shows what a single data bit looks like for OOK modulation when data bit '0' or '1' is transmitted. As mentioned above, in the case of data bit '0' the OOK spreading signal is characterized by a blank transmission. Another way is to utilize OOK after code spreading.

3.3.4.2 TH-OOK

The TH spreading approach was not implemented for OOK. As a matter of fact, due to the blank transmission in the case of bit '0', this kind of modulation could not take advantage of TH spreading, and it would create further problems for synchronization.

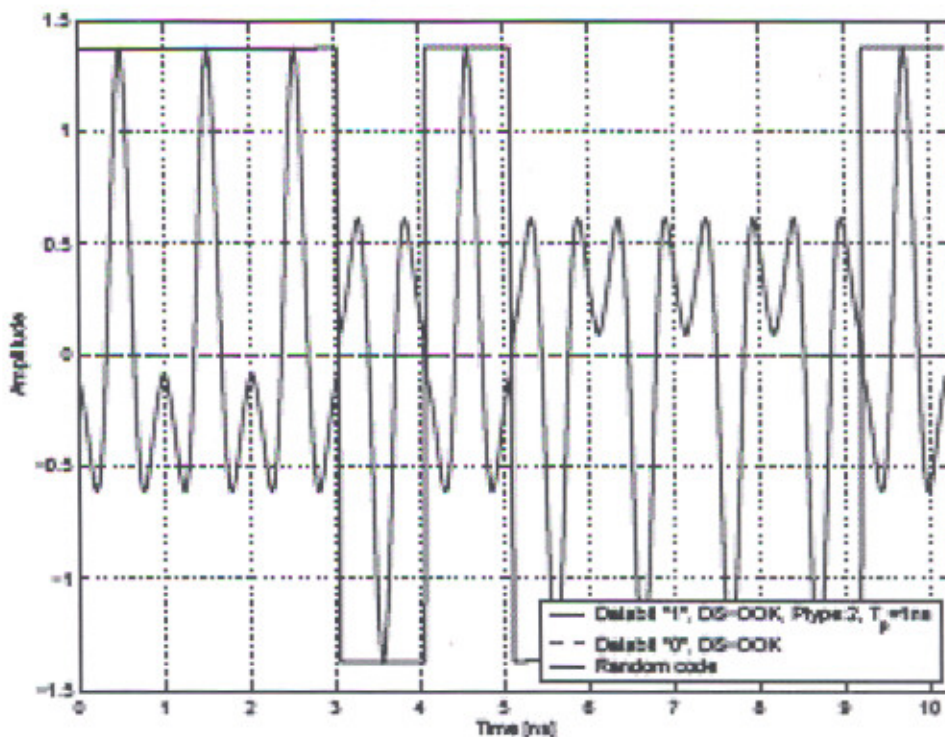


Figure 3.8 OOK with DS spreading.

3.3.5 Other modulation schemes

Bipolar Modulation scheme can also be used to modulate the ultra wideband pulse. Bipolar modulation is similar to OOK, but a binary '1' is represented by alternately positive or negative pulses. Because of the alternating polarity pulses for '1's, this scheme has error detection capability. But on the other hand, a long string of '0's may result in

loss of synchronization. Chirp Modulation is also proposed by some researchers, but the critical point of it is the design and realization of relevant SAW devices with adequate production tolerance and temperature drift.

3.3.6 Selected modulation scheme

After introducing the several different modulation techniques such as PAM, OOK, PPM and BPSK, we used PAM and BPSK as modulation schemes for system simulation and receiver design. Although PPM is not the most power efficient method compared to BPSK in the constellation diagram.

There are three concerns for which PPM also used in this work along with BPSK. Firstly, because the multipath channel is causal in time, PPM can utilize this feature very well to be tolerated with the reflective wireless channel and as well has good spectral properties. On the other hand, BPSK modulation encodes the transmitted data in the pulse polarity that can be distorted by the reflective wireless channel easily. Secondly, since PPM can use for accurate timer implementation. Which is important for building a real system and therefore, the problem of timing accuracy can be more or less solved. The third reason of choosing PPM is that it is also used by Time Domain Inc, one of first companies who are working on commercial UWB products. Time Domain Inc already made some successful UWB communication chipsets based on this modulation scheme, which indicates that PPM is acceptable as a mature modulation scheme.

In order to compare the analyzed multi-access and modulation techniques under the chip-synchronous assumption, we focus on a particular scenario for UWB applications, characterized by:

- Indoor environment
- High bit rates (> 50 MBit/s)
- Limited number of users (less than 14).

The first assumption does not influence our analysis, as the channel is supposed to be a simple AWGN one. The high bit rate requirement limits the length of the frame and consequently, the number of chips it can be divided into. The last point should be taken into account in the design of the codes for multi-access. Assuming a random time hopping scheme we can admit the presence of an arbitrarily large number of users; the same consideration can be extended also to DS systems with random interference in each

chip, while for OOC ones, equation (3.17) must be taken into account. As far as bit rate is concerned, it is also worth pointing out that the PPM technique requires longer chip interval than PSK. This observation must be taken into account in order to fairly compare the two strategies.

In our analysis we will consider a target bit rate of 50 Mbit/s per user, and will compare the bit error probabilities for different values of signal-to-noise ratio E_b/N_0 , defined as

$$E_b / N_0 = \begin{cases} N_s E_x / N_0 & \text{for } TH_PPM / BPSK \\ kE_x / N_0 & \text{for } OOC_PPM \\ KE_x / N_0 & \text{for } DS_BPSK \end{cases} \quad (3.29)$$

The transmitted waveform is the fifth derivative of a Gaussian pulse. The minimum chip width has been chosen equal to 0.5ns for PSK systems and to 0.6ns for PPM ones, in order to avoid interchip interference.

3.4 Power analysis

In the FCC specification, the power limit for the frequencies from 3.1 GHz to 10.6 GHz is .41.25dBm/MHz. Since the working frequency band is 7.5GHz bandwidth in total, the upper limit of the transmission power P_{Tx} of UWB system can be calculated as:

$$P_{Tx} = -41.25dBm / MHz \cdot 7500MHz = -2.5dBm = 0.56milliwatts \quad (3.30)$$

Based on the value of transmitted power, we can calculate the received power P_{Rx} in UWB receiver, using the UWB channel model. A practical UWB channel model indicates that while increasing the distance between Tx and Rx , the received UWB signal power will decay by e to the power -1.9 for LOS environment and e to the power of -3.4 for non-LOS environment.

$$\text{For LOS:} \quad P_{Rx} = e^{-1.9d} \cdot P_{Tx} \quad (3.31)$$

$$\text{For non-LOS:} \quad P_{Rx} = e^{-3.4d} \cdot P_{Tx} \quad (3.32)$$

where d is the distance between Tx and Rx in meters.

The power budget of a UWB system is shown in Table3-1.

Table 3-1 Power budget of UWB system

UWB signal bandwidth	7.5 GHz (3.1 GHz . 10.6 GHz)
FCC signal power limit	-41.25 dBm/MHz
Maximum transmitted power	-2.5 dBm (0.56 milliwatts)
Distance between Tx and Rx	10 meters
Received power (Using .1.9 model)	-115.0341 dB
Noise power	-98.2900 dB
Duty cycle factor	0.01 (20 dB gain for received power)
<i>SNR</i> _{simultaneous}	3.2559 dB

3.5 Transmission effects on UWB signals

3.5.1 Multipath effects

Multipath is one problem that is faced by almost all wireless communication systems. It is the result of the receiving antenna picking up reflected signals from the transmitter as well as the signal that travels directly to the receiver. If a single UWB pulse (Gaussian monocycle) is transmitted, the received signal will contain a direct path signal and reflected signals. Such a received signal $r(t)$ without the consideration of noise can be represented by:

$$r(t) = \sum_{n=1}^L a_n s(t - \tau_n) \quad (3.33)$$

Where $\tau_1 < \tau_2 < \dots < \tau_n$. The parameters τ_n and a_n are the time delay and the amplitude of the n^{th} multipath component, among which τ_1 and a_1 stand for the direct path. The waveform $s(t)$ denotes the single received UWB pulse. L is the number of multipath signals

As we know, the pulse width of $s(t)$ is typically less than $200ps$. Therefore, the multipath components with differential delays larger than the pulse width can be measured unambiguously. We can conclude that UWB system can be very robust to the effects of multipath interference.

However the long time delayed multipath components $a_n s(t - \tau_n)$ may cause ISI problem especially when $\tau_n > T_f$. To prevent the ISI problem, T_f cannot be chosen as a too small value when the transmitting pulse train is built.

3.5.2 Effects caused by related moving between Tx and Rx

A normal indoor office can be simulated as a high-density multipath environment, and one problem we are going to face is the effect on the propagation channel by the moving objects. The highest speed of a moving object can be set as $2m/s$, which is quite reasonable in office. By simple geometric analysis, we can see the change in path lengths led by a $2 m/s$ moving object within $100 ns$ should be smaller than $4 e-7$ meters. Since the speed of microwave signal is $3e 8m/s$, the time shift within $100ns$ will be $4e-7/3e 8$, which is around $1e-15$ seconds, $1e-6ns$. Compare to the pulse width of $0.1ns$, the time shift resulted by moving object in office can be neglected in a short time period. If we observe the system in a long time period, the moving object can cause the problem that the locking on one or several resolvable UWB signal paths is lost at the receiver.

3.5.3 Relocking on the most resolvable path(s)

If the wireless transmission channel makes a significant change, which means the resolvable path was lost tracking. The pulse detection for locking on the right path needs to be redone. The problem here is how to detect loss of lock to the strongest path.

A good suggestion would be doing the pulse detection in parallel with the demodulation. When the pulse detection observes the strongest path shifted too much, for example exceeds a certain threshold value, it will start adjusting the timing information of input UWB pulses to assure that the template pulse at the receiver always overlapping with the strongest input pulse (most resolvable path). Later, the demodulation will work with the new template signals, and importantly, still under the monitoring of the pulse detection.

Chapter 4

RAKE RECEIVER

**Performance Analysis of TH-PPM and DS-BPSK
in AGWN Channels for UWB Communication**

4.1 Introduction

The Rake receiver got its name from its inventors R. Price and P. Green in 1958. When a signal is received over a multi-path channel, the multi-path component delays appear at the receiver as in figure 4.1. By attaching a "handle" to the plot a picture of an ordinary garden rake is created. It is from this figure the Rake receiver got its name.

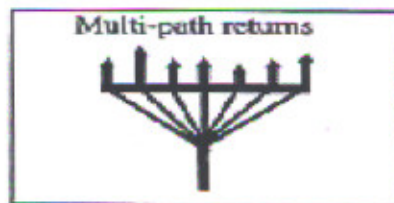


Figure 4.1 A rake

Conventional RAKE receiver structure and traditional DPSK receiver structure are two possible structures for detecting UWB impulses that include the effects of multi-path propagation, inter-symbol interferences "narrowband" jammers, and additive white gaussian noise (AWGN). The performance and complexity trade-offs for these two structures are compared in [31] and it is seen that RAKE receiver has better performance than DPSK receiver for detecting the UWB impulses. One of the benefits of UWB transmission is its ability to resolve individual multipath components. This feature motivates the use of RAKE multipath combining techniques to provide diversity and capture as much energy as possible at UWB receiver [32].

The key issue in designing a UWB RAKE receiver is its complexity. For full recovery of all considered multi-path components, the system requires a RAKE Receiver with a large number of fingers, in order to capture the majority of available energy. In a dense multipath environment (in case of UWB), the number of multi-path components increases linearly with the signal bandwidth. Even in a sparse environment, up to 80 fingers are required to collect the 80% of the available energy [33]. This is problematic from a cost perspective. There is a trade-off between UWB RAKE receiver complexity and its performance. Consequently, there is a need to design an UWB RAKE receiver that

has reasonable number of fingers, in terms of cost, and that also has an ability to collect the majority of the available energy from the multi-path channel, without compromising the receiver performance. The standardization for this technology is still in motion. Some of the potential applications of UWB transmission are wireless links connecting all fixed and smart home appliances such as computers, security systems, VCR's, TV's, stereos, short-range data and video communications, through wall sensing, wireless USB (USB2), wireless personal area network, underground imaging and establishing the security zones for home/ business security systems.

But the UWB systems with two-finger RAKE Receiver over two-path channel model make it simple to understand, and is used in this thesis.

4.2 Conventional Rake receiver

In a conventional Rake receiver each multi-path component ('finger') has dedicated Rake finger device consisting of scramble/channelization code generator, correlator, integrator and First In First Out (FIFO) as shown in figure 4.2. The separate code generators are time-aligned with their respective multi-path component. The more multi-path components that you want to be able to combine, the more Rake finger receivers you need. The received symbols are stored in a FIFO to be time-aligned before they are sent to the Maximum Ratio Combiner (MRC). Each Rake finger device operates at chip-rate (3.84MHz in WCDMA).

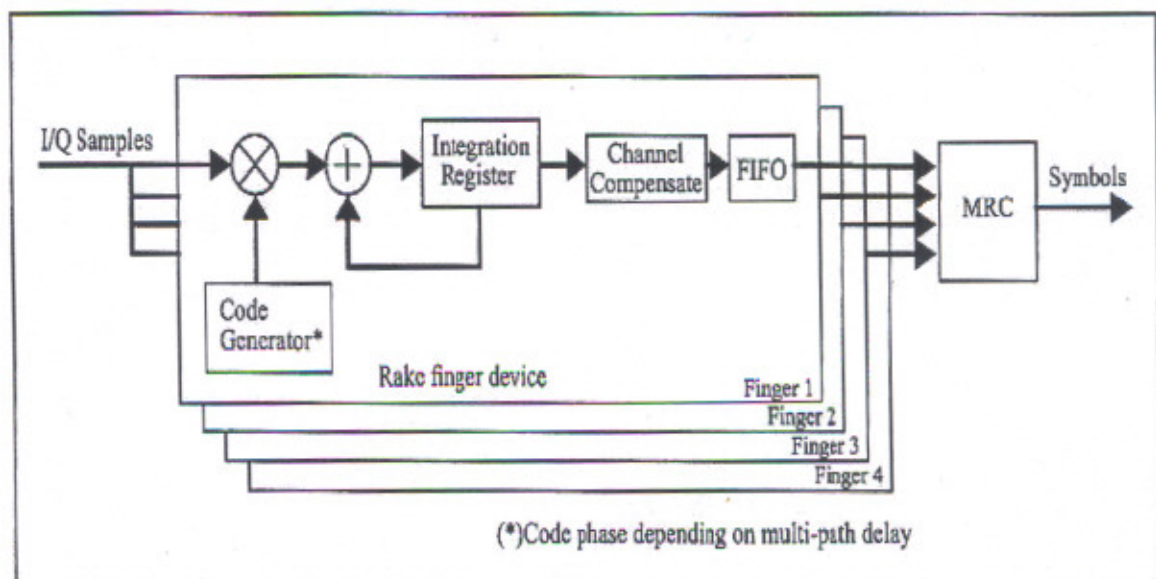


Figure 4.2 Conventional Rake Receiver

4.3 Types of Rake Receivers for UWB

Following are the types of RAKE receivers generally used for ultra wideband communication systems:

Flex Rake receiver

Post Buffer Rake Receiver

4.3.1 Flex Rake receiver

The Flex Rake receiver is much more efficient than the standard Rake receiver approach. The main optimization is that Flex Rake uses one big circular sample buffer to store the incoming I/Q samples and only one correlator engine that works time-multiplexed between the Rake-fingers that are active. This saves very much hardware.

The Flex Rake consists of a Sample Buffer and a Correlator Engine. The correlator engine works time-multiplexed so that it correlates one sample (chip) from each active finger in turn. This means that to be able to process up to eight active fingers, the correlator needs to be eight times faster than the conventional Rake receiver that has one correlator for each active finger. The correlator engine consists of code generators, complex multiplier, a number of integration registers (one for each active finger) and a FIFO-buffer for the correlated symbols as shown in figure 4.3.

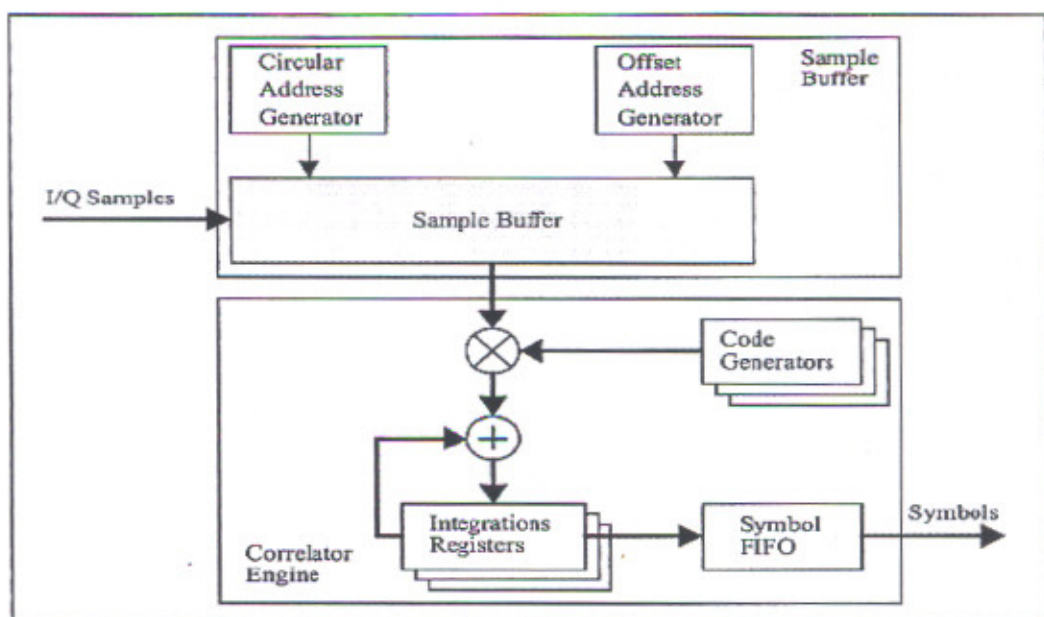


Figure 4.3 Block diagram of Flex Rake Receiver

The correlator performs a complex multiplication of I/Q samples with the combined scramble and channelization code. The result is accumulated with the previous correlated sample and stored in the integration registers for that particular finger. Then the next finger is processed.

When one finger has been integrated spreading factor (SF) times the resulting symbol is stored in the symbol FIFO to later be combined with the corresponding symbol from the other active fingers. The sample buffer consists of a data buffer and two address generators. The data stored in the buffer is I/Q samples coming in from the ADC (via a pulse shaping filter). The sample buffer is implemented as a time-sliding window with three parts as shown in figure 4.4, write window, pre-window and post-window. The write window prevents the pre-window from being overwritten. The pre-window makes it possible to catch a new multi-path finger that has much shorter delay than the current active fingers. The post-window is big enough so that it can contain I/Q samples for different fingers that have the longest supported delay between them.

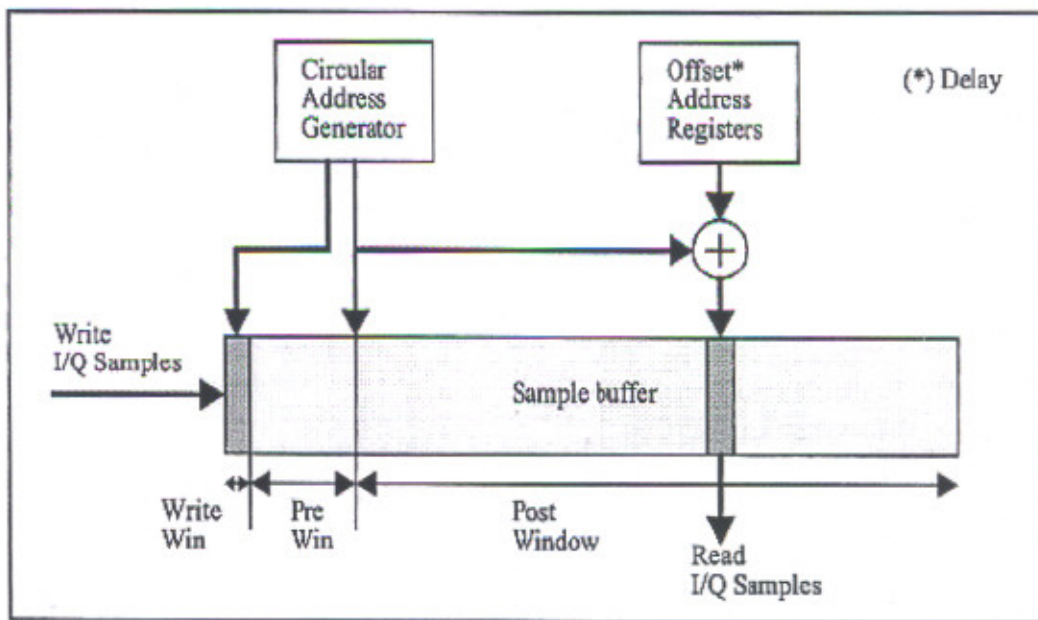


Figure 4.4 Sample Buffer read and write accesses

4.3.2 Post Buffer Rake Receiver

The Post Buffer Rake receiver takes a different approach to the buffering problem. It instead processes each finger individually, and keeps track of their respective delay (τ). In

this receiver the time alignment is also done at very end. Since the time alignments are then done on symbols instead of samples, the data rate to/from the post-VDB is much lower.

To handle each finger individually in a time multiplexed manner, each block needs to know each fingers respective delay (τ_{finger}). Enclosed with each Chip and Symbol is their delay value. This eliminates the need for each block to store the different delay values for each finger. The Post Buffering Rake Receiver is designed to handle eight fingers with a maximum delay of $296T_c$ and six different scrambling codes. It is also easy to include more than one dedicated physical channel by instantiating more than one Despreader. In figure 4.5 the overall structure of the Post Buffering Rake Receiver is shown.

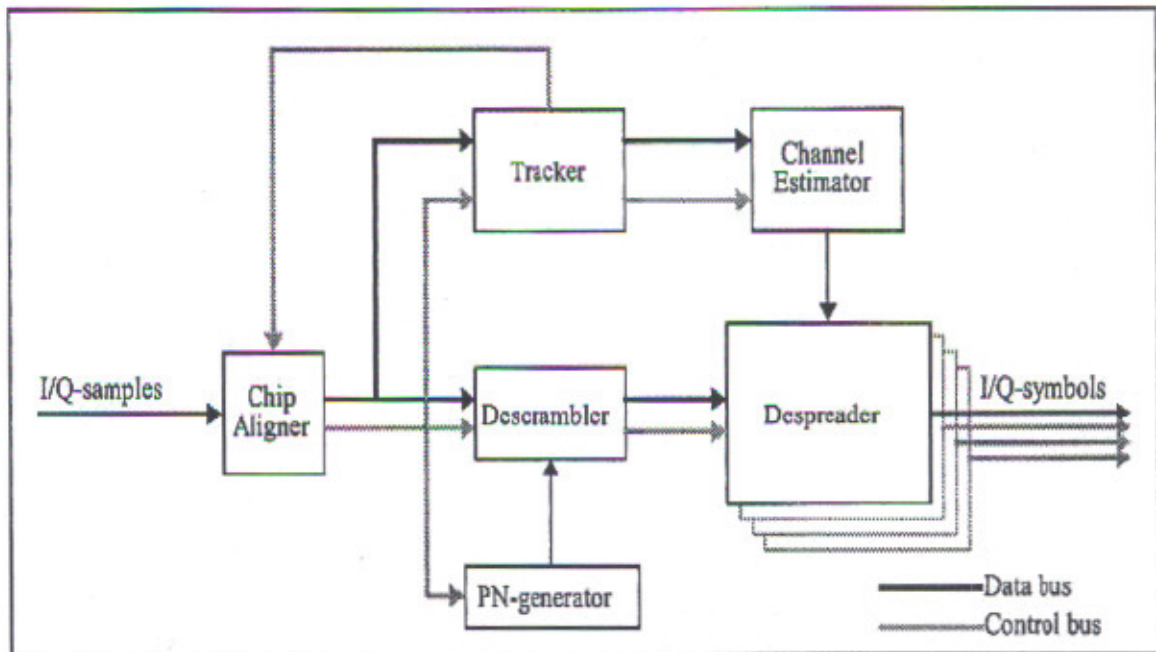


Figure 4.5 Block diagram of Post Buffering Rake Receiver.

4.4 RAKE Receiver Performance Analysis

The transmitted UWB waveform is defined as

$$s(t) = \sqrt{P} \sum_{i=-\infty}^{\infty} b_i a(t - iT_r) \quad (4.1)$$

where $a(t)$ is the equivalent RF pulse shape, $\{b_i\}$ are the modulated data symbols, T_r is the pulse repetition period, and P is the transmitted power of the impulse. For simplicity, the transmitted waveform is normalized in the following manner. Let

$$B_s \int_{-\infty}^{\infty} a^2(t) dt = 1 = B_s \int_{-\infty}^{\infty} |A(f)|^2 df \quad (4.2)$$

where B_s is the occupied bandwidth of the waveform and $A(f)$ is the Fourier transform of $a(t)$. The average transmit power is then given by

$$P_{avg} = \frac{1}{T_r} \int_0^{T_r} E[s^2(t)] dt = \frac{B_r}{B_s} P B_s \int_0^{T_r} a^2(t) dt = \frac{B_r}{B_s} P \quad (4.3)$$

Where $B_r = 1/T_r$ can be interpreted as the symbol rate or the pulse repetition frequency (PRF), and the modulated symbols are assumed to be bipolar (i.e., $b_i \in \pm 1$). Note that this results in the following equality $P = (B_s / B_r) P_{avg} = N_s P_{avg}$ where $N_s = B_s / B_r$ can be considered the pulse processing gain. The received waveform, which includes multipath and ‘narrowband’ interference, can be written as follows:

$$r(t) = \sum_{l=0}^{L-1} \alpha_l s(t - \tau_l) + n(t) + I(t) \quad (4.4)$$

where L is the number of multipath components present due to the frequency selective nature of the channel, $\{\alpha_l\}$ are the received amplitudes of the paths, $\{\tau_l\}$ are the associated delays of each path, $n(t)$ is the AWGN with two-sided power spectral density $(\eta_0/2)$ and $I(t)$ represents a ‘narrowband’ interferer. This interference term is modeled as a traditional modulated single carrier waveform, where

$$I(t) = \sqrt{2P_I} \cos(\omega_0 t + \theta) \sum_{k=-\infty}^{\infty} g_k v(t - kT_I - \tau_I) \quad (4.5)$$

P_I is the average transmit power of the ‘narrowband’ waveform, ω_0 is the carrier frequency of the ‘narrowband’ waveform, θ is a random phase of the carrier, $\{g_k\}$ are

the randomly modulated symbols where $b_k \in \{\pm 1\}$, T_I is the ‘narrowband’ symbol period, τ_I is a random delay uniformly distributed in the interval $[0, T_I]$, and $v(t)$ is the baseband waveform shape. Although the analysis is valid for any ‘narrowband’ baseband waveform, the results will assume a root raised cosine shape with a bandwidth expansion factor of $\alpha=0.25$ [34].

In order to simplify the analysis, a discrete model for the UWB multipath channel is used, which assumes that the multipath components arrive at some integer multiple of a minimum path resolution time, T_m . Also, in order to avoid partial correlations of the waveform, the modulated waveform, $a(t)$, is assumed to be effectively zero outside the interval $0 \leq t \leq T_m$. The RAKE receiver is modeled as having L_p arms, where each arm independently tracks a different path with a delay $p_m T_m$, p_m is an integer in the interval $[0, N_r-1]$ corresponding to path delay m , and $N_r = T_r / T_m$ represents the number of possible paths per pulse period separated by the minimum resolvable path spacing of T_m . The sampled output of the RAKE receiver can then be written as $h_j = d_j + n_j + I_j$, where each term corresponds to the desired signal, additive noise, and interference signal, respectively, and is described in the following subsections:

4.4.1 Desired term

The desired signal term is given by

$$d_j = c^T y_j, \quad (4.6)$$

where $y_j = [y_{P_0,j}, y_{P_1,j}, \dots, y_{P_{L_p-1},j}]^T$, p_m is the delay of the m^{th} RAKE arm where $m=0 \dots L_p-1$, $c = [c_0, c_1, \dots, c_{L_p-1}]^T$ is the vector of RAKE tap combining weights, and

$$y_{P_m,j} = \sum_{l=0}^{L-1} \sum_{f=-\infty}^{\infty} \alpha_l b_l^f \sqrt{P} \int_0^{T_m} a(u) a(u + (j-i)T_r + (P_m - l)T_m) du \quad (4.7)$$

Let b_0^j be the symbol of interest at time j , and b_i^j for $i=1\dots Q$ be the symbols that have a non-zero channel tap weight associated with them, which represent the inter-symbol interference. For L non-zero channel weights, then $Q = \text{ceil}[(L-1)/N_r]$, where $\text{ceil}[x]$ is the largest integer less than or equal to x . Also, define the L length column vector of channel tap weights $\alpha = [\alpha_0, \alpha_1, \alpha_2, \dots, \alpha_{L-1}]^T$. Note that, if there is no multipath component at a particular delay, $l T_m$, then the tap weight shall be $\alpha_l = 0$. Also, since the pulses are non-overlapping in order to neglect the effects of inter-pulse interference, the following equality is obtained:

$$\int_{-\infty}^{\infty} a(u)a(u+(j-i)T_r+(m-l)T_m)du = \begin{cases} 1/B_s & \text{when } (j-i)T_r+(m-l)T_m=0 \\ 0 & \text{otherwise} \end{cases} \quad (4.8)$$

Then, the desired term can be simplified to $d_j = \sqrt{P}/B_s c^T A_j \alpha$, where $A_j = \sum_{i=0}^Q b_i^j E_i$, and E_i is an $L_p \times L$ matrix. Each row, m , where $m=0\dots L_p-1$, of this matrix consists of a zero in all places except for a one in position $(N_r i + p_m)$. If $|N_r i + p_m| > L$, then the row is an all zero vector.

4.4.2 Noise term

The noise output of the RAKE combiner is given by

$$n_j = c^T n_j, \quad (4.9)$$

where $n_j = [n_{p_0,j}, n_{p_1,j}, \dots, n_{p_{L-1},j}]$ whose components $n_{p_m,j} = \int_{-\infty}^{\infty} a(u)n(u+jT_r+p_mT_m)du$ are independent; Gaussian distributed random variables with a zero mean and variance $\sigma^2 = \eta_0/2B_s$, for all m and j .

4.4.3 Interference term

Note that the sampled output of the correlator receiver is equivalent to the sampled output of a filter matched to the waveform $a(t)$. The frequency response for the pulse matched

filter is given by $H(f) = e^{-j2\pi fT_r} A(f)$, where $A(f)$ is the (real) amplitude response. In order to simplify the analysis, the frequency response of the impulse is assumed to be a perfect bandpass waveform, as shown in Figure 4.6. If the narrowband interference is fully contained within the bandwidth of the UWB waveform (and therefore within the bandwidth of the pulse matched-filter), the output of the pulse matched filter due to the interference term is simply $I(t - T_r) / \sqrt{2B_s}$. Hence, the output of the RAKE receiver due to the interference term is given by $I_j = \sqrt{P_I} / B_s c^T y_j^I$ where:

$$y_j^I = [y_{p_0 \cdot j}^I, y_{p_1 \cdot j}^I, \dots, y_{p_{p-1} \cdot j}^I]^T \quad (4.10)$$

$$y_{p_m}^I = \cos(\omega_0(jT_r + p_m T_m) + \theta) \sum_{k=-W/2}^{W/2} g_k^f v(jT_r + p_m T_m - kT_I - \tau_I). \quad (4.11)$$

The summation over the ‘narrowband’ modulated symbols is truncated to $W=6$, which is sufficient for $T_I > T_r$ due to the roll-off of the root raised cosine waveform and the limit on the RAKE arm delays such that $p_m T_m < T_r$.

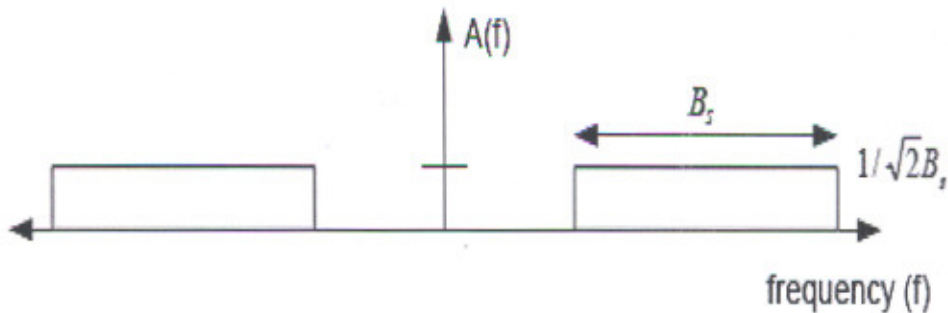


Figure 4.6 Frequency domain representation of UWB impulse used to evaluate effect of narrowband interference on UWB performance.

4.4.4 RAKE Receiver Output

Now, the RAKE receiver output can be written as:

$$h_j = \frac{\sqrt{P}}{B_s} (c^T A_j \alpha + \frac{1}{\sqrt{N_s L_I}} c^T y_j^I) + n_j \quad (4.12)$$

where $L_I = P_{avg}/P_I$ represents the signal-to-interference ratio (SIR) and $\{n_j\}$ are independent, identically distributed, Gaussian random variables with zero mean and variance equal to $\sigma^2 = c^T c \eta_0 / 2B_s$. This equation shows the effect of the pulse processing gain, N_s , reducing the impact of the interference similar to traditional spread spectrum systems [35].

4.4.5 Average Bit Error Probability

By conditioning on the channel path weights, the desired symbols, and the ‘narrowband’ interfering symbols, the output of the RAKE receiver is simply a conditional Gaussian random variable whose bit error probability is well known [35]. Averaging over the desired signals interfering symbols (ISI) and the ‘narrowband’ interfering symbols yields the following conditional probability of error:

$$P_b(e/\alpha) = \frac{1}{2^Q 2^{W+1}} \sum_{j=1}^{2^{Q-1} 2^{W+1}} P_s(e/\alpha, b_j, g_j) \quad (4.13)$$

Where

$$P_s(e/\alpha, b_j, g_j) = \frac{1}{2} \text{erfc}(\gamma_j) \quad (4.14)$$

$$\gamma_j = \sqrt{\frac{\gamma_{avg}}{c^T c}} \left(c^T A_j \alpha + \frac{1}{\sqrt{N_s L_I}} c^T y_j^I \right) \quad (4.15)$$

$$\gamma_{avg} = E_b / \eta_0, \quad g_j = [g_{-W/2}^j, g_{-W/2+1}^j, \dots, g_{W/2}^j]^T \quad (4.16)$$

where $g_i^j \in \pm 1$, and

$$b_j = [b_0^j, b_{-1}^j, b_{-2}^j, \dots, b_{-Q}^j]^T \quad (4.17)$$

where $b_0^j = 1, b_i^j \in \pm 1$ and j spans all the possible combinations of the interfering symbols in the vector b_j and g_j . There are several options for determining the tap combining weights, which can be analyzed using the above equations [37]. For example, the tap

coefficients for a RAKE receiver using maximal ratio combining are determined by first finding the path delays corresponding to the strongest L_p multipath components, which is defined as $\tau_c = \text{index} \left\{ \max_{L_p} \left[\left| \alpha(1 : N_r) \right| \right] \right\}$, and assigning the RAKE coefficients as $c(\tau_c) = \alpha(\tau_c)$. Similarly, the performance of an equal gain combining RAKE can be determined by setting $c(\tau_c) = 1$ for the strongest paths, or by only selecting the first L_p non-zero paths ($\tau_c = \text{index} \left\{ \text{find}_{L_p} \left[\left| \alpha(1 : N_r) \right| > 0 \right] \right\}$) and setting $c(\tau_c) = 1$. The channel estimation and tracking algorithms are not covered in this paper, but this analysis can be used to compare the optimal performance of several different algorithms, although the results shown here focus only on the performance of a maximal ratio combining rake for brevity. The final average probability of error is then obtained by averaging over several realizations of the multipath channel.

Chapter 5

RESULTS AND DISCUSSIONS

**Performance Analysis of TH-PPM and DS-BPSK
in AGWN Channels for UWB Communication**

RESULTS AND DISCUSSIONS

5.1 Monocycle shape

The monocycle shape and its duration are important design parameters, affecting the signal spectrum and the system performance. As already discussed in sec 2.6 Gaussian fifth order derivative has been used for initial system analysis and simulations as it satisfies the FCC recommendations. The various parameters used for the analysis are:

Table 5.1 Design parameters for TH-PPM/DS-BPSK

Symbol	Meaning	Value and comments
$p(t)$	Monocycle	Gaussian fifth derivative
T_p	Monocycle duration	1 nsec
T_c	Chip time	1 nsec
T_f	Frame duration	15 nsec (1 nsec for DS-BPSK)
δ	Delay (PPM)	1 nsec
N_s	Monocycles per data bit	1
T_d	Bit duration = $N_s T_f$	15 nsec
R_b	Bit rate = $1/T_d$	~56.6 Mbps
N_c	Chip sequence length	15
P	Maximum transmitted energy	-41.25 dBm/Mhz

Note: The pulse width $T_p = 1$ nsec is chosen to reduce the simulation time. But for practical transmission $T_p < 1$ nsec is used.

The maximum transmitted UWB signal power according to FCC specification is $P = -41.25$ dBm/MHz = $-41.25 * 7500 = -2.5$ dBm = 0.56 mill watts,

Figure 5.1(a) shows the fifth derivative of Gaussian pulse and 5.1(b,c) shows TH-PPM & DS-BPSK monocycle trains in time domain respectively.

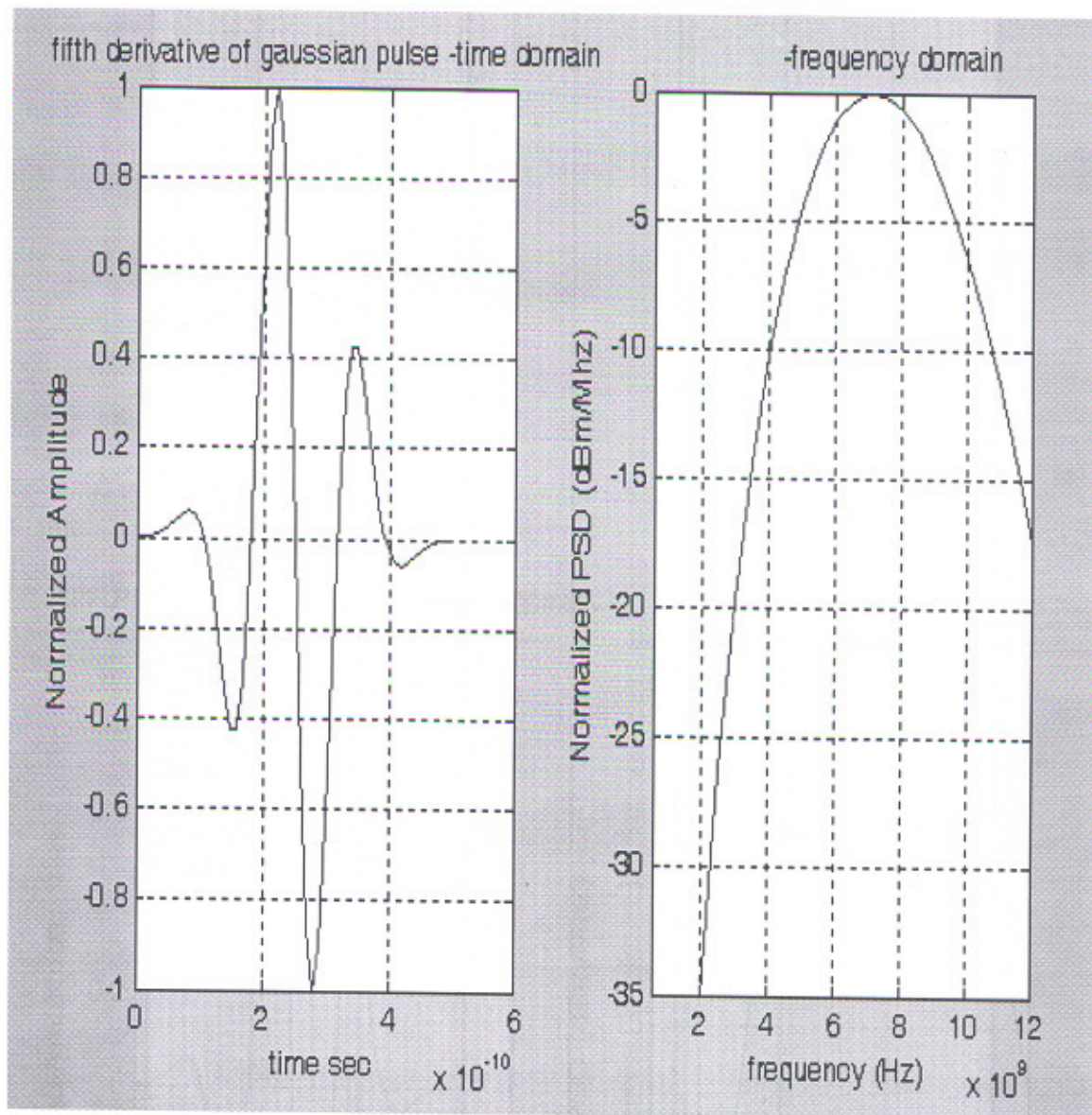


Figure5.1 (a) Gaussian fifth derivative in Time domain and Frequency domain

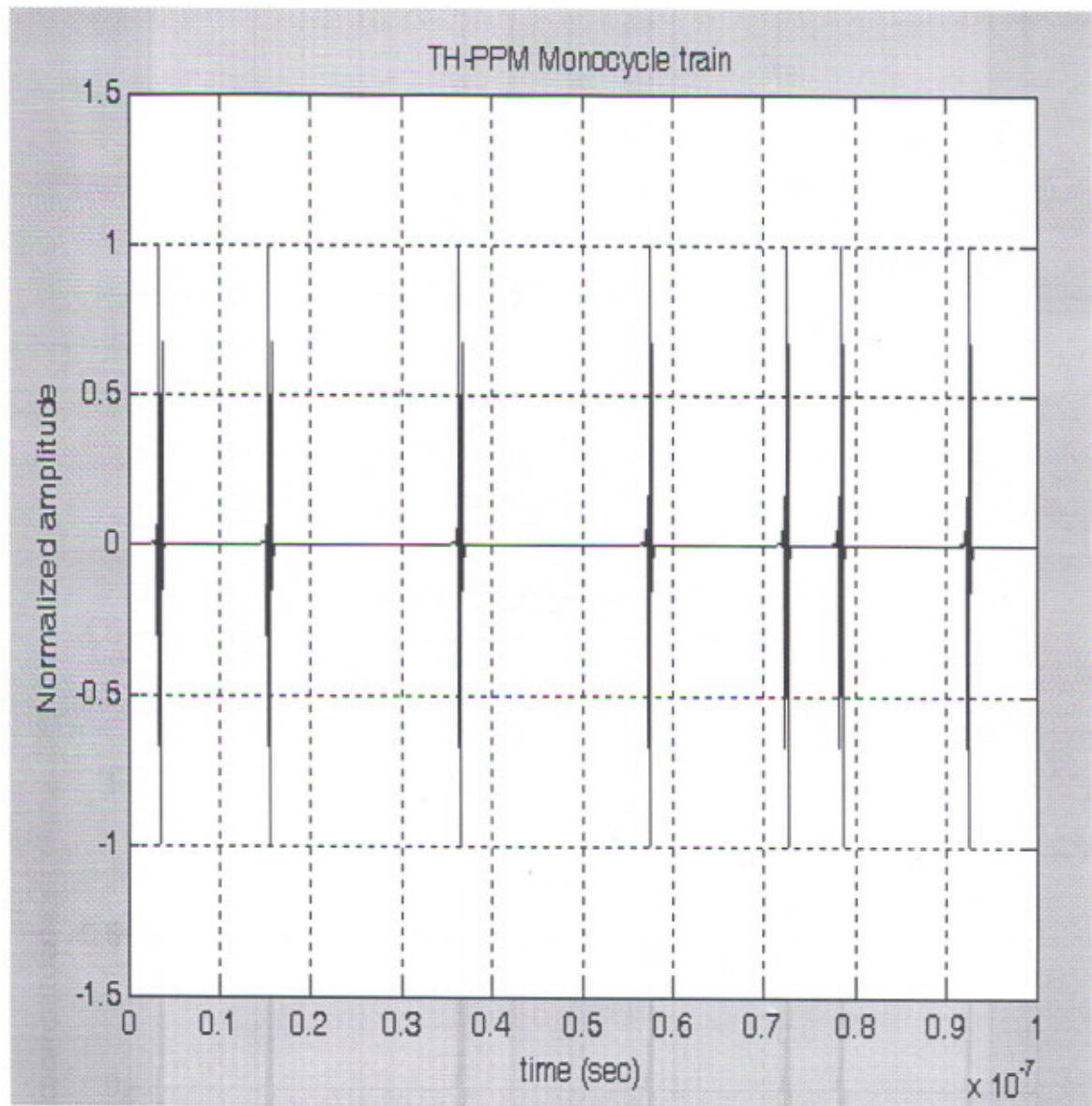


Figure 5.1(b) TH-PPM monocycle train in time domain

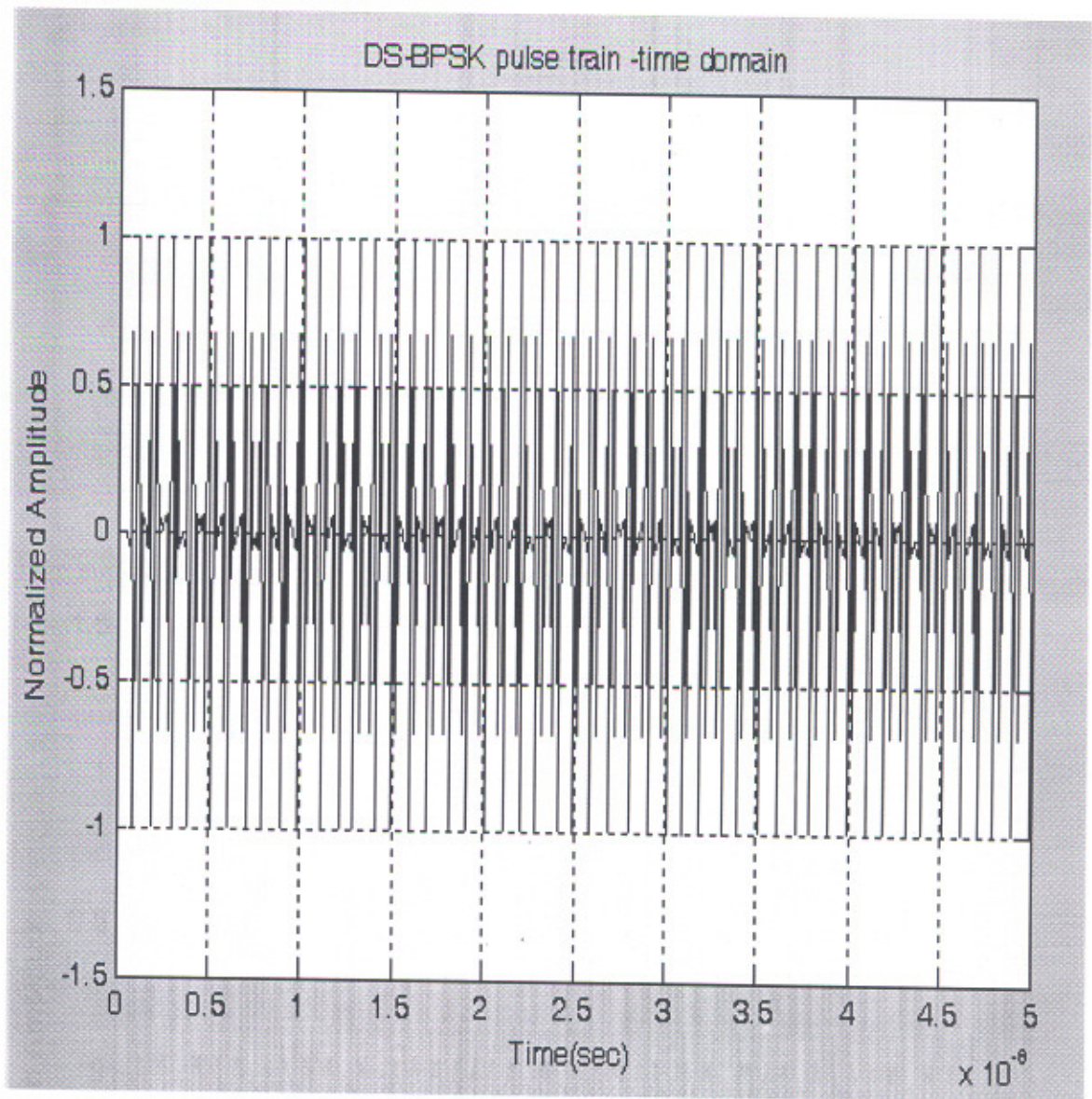


Figure 5.1(c) DS_BPSK monocycle train in time domain

5.2 Performance Analysis of TH-PPM & DS- BPSK in AWGN channel

In this work single-user performance of the two techniques assuming free space propagation conditions and additive white Gaussian noise (AWGN) is studied and in later section subsequently extended to incorporate multipath channels.

A fair evaluation of TH and DS is accomplished using a fixed average signal when characterizing performance. Since DS provides an inherent processing gain N_c which is N_s times greater than TH, simulations are performed using a received TH-PPM SNR equaling N_c times the received DS-BPSK SNR within each PRI;

Fundamentally, TH-PPM represents a form of orthogonal signaling and DSBPSK represents a form of antipodal signaling. For communicating over an AWGN channel with a matched filter receiver, the theoretical probability of bit error:

$$P_b = Q\left(\sqrt{\frac{E_b(1-\rho)}{N_0}}\right)$$

$$\rho = 0 \text{ (Orthogonal Signaling)}$$

$$\rho = 1 \text{ (Antipodal Signaling)}$$

where Q is the complementary error function, E_b/N_0 is the average energy per bit divided by the AWGN power spectral density, and ρ is the correlation coefficient.

5.2.1 Performance of TH-PPM in AWGN channel at different data rate

Simulations for this modulation scheme for different values of data rate have been performed as shown in Figure 5.2(a-f). The modulation scheme use Gaussian fifth derivative with pulse width of 1 nsec and Spreading factor (SF) =15. It is seen from simulation results as we increase the data rate from 500 bits/sec, the curves between Bit Error Rate and Signal to Noise Ratio becomes linear till 10 Kbps and also remain approximately same after that. In this work due to very long simulation time the maximum data rate used for simulation was 50 Mbps. These results shows that it is possible to transmit data, with data rate as high as 50 Mbps with this technology.

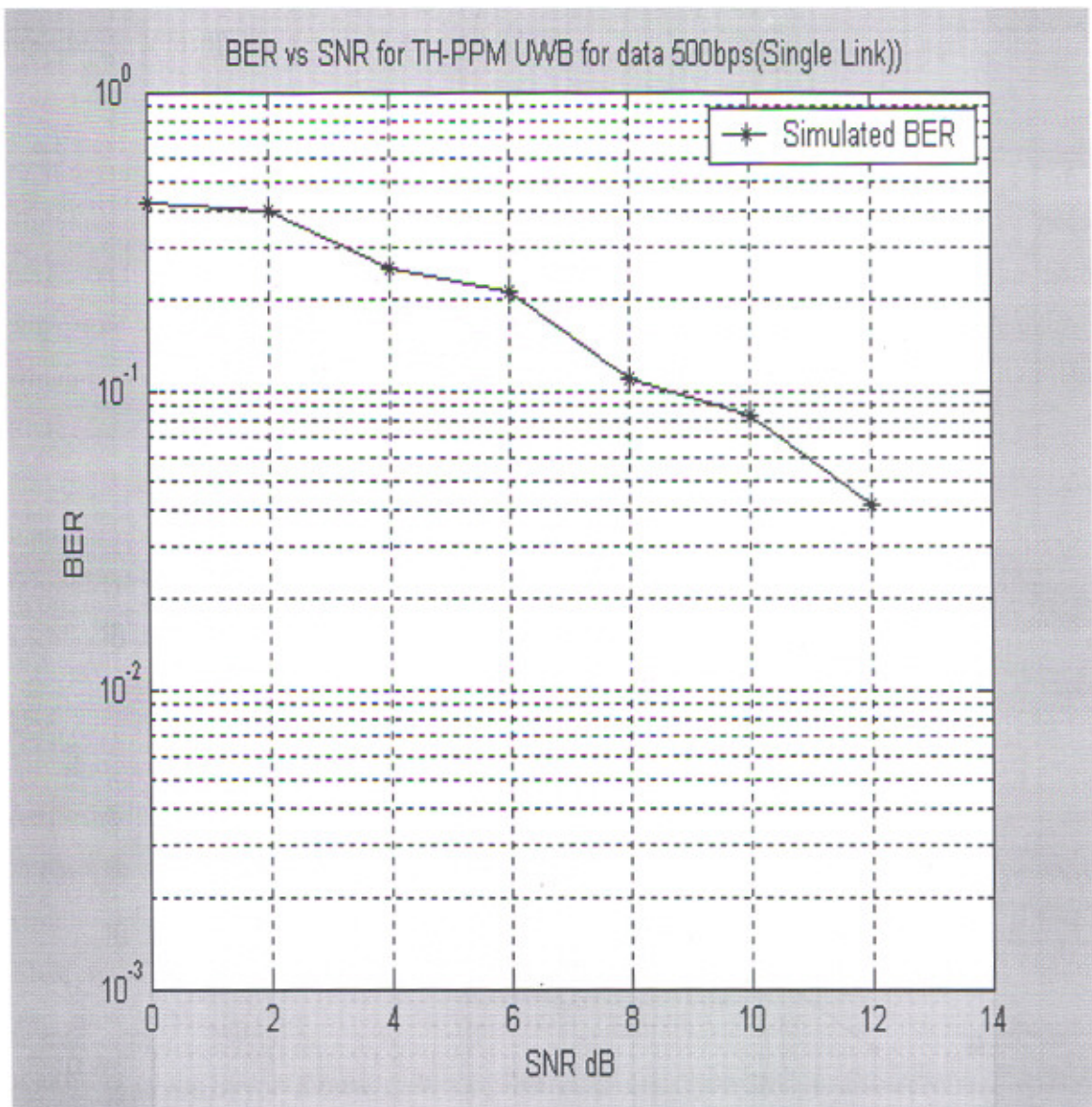


Figure 5.2(a) Performance of TH-PPM for data rate 500 bps

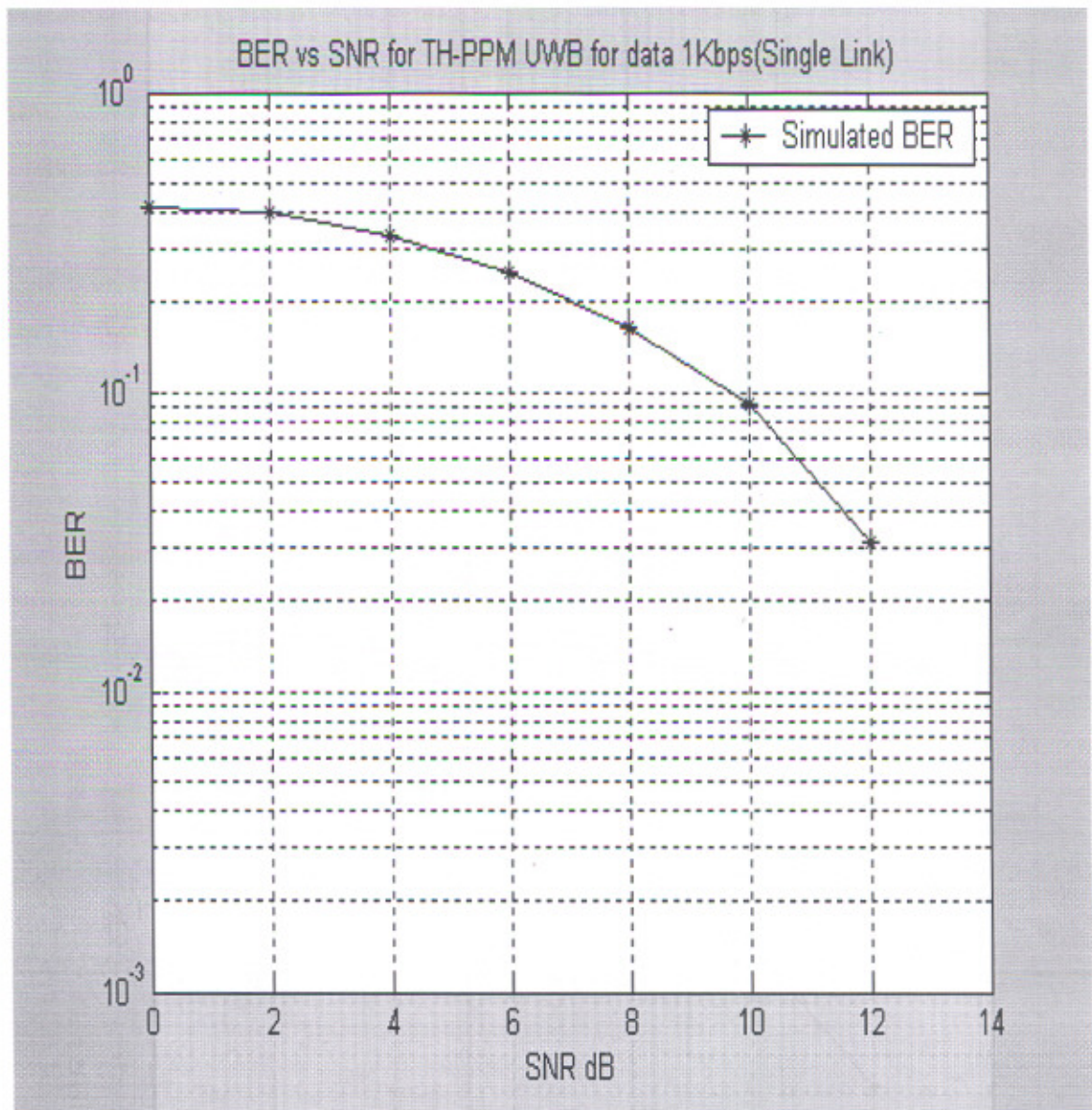


Figure 5.2(b) Performance of TH-PPM for data rate 1 kbps

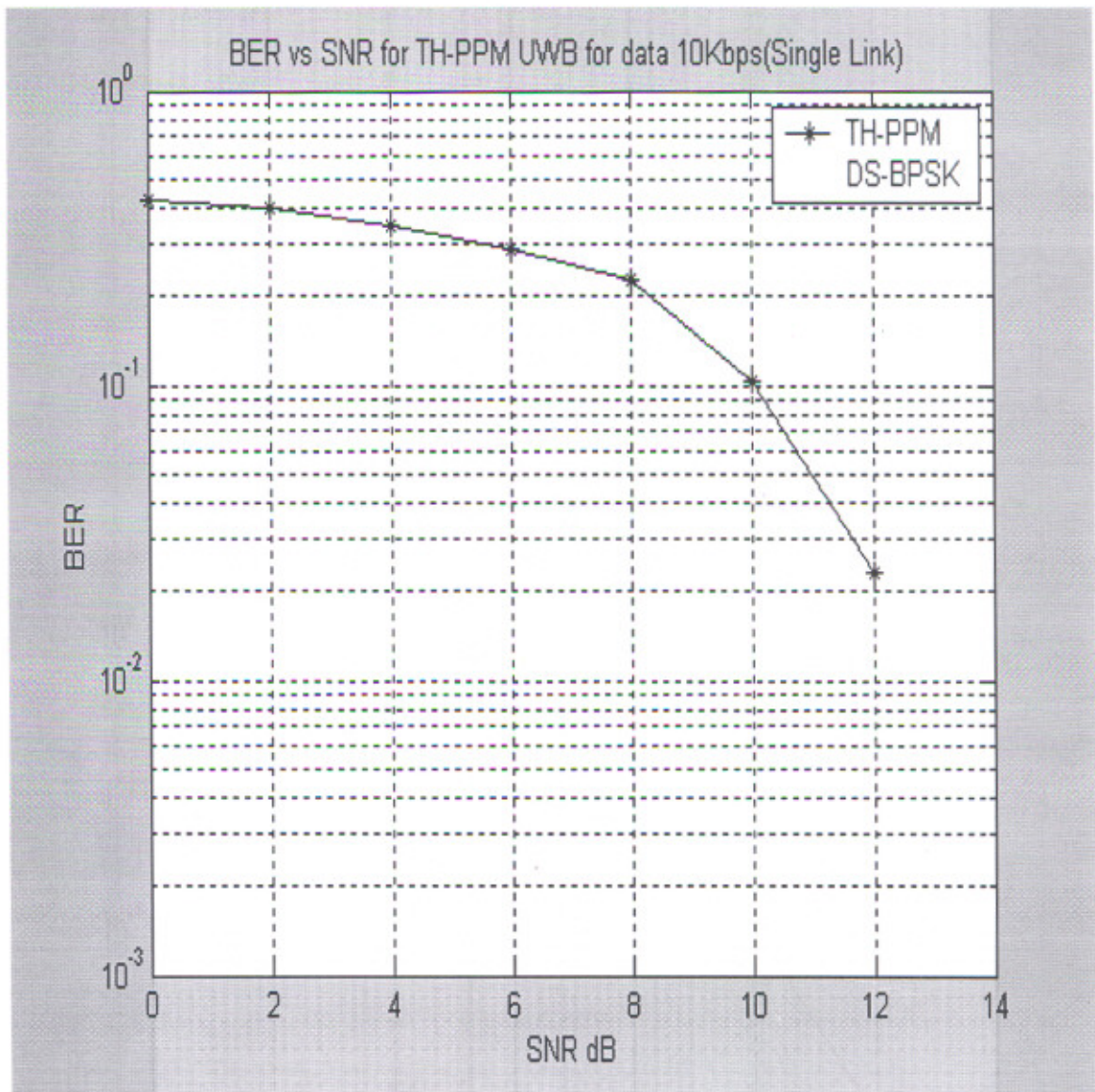


Figure 5.2(c) Performance of TH-PPM for data rate 10 Kbps

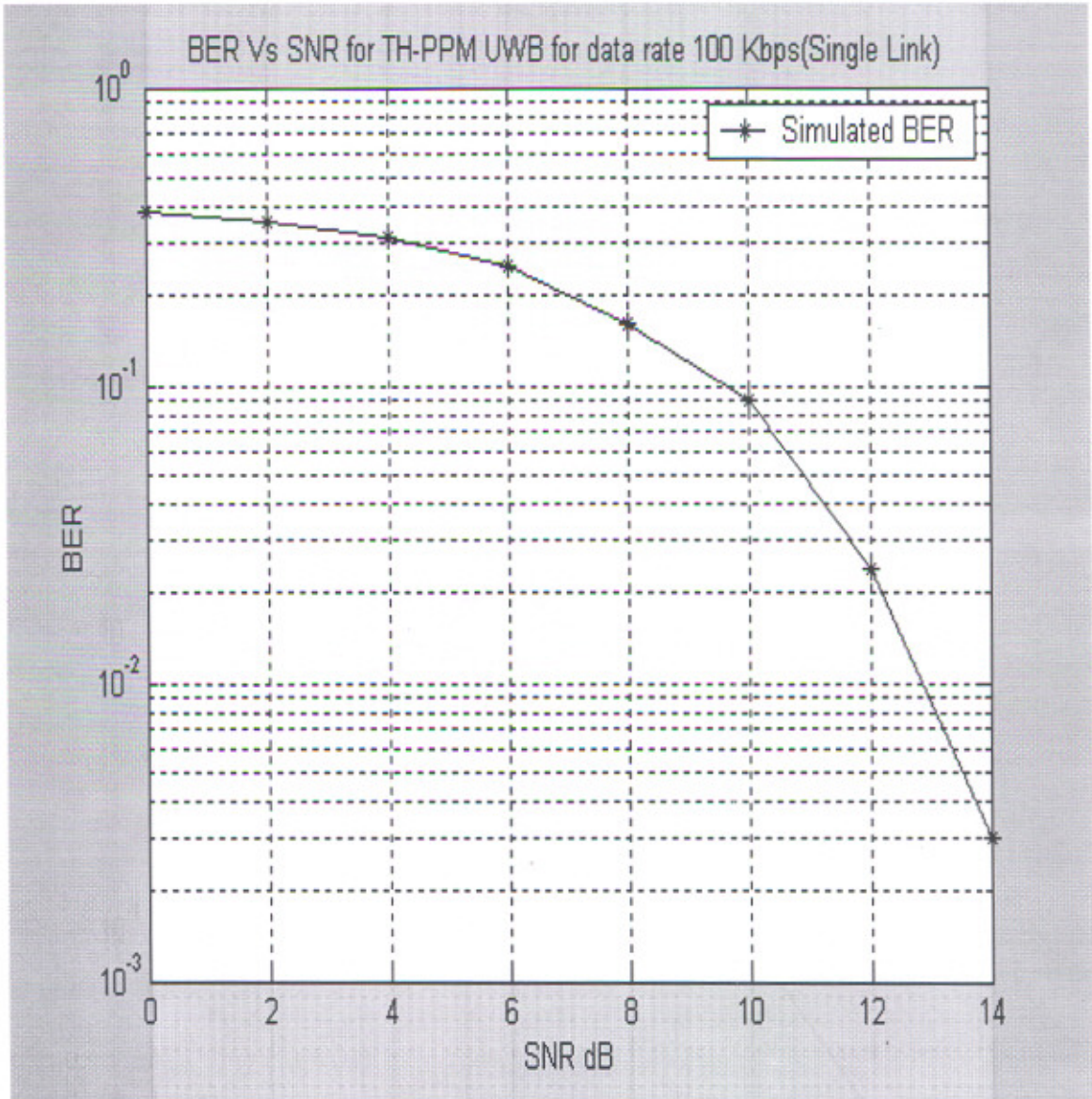


Figure 5.2(d) Performance of TH-PPM for data rate 100 Kbps

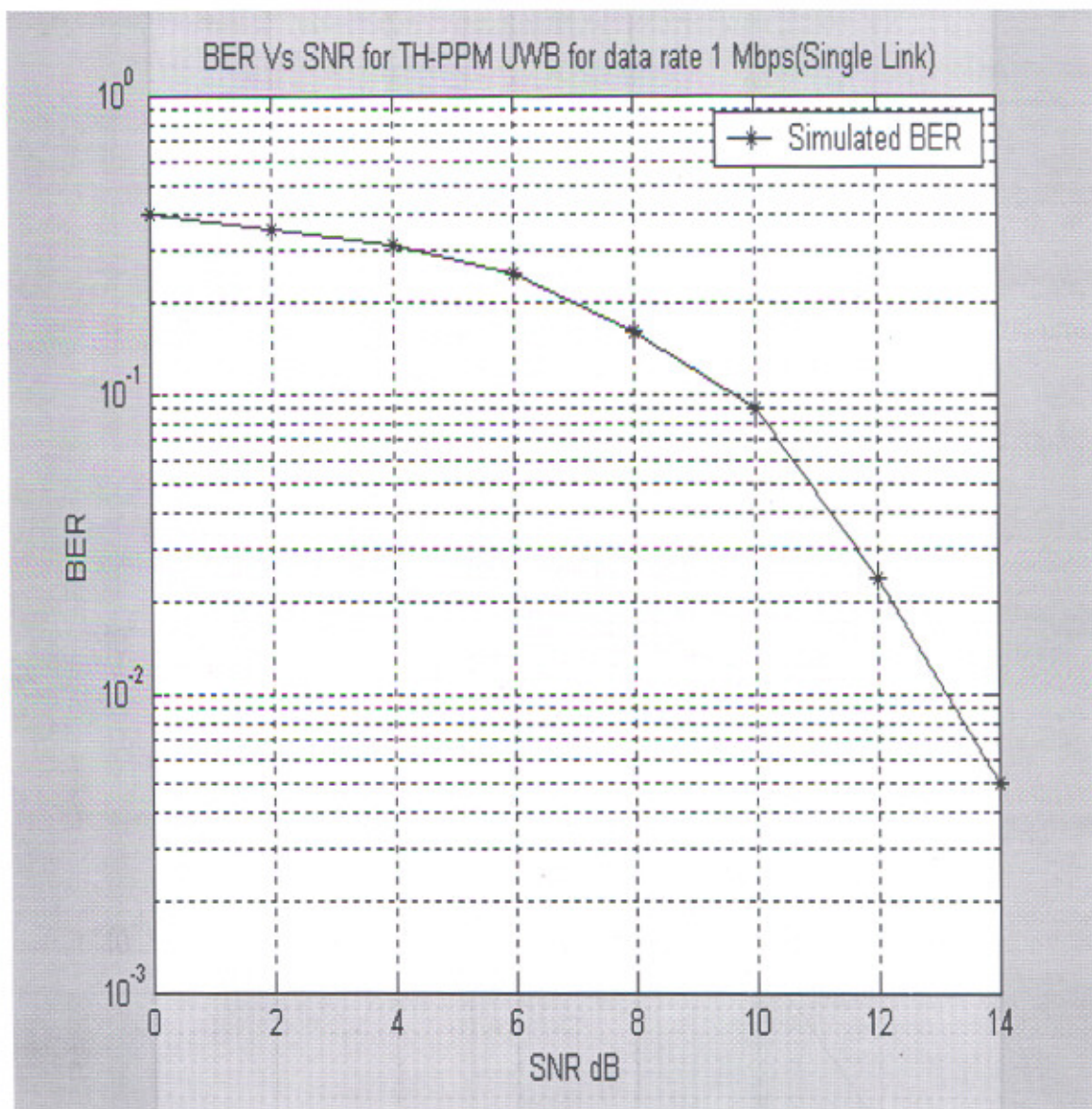


Figure 5.2(e) Performance of TH-PPM for data rate 1 Mbps

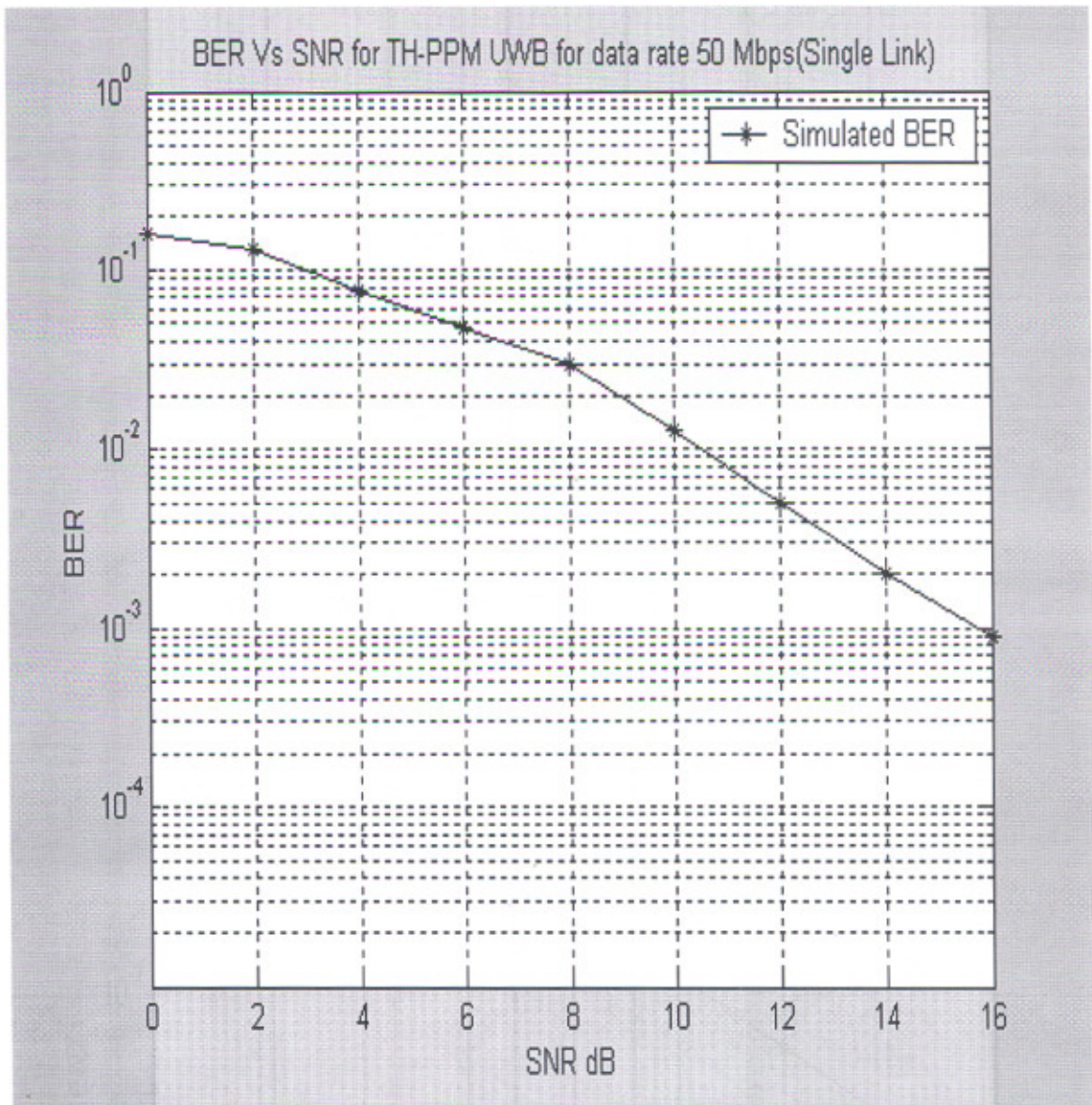


Figure 5.2(f) Performance of TH-PPM for data rate 50 Mbps

5.2.2 Performance of DS-BPSK in AWGN channel at different data rate.

Simulations for this modulation scheme for different values of data rate have been performed as shown in Figures 5.3(a-f). The modulation scheme use Gaussian fifth derivative with pulse width of 1 nsec and Spreading factor (SF) =15. It is seen from simulation results as we increase the data rate from 500 bits/sec, the curves between Bit Error Rate and Signal to Noise Ratio becomes linear till 10 Kbps and also remain approximately same after that. In this work due to very long simulation time the maximum data rate used for simulation was 50 Mbps. These results shows that it is possible to transmit data, with data rate as high as 50 Mbps with this technology.

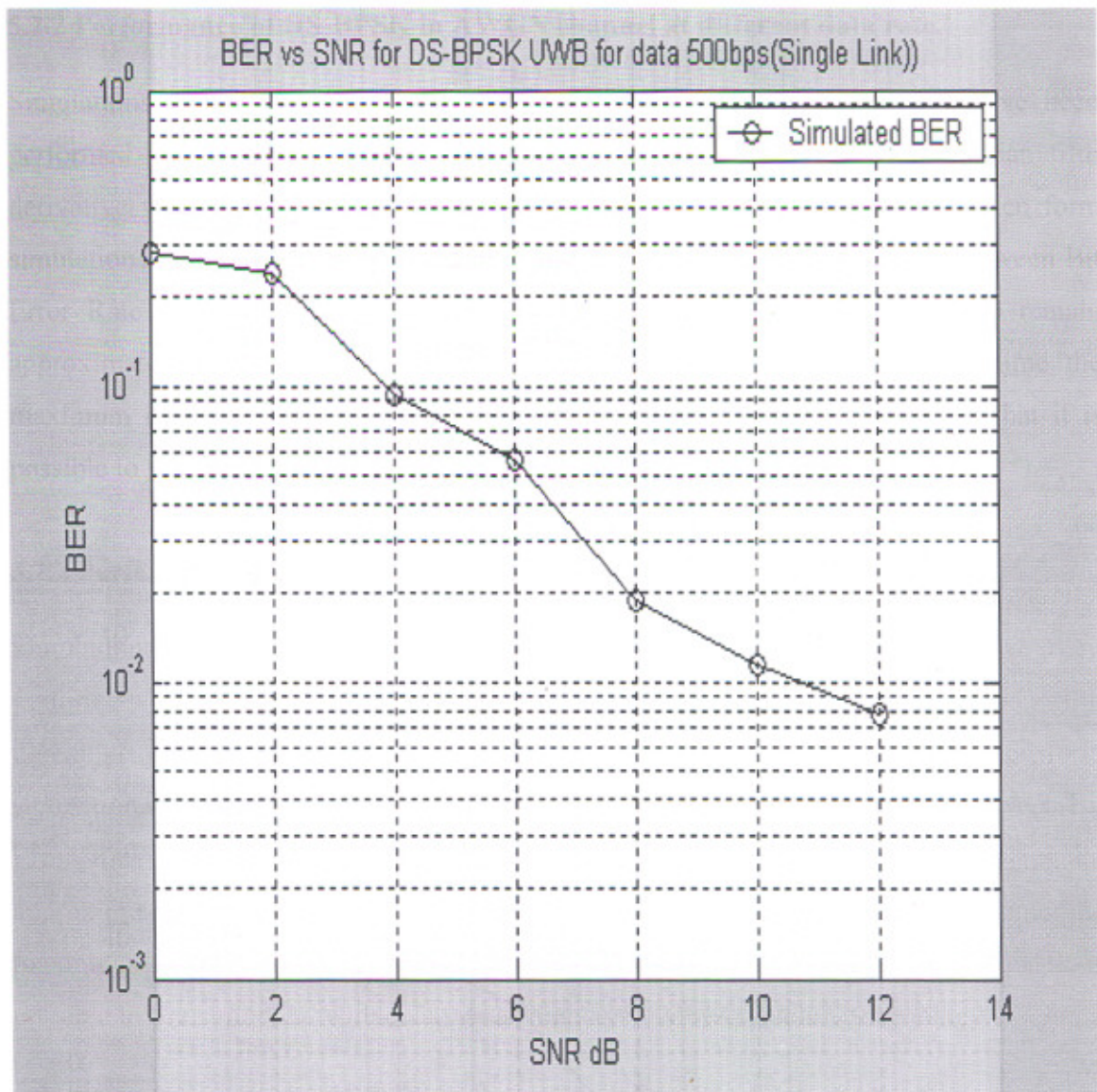


Figure 5.3(a) Performance of DS-BPSK for data rate 500 bps

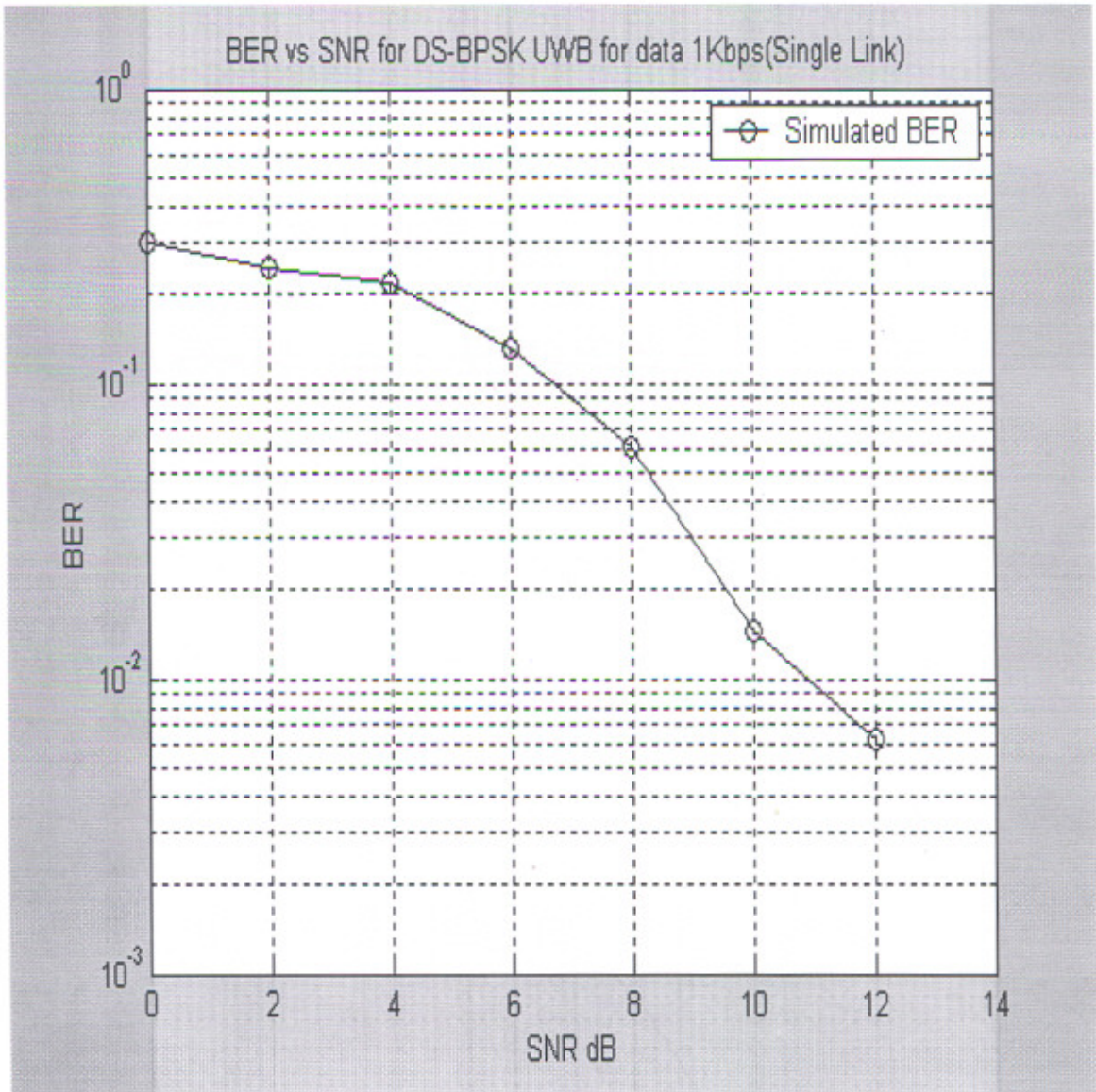


Figure 5.3(b) Performance of DS-BPSK for data rate 1 Kbps

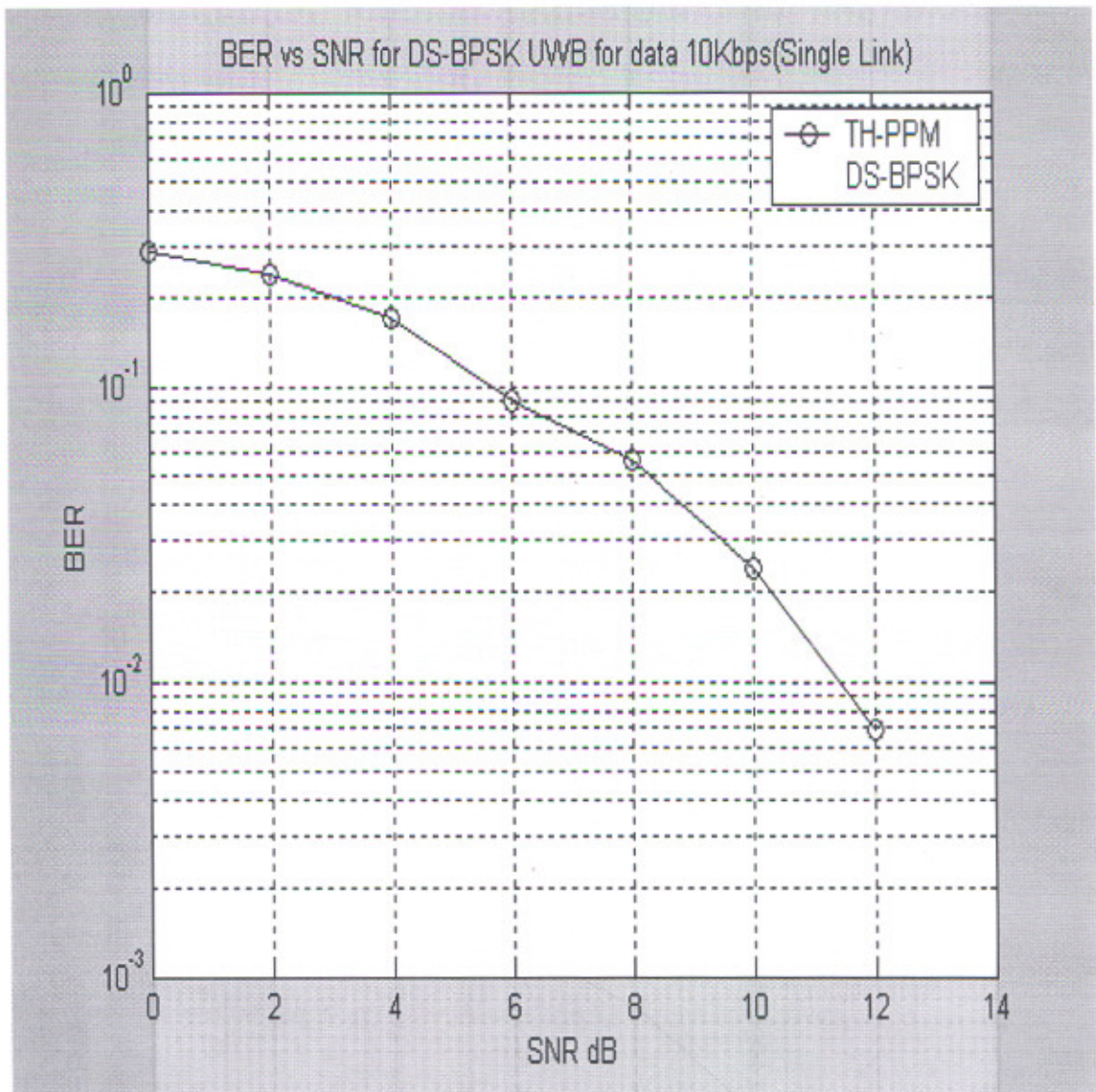


Figure 5.3(c) Performance of DS-BPSK for data rate 10 Kbps

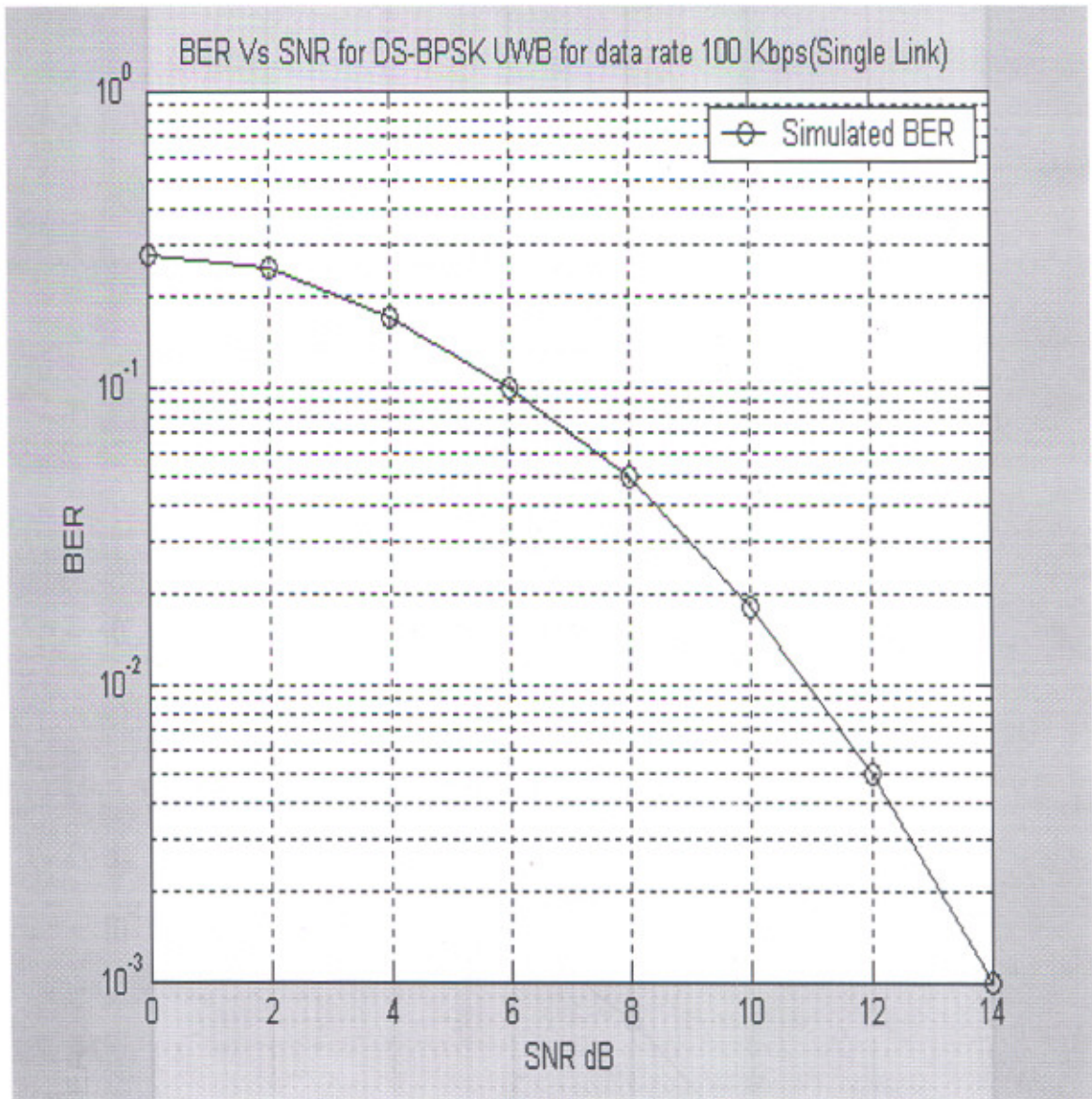


Figure 5.3(d) Performance of for DS-BPSK for data rate 100 Kbps

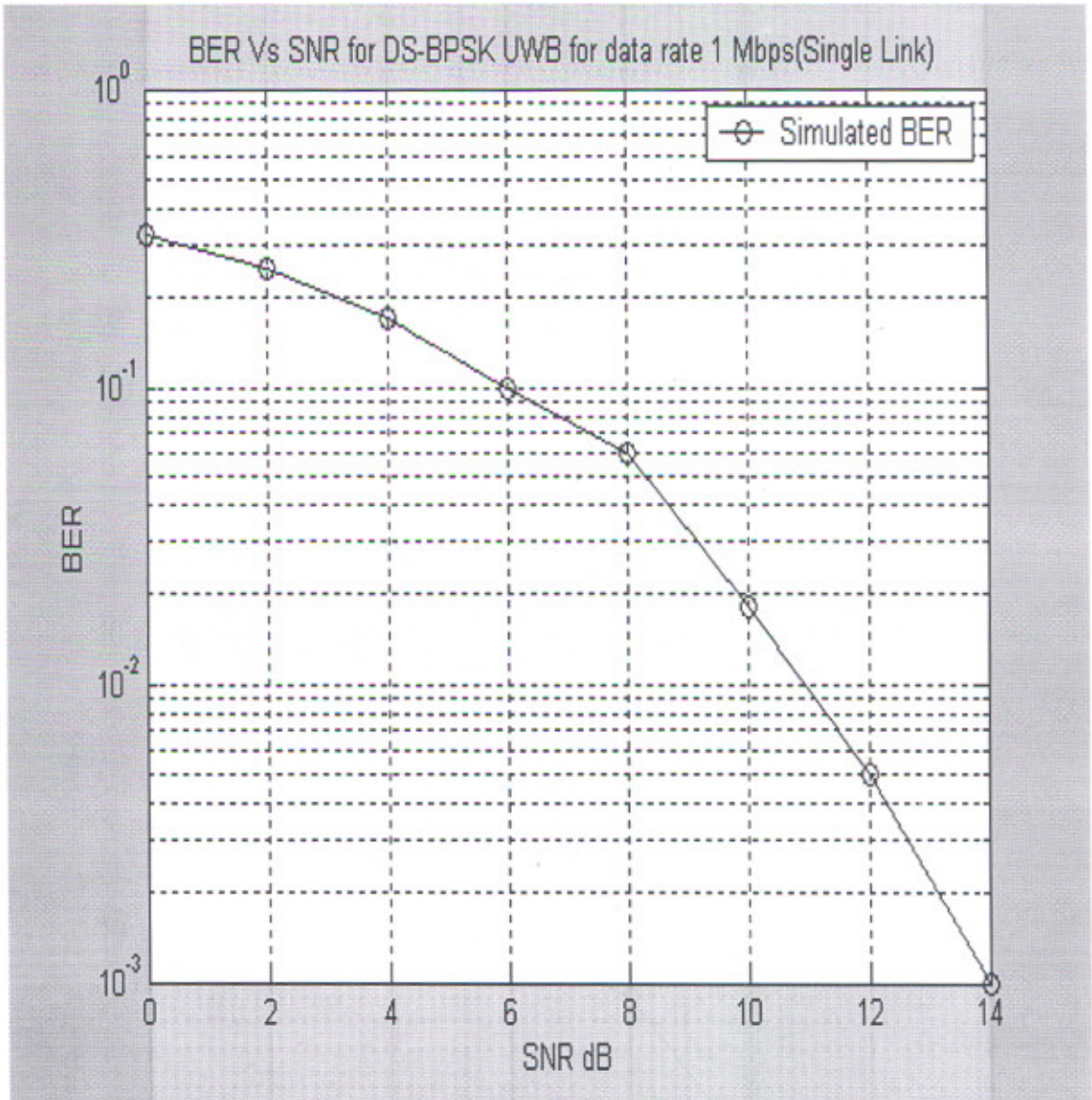


Figure 5.3(e) Performance of DS-BPSK for data rate 1 Mbps

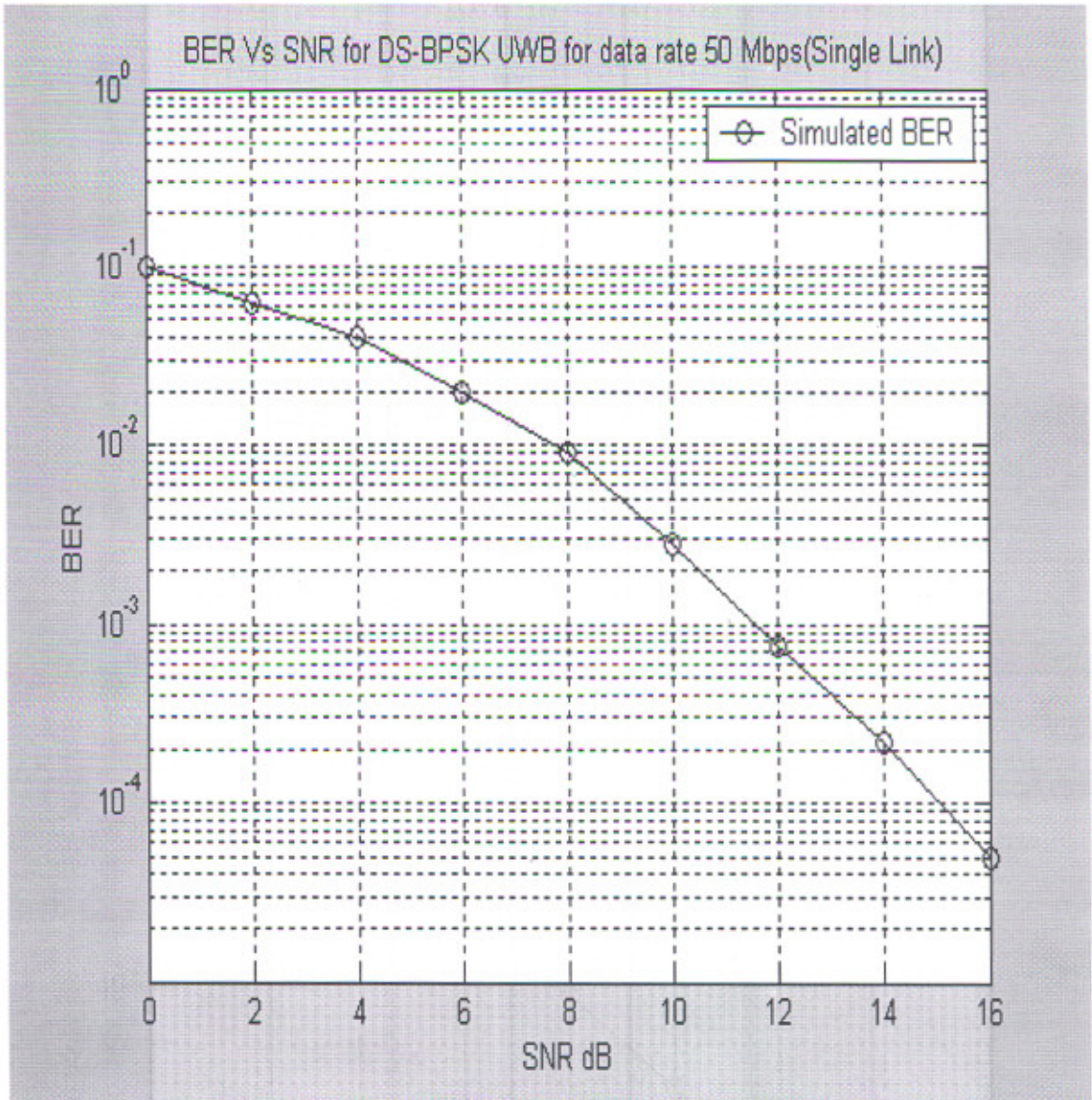


Figure 5.3(f) Performance of DS-BPSK for data rate 50 Mbps

5.2.3 Performance of TH-PPM & DS-BPSK in AWGN channel

Combine simulation of these modulation schemes have been performed as shown in Figures 5.4(a-f). For a single user, single path case, the performance of TH-PPM when compared with DS-BPSK, it is found that the performance of DS-BPSK is better than TH-PPM irrespective of data rate. For a BER= 10^{-4} DS-BPSK gives a 1.8dB performance improvement over THPPM at 50Mbps data rate.

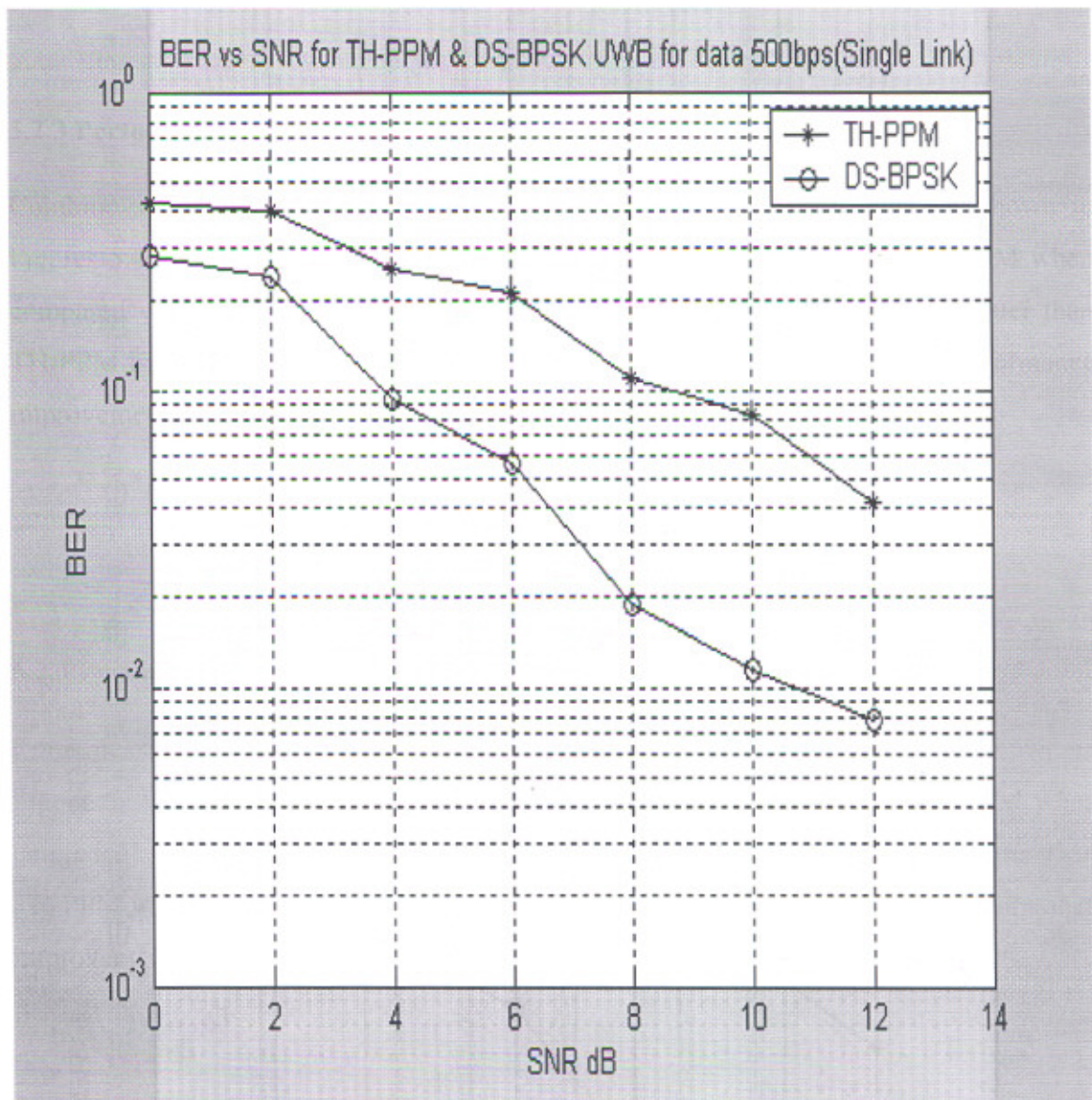


Figure 5.4(a) Performance of TH-PPM & DS-BPSK for data rate 500 bps

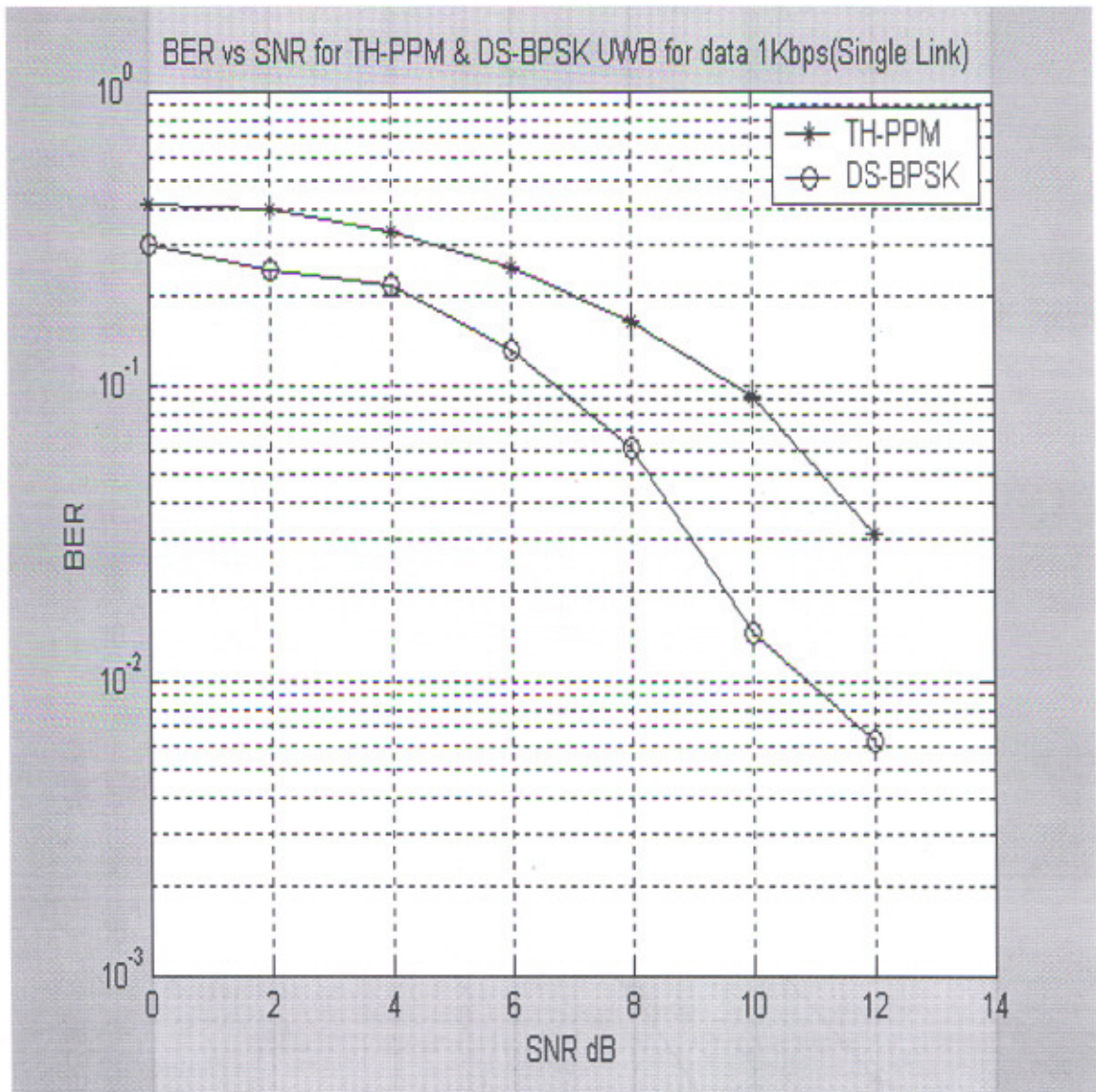


Figure 5.4(b) Performance of TH-PPM & DS-BPSK for data rate 1 Kbps

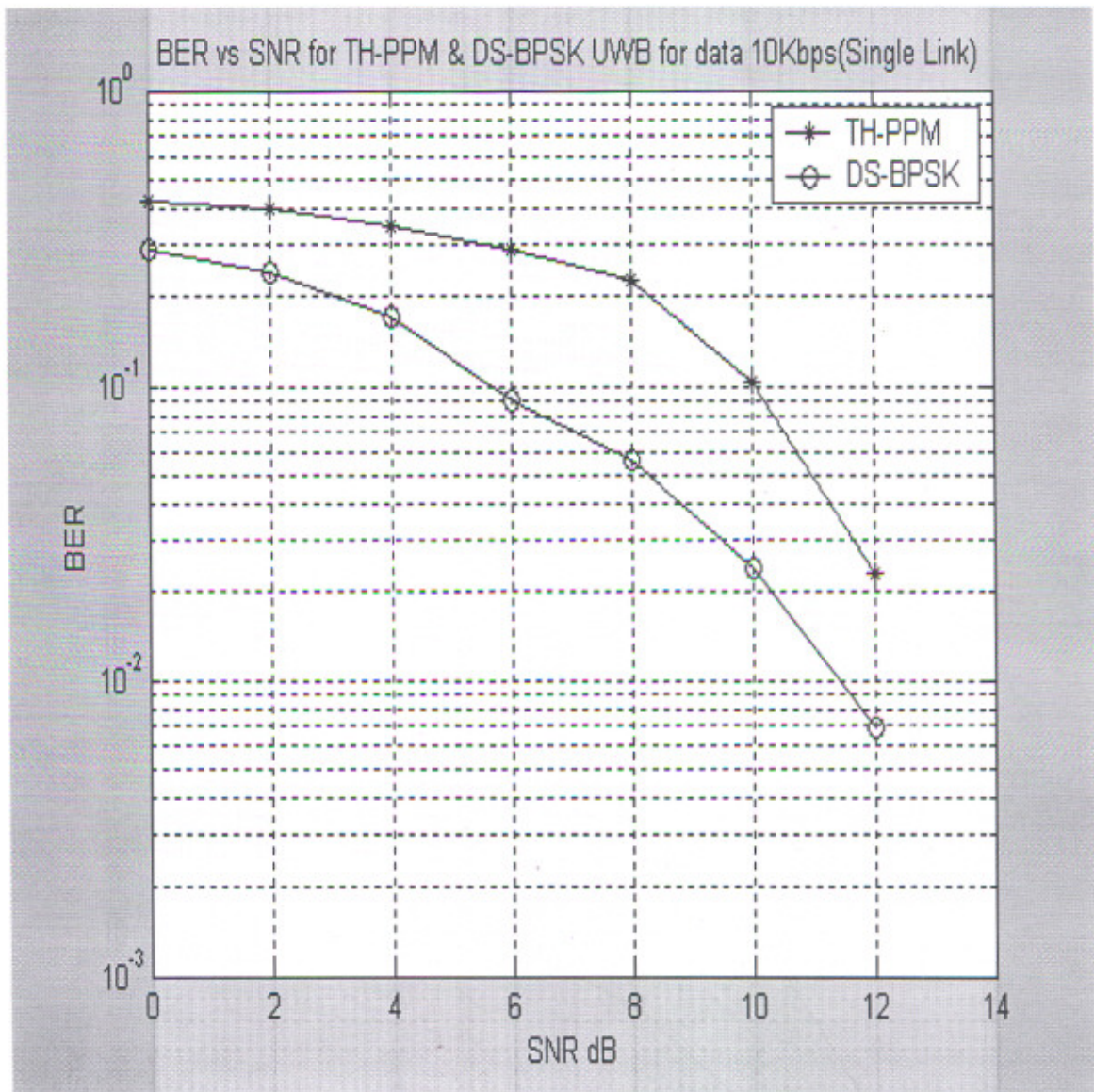


Figure 5.4(c) Performance of TH-PPM & DS-BPSK for data rate 10 Kbps

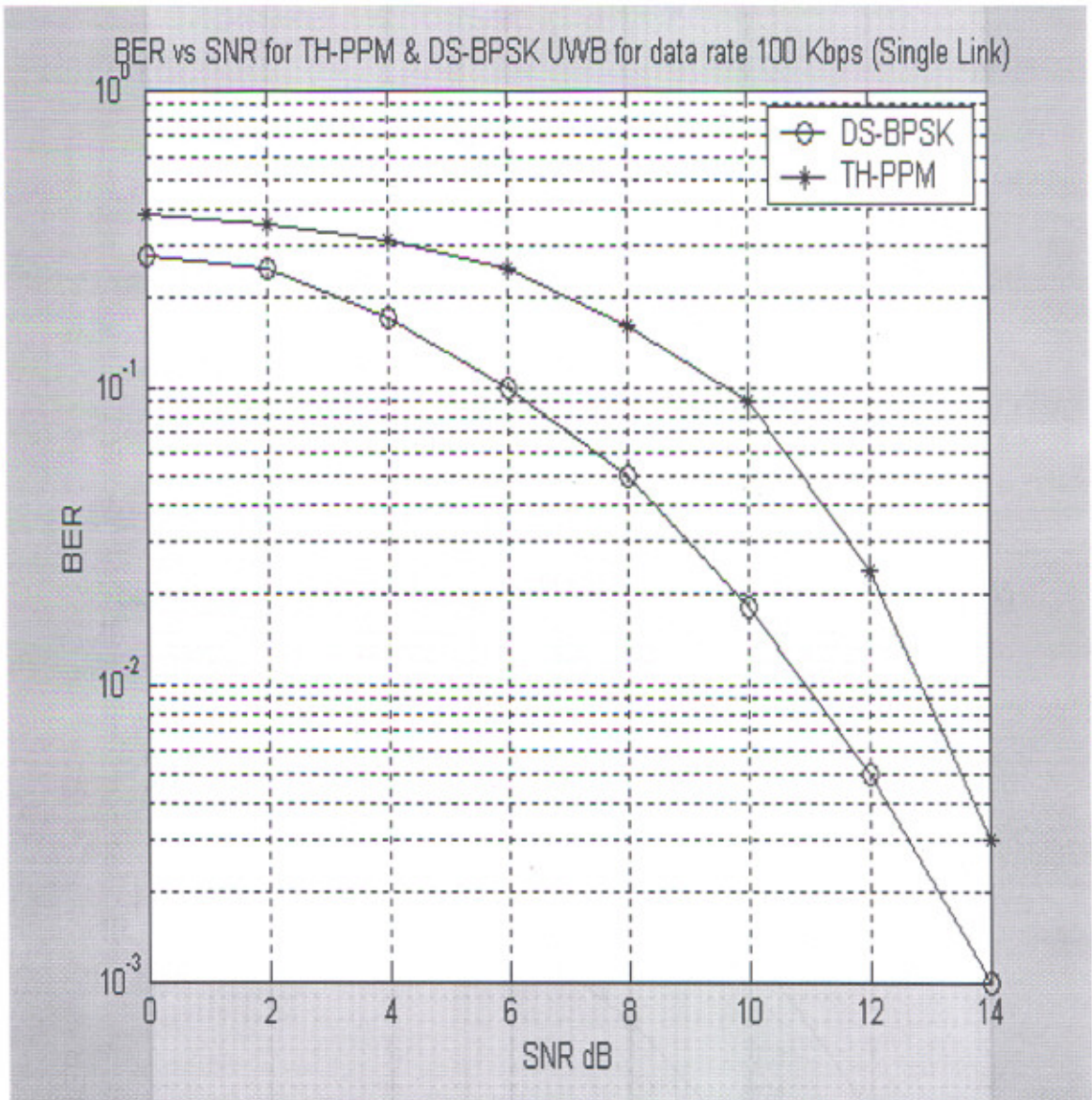


Figure 5.4(d) Performance of TH-PPM & DS-BPSK for data rate 100 Kbps

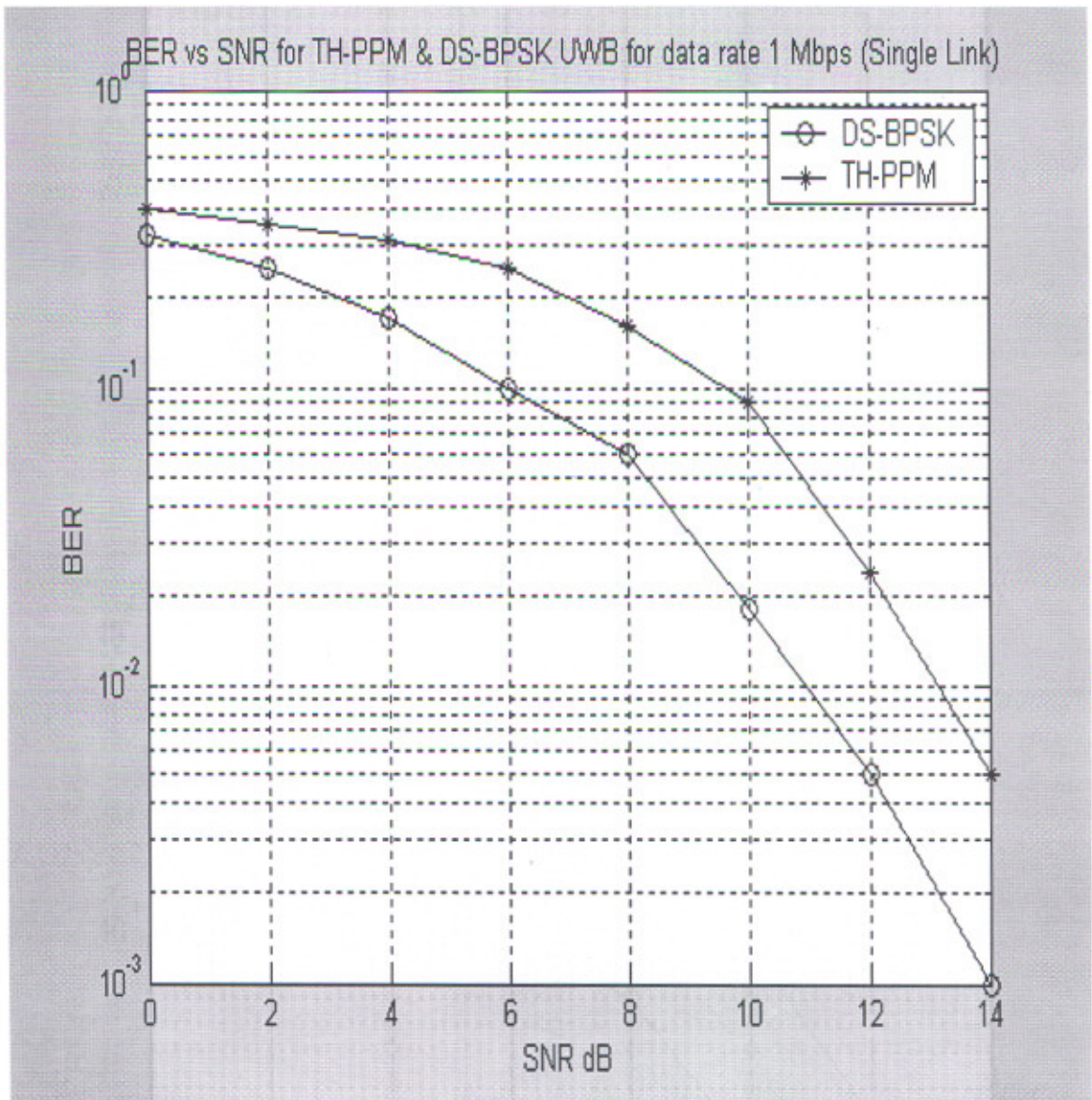


Figure 5.4(e) Performance of TH-PPM & DS-BPSK for data rate 1 Mbps

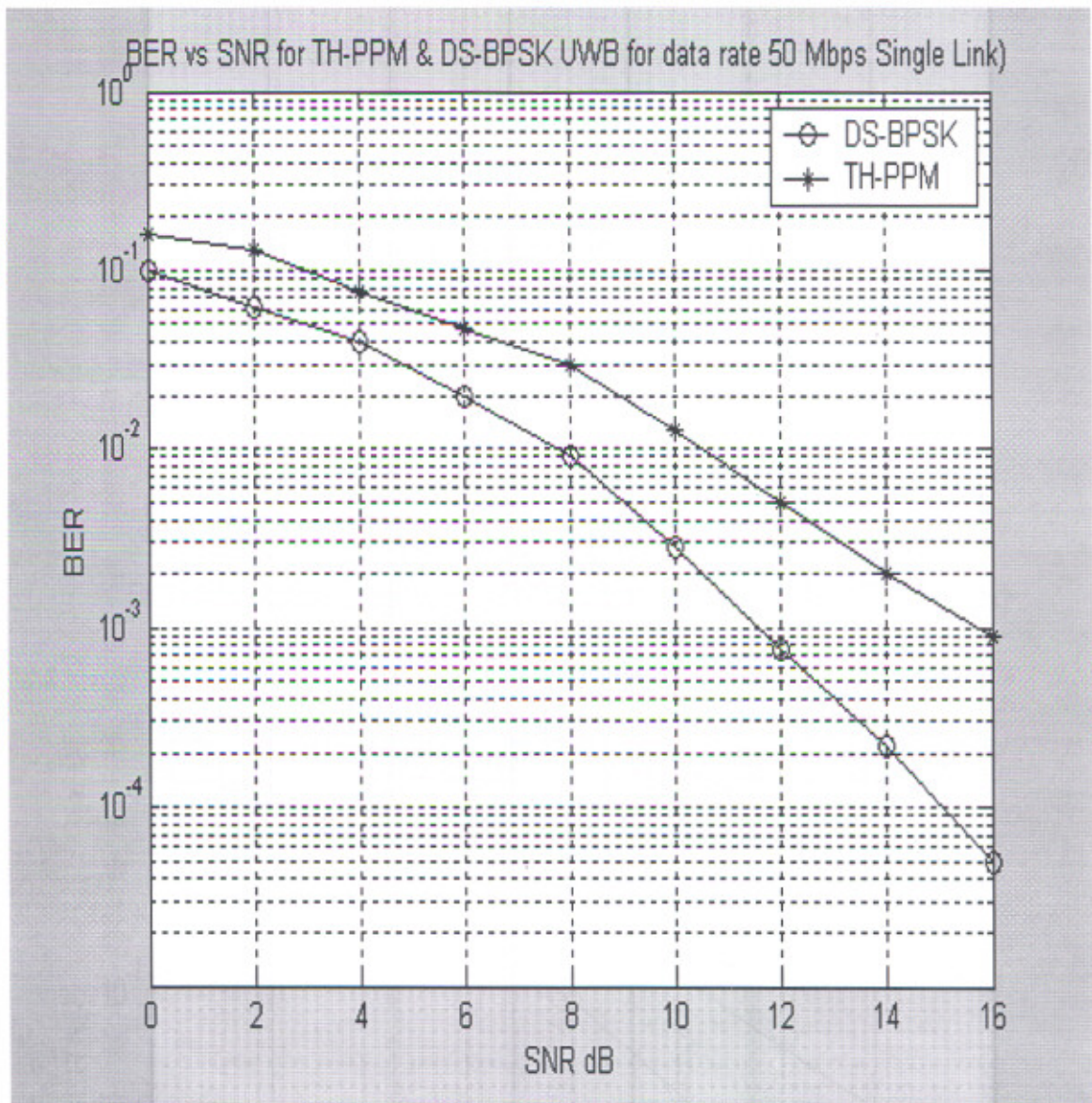


Figure 5.4(f) Performance of TH-PPM & DS-BPSK for data rate 50 Mbps

5.3 Performance comparison of TH-PPM & DS-BPSK in AWGN & multipath channel

Simulation results of single-user UWB system employing PPM and BPSK in multipath environment have been shown in figures 5.5(a-c). From the simulated results it is observed the performance of both PPM and BPSK degrades in multipath environment. But when performance of PPM is compared with BPSK, it is observed performance of BPSK degrades more than PPM. The multipath channel is modeled by exponential inter-arrival times and the path gains of each path are modeled as Rayleigh distributed. This shows TH-PPM is better than DS-BPSK in multipath. This is due to the inter-chip interference caused by the multipath in case of DS system

To show inter-chip interference in DS system .DS system with different number of chips per data bit (N_c) is simulated and have been show in figures 5.5 (d-g). Simulation result shows as the number of chips per data bit N_c increases the performance DS degrades in multipath as well in AGWN.

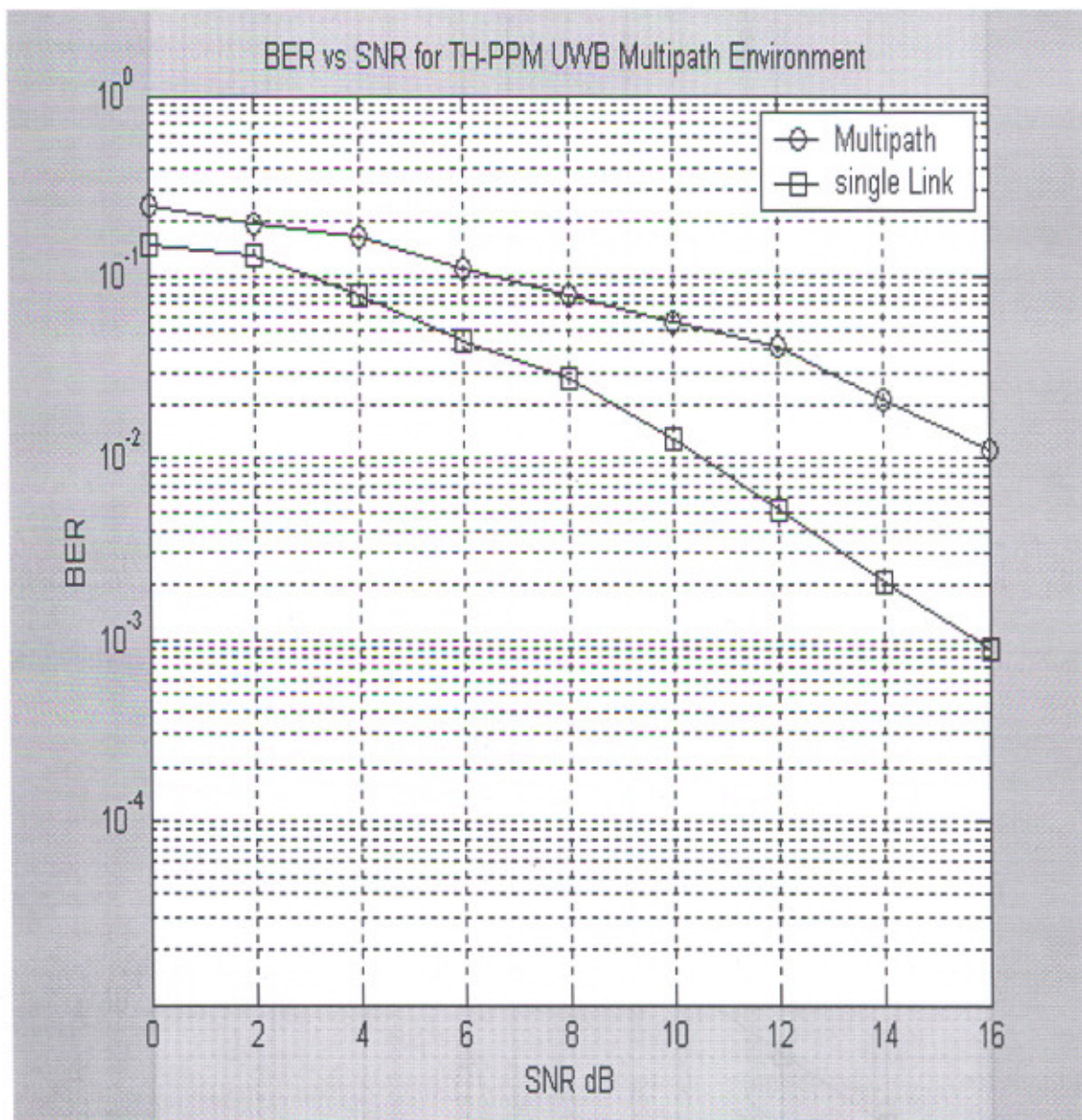


Figure 5.5(a) Performance of TH-PPM in multipath and AGWN

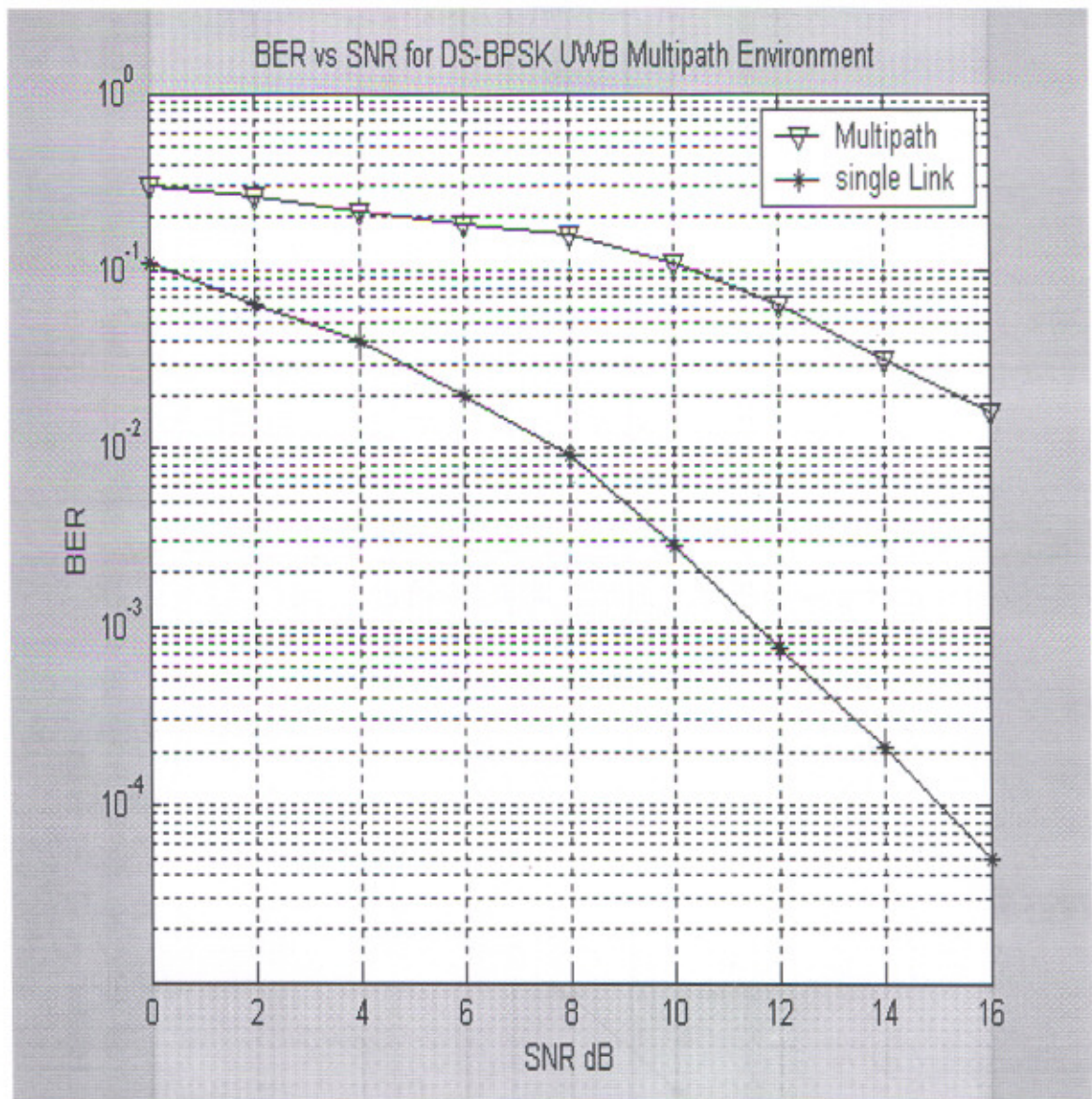


Figure 5.5(b) Performance of DS-BPSK in multipath and AGWN

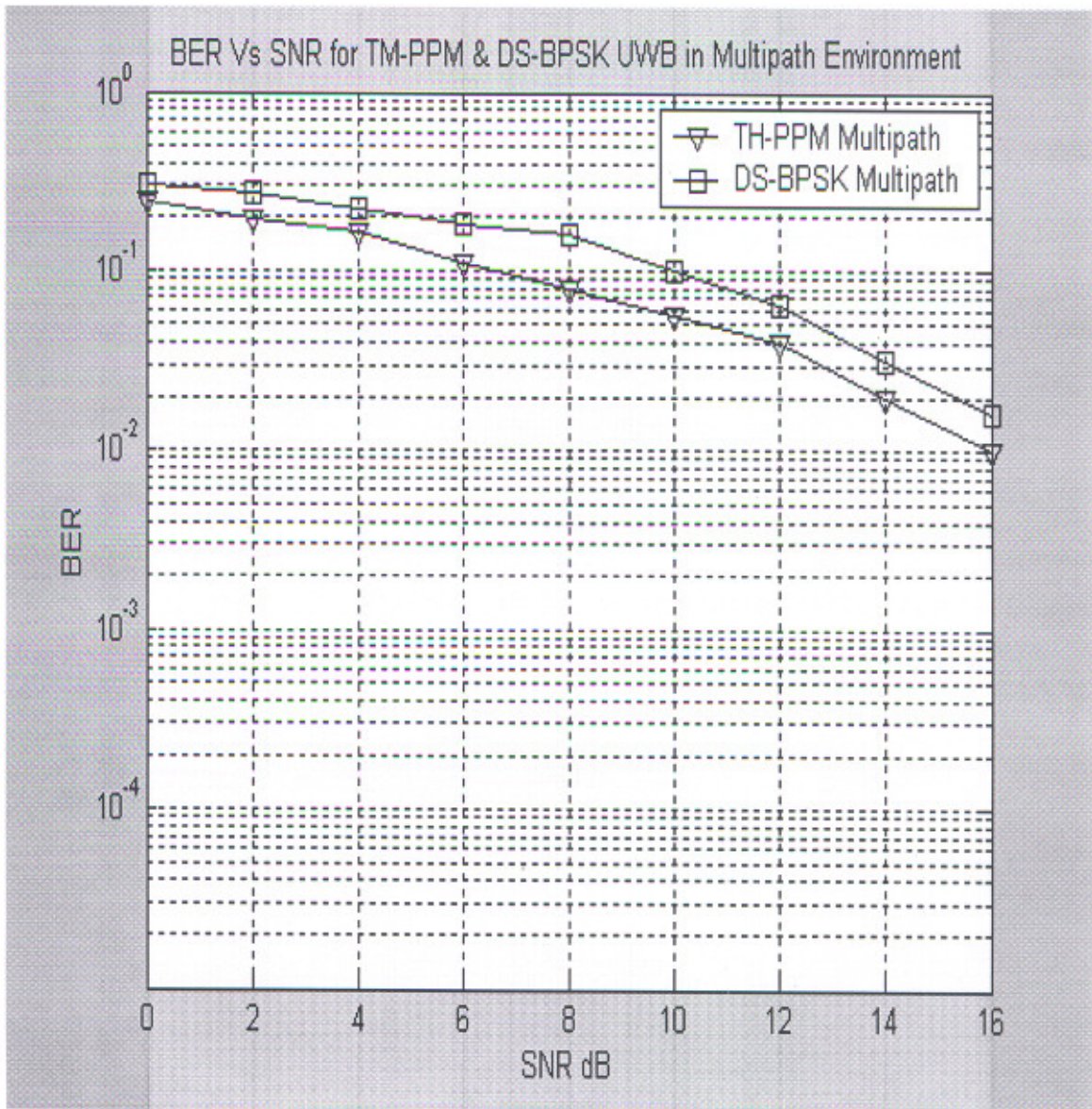


Figure 5.5(c) Performance of TH-PPM and DS-BPSK in multipath.

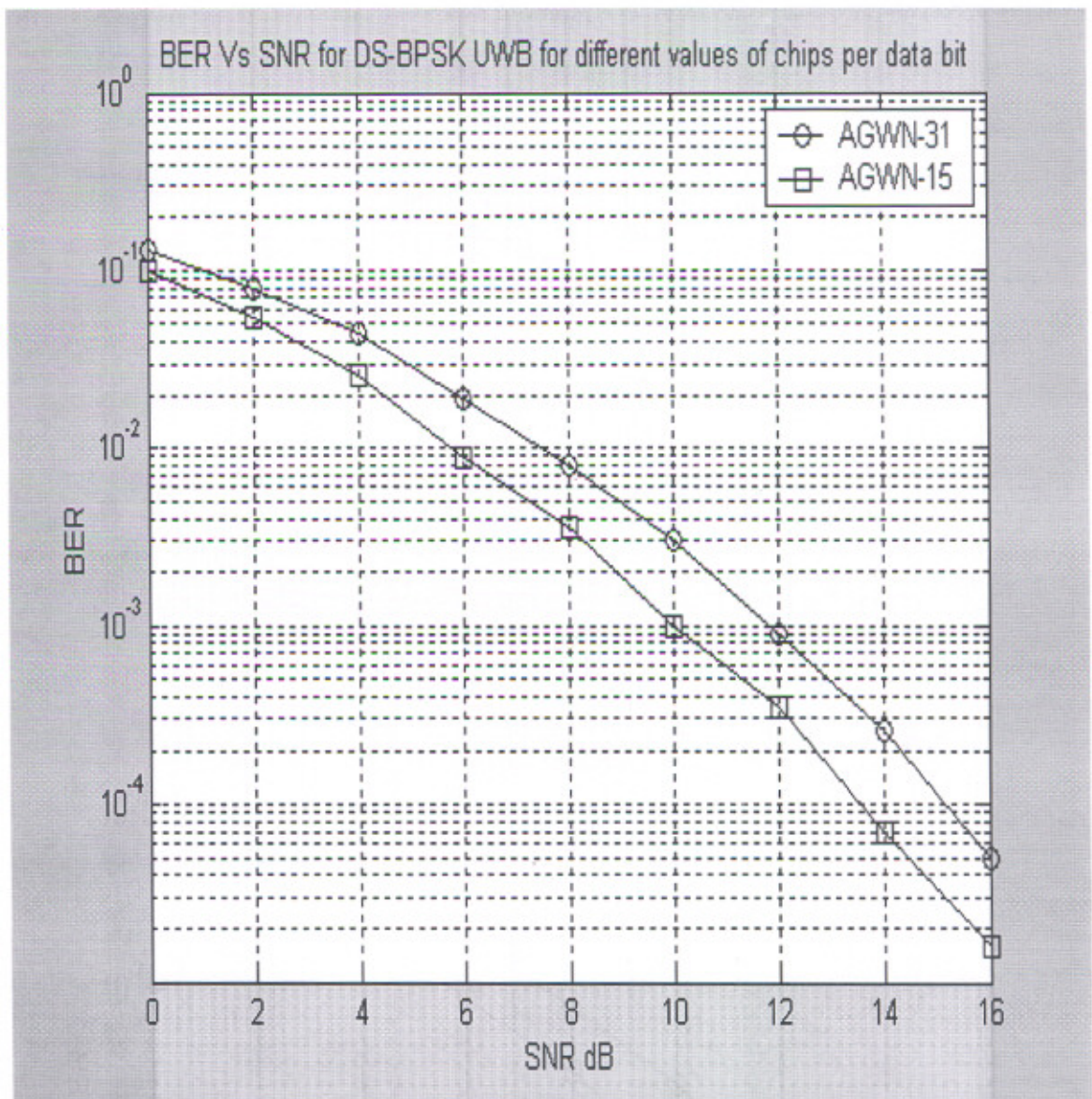


Figure 5.5(d) Performance of DS-BPSK different no. of chips per data bit in AGWN

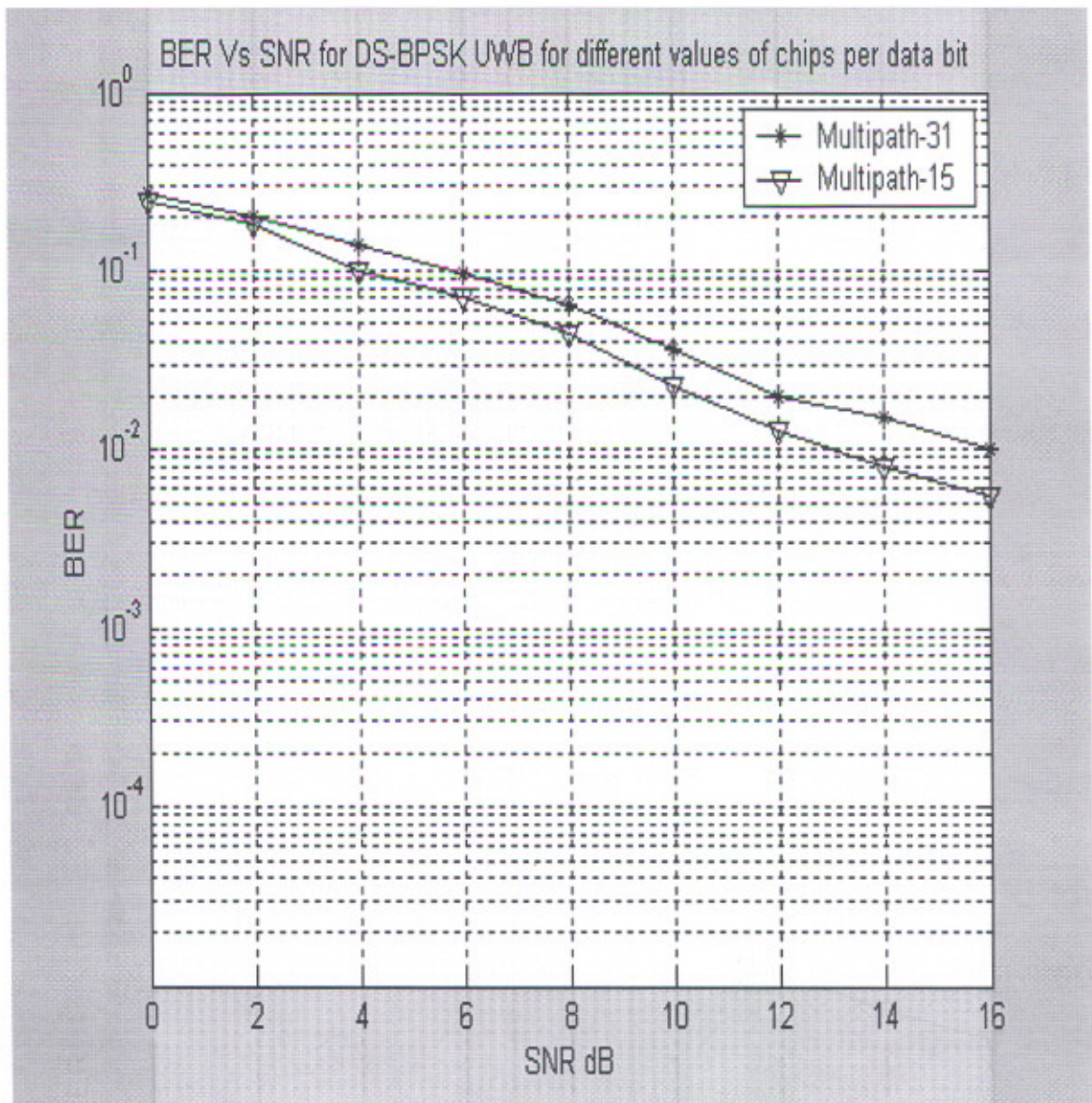


Figure 5.5(d) Performance of DS-BPSK at different no. of chips per data bit in multipath environment

5.4 Performance of Rake Receivers

A number of simulations have been performed to observe the performance of Rake receivers in a UWB multipath channel. The results are shown in figure 5.6(a,b). The Rake performs EC combining with the channel coefficients. Here the Rake is having perfect knowledge of the channel. The performance of Rake is compared with different fingers. Here we use partial Rake (PRake) receiver that combines the first L_r paths out of the L_r available resolved multipath components. This makes the Rake design simpler. Simulation results show the performance of Rake receiver improves as the number of fingers is increased.

However for DS-BPSK there is a significant performance improvement by using Rake receivers

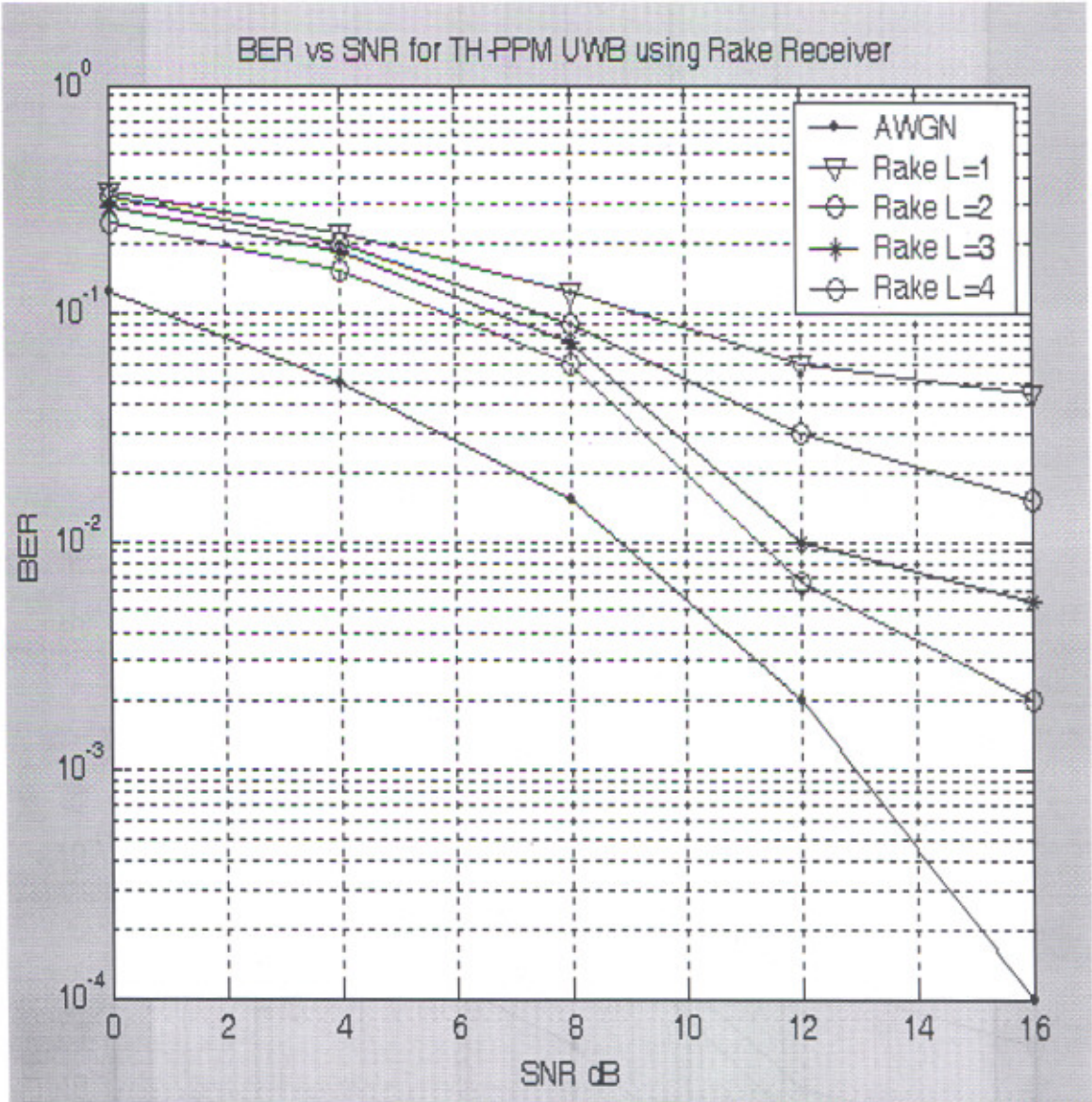


Figure 5.6 (a) Performance comparison of Rake Receivers for TH-PPM.

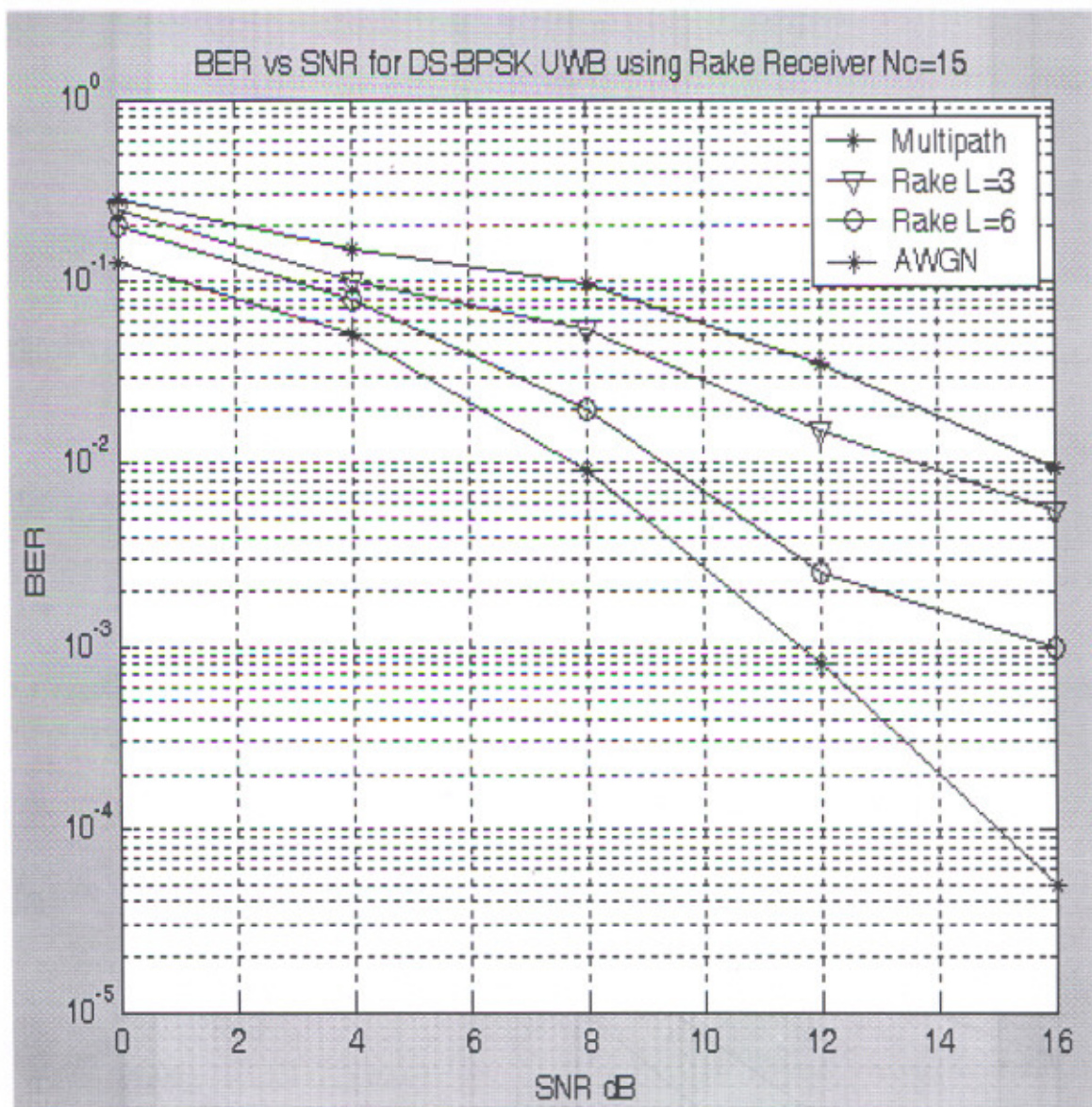


Figure 5.6 (b) Performance comparison of Rake Receivers for TH-PPM

5.5 Performance comparison of TH-PPM & DS-BPSK in case of Multi-user

A number of simulations have been performed to observe the performance of TH-PPM and DS-BPSK in case of multi-user conditions. The results are shown in figure 5.7(a-c). From simulated results it is observed that as the number of users increases the performance of ultra wideband communication systems decreases with both the modulation schemes, but when these techniques are compared with each other TH-PPM perform better then DS-BPSK in case of multi user conditions

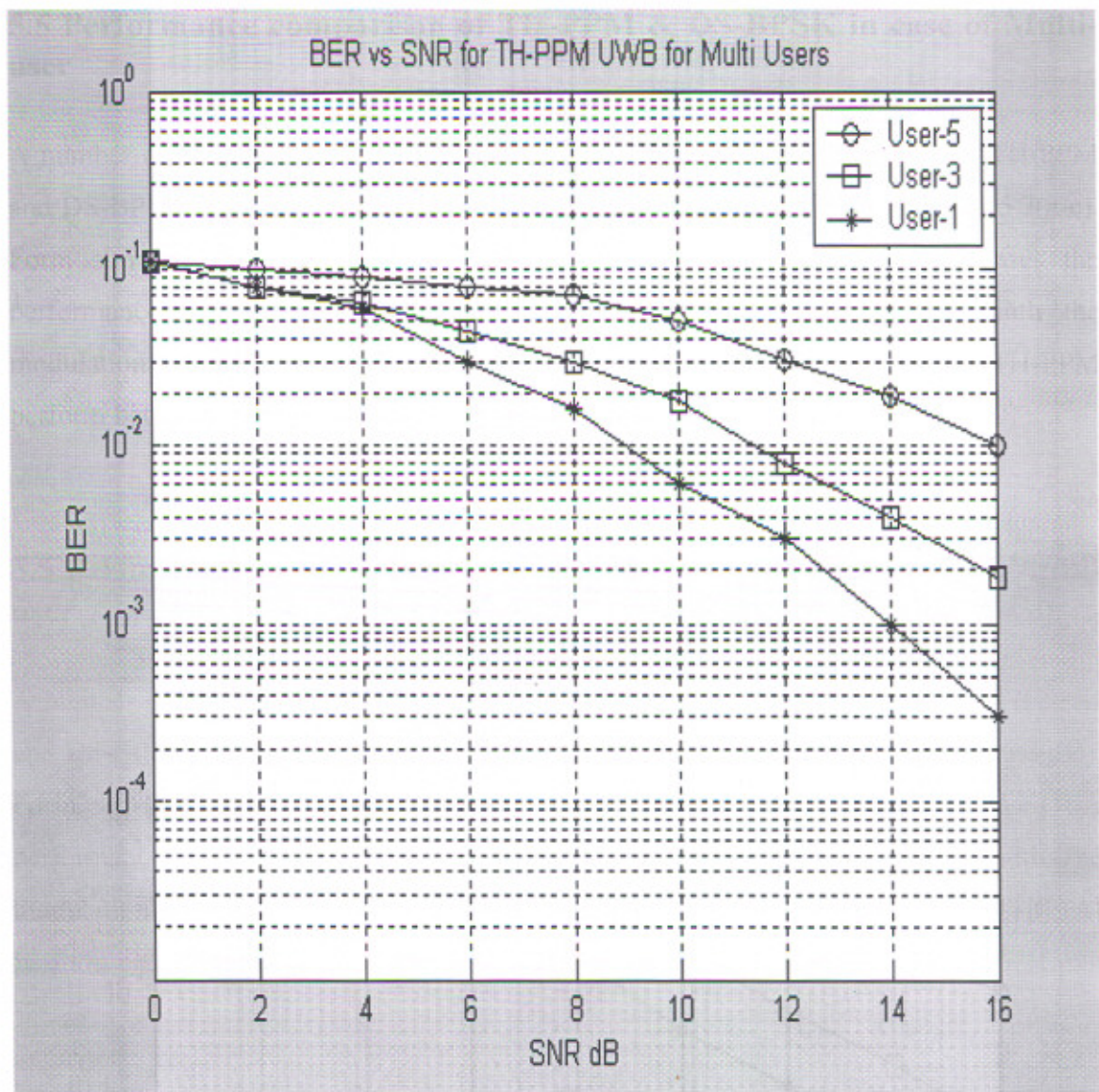


Figure 5.7 (a) Performance of TH-PPM in case of multiuser

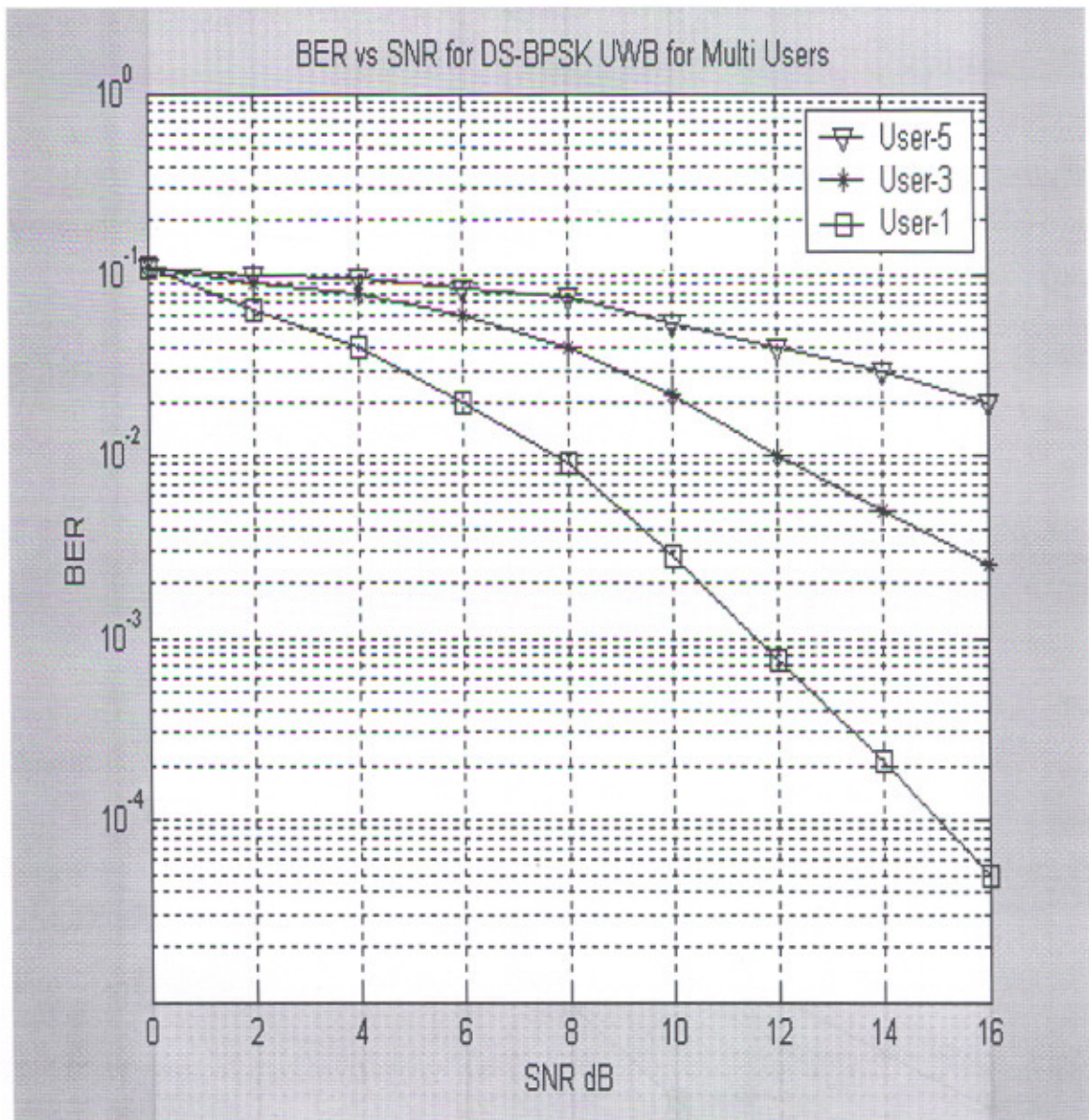


Figure 5.7 (b) Performance of DS-BPSK in case of multiuser

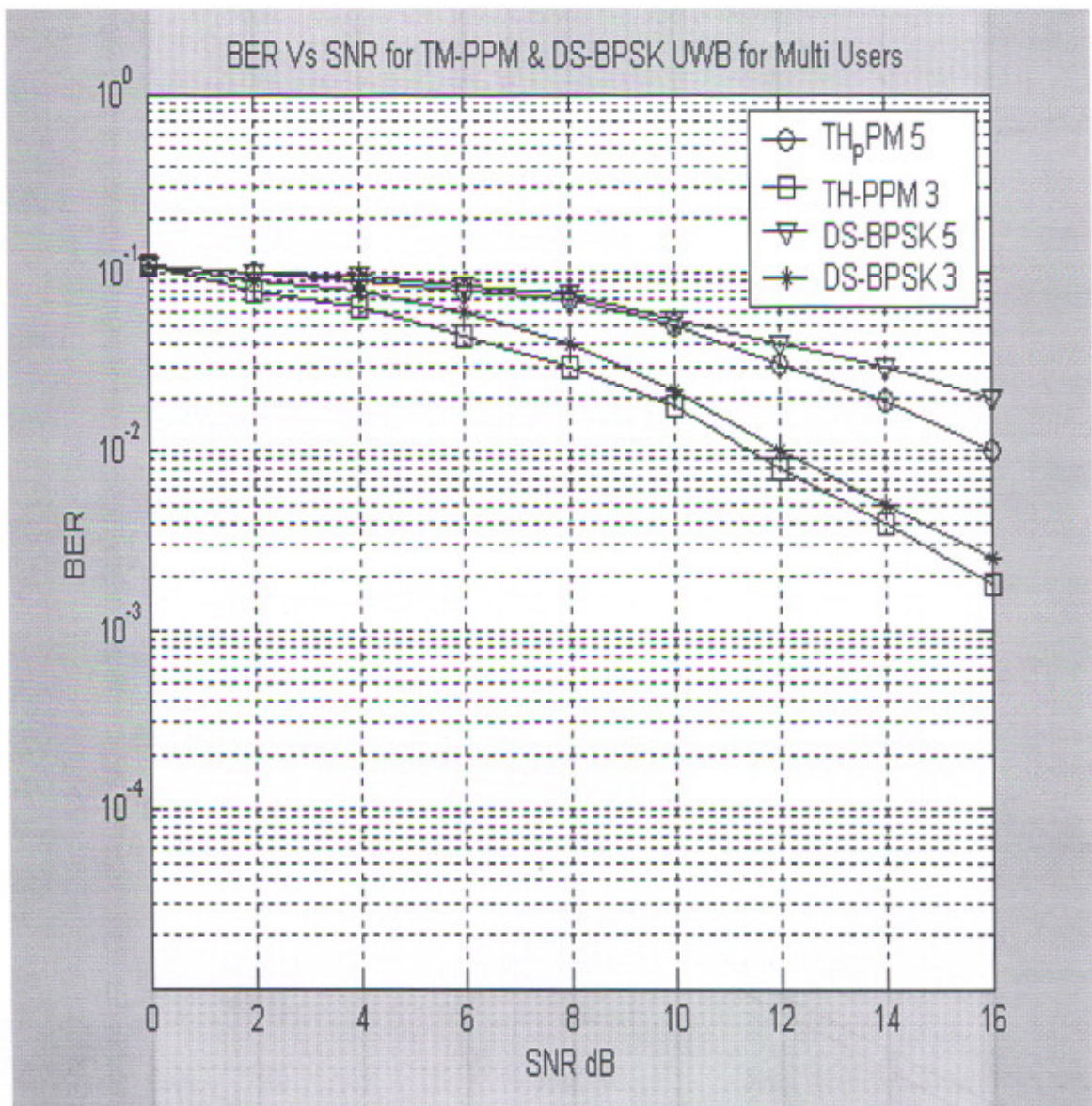


Figure 5.7 (c) Performance comparison of TH-PPM and DS-BPSK in case of multi-user

Chapter 6

CONCLUSION

**Performance Analysis of TH-PPM and DS-BPSK
in AGWN Channels for UWB Communication**

Conclusions

This thesis has identified several features of ultra wideband systems that show the promise of UWB for use short- to medium-range communications. These include very high data rate, potential low power consumption due to limits on transmit power spectral density, and favorable multi-path fading robustness due to the nature of the short impulse. The results show that the Ultra wideband communications systems operates at very high data rate using very short Gaussian pulse and very wide frequency spectrum.

Analysis of time hopping pulse position and direct sequence bi-phase shift keying shows that TH-PPM is more suitable than DS-BPSK for UWB under multipath and multi-user conditions. It can be concluded that UWB system can operate perfectly in a low SNR environment due to the properties of UWB signal and matched filter reception combined with Rake structure. Rake receiver is more suitable for DS-BPSK as BER Vs SNR curves are similar for same number of fingers.

To fully exploit the benefits of UWB systems, enhanced interdisciplinary links need to be established across the signal processing, communications, and networking communities. Today, research in signal processing for UWB is still at its infancy, offering limited resources in handling the challenges facing UWB communications. Understanding the unique properties and challenges of UWB communications, and applying competent signal processing techniques are vital to conquering the obstacles towards developing exciting UWB applications. It is clear that innovative research in this area is required in meeting the future challenges and demands of the dynamic communications industry.

References

- [1] Taylor, J. D., Introduction to Ultra-wideband Radar Systems, CRC Press, Boca Raton, Florida, 1995.
- [2] Foerster, J. R., "Ultra-Wideband Technology for Short-Range, Medium-Range Wireless Communications", Intel Technology Journal, Q2, 2001.
- [3] FCC Notice of Proposed Rule Making, "Revision of Part 15 of the Commission's Rules Regarding Ultra-wideband Transmission Systems", pp. 98-153, 2002.
- [4] Cover, T. Thomas, M. J. A., Elements of Information Theory, John Wiley & Sons, Inc., New York, 1991.
- [5] Harmuth, H.F., "A Generalized Concept of Frequency and Some Applications," IEEE Transactions on Information Theory, Vol.14, pp. 375-382, May 1968.
- [6] Durisi, G. Benedetto, S., "Performance Evaluation and Comparison of Different Modulation Schemes for UWB Multiaccess Systems", IEEE International Conference on Communications, Vol. 3, pp. 2187 – 2191, 2003.
- [7] Multispectral Solutions Inc., "A Brief History of Ultra Wideband." <http://www.multispectral.com/history.html>. 10 June 2001.
- [8] Hussain, Malek, "An Overview of the Principles of Ultra-wideband impulse Radar," CIE International Conference of Radar, pp. 24-28, 1996.
- [9] Bennett, C. Leonard, Ross, Gerald, F., "Time-Domain electromagnetics and Its Applications," Proceedings of the IEEE, Vol. 66, pp. 299-318, Mar. 1978.
- [10] Cramer, J. R. Win, M. Z. Scholtz, R. A., "Evaluation of the Multipath Characteristics of the Impulse Radio Channel, Personal, Indoor and Mobile radio Communications", PIMRC, vol. 2, pp. 864-868, 1998.
- [11] Young, J., "VHF/UHF Ultra-Wideband Measurements of Scattering Targets in Foliage", IEEE Antennas and Propagation Society International Symposium, Vol. 1, pp. 586, 1992.
- [12] Time Domain C., "UWB Technology." Article. <http://www.timedomain.com>. August 2001.
- [13] UWBWG Ultra Wide-Band Working Group "Comments on the FCC Part 15 Notice of Inquiry." <http://www.uwb.org/standards.htm>. June 2001.
- [14] FCC, "Federal Communications Commission" <http://www.fcc.gov>. 04 Sep 2001.

- [15] NTIA "National Telecommunications and Information Administration."
<http://www.ntia.doc.gov>. 15 July 2001
- [16] FCC Notice of inquiry, NOI, ([http://www.fcc.gov/Bureaus/Engineering Technology /Documents/fedreg/63/5018 4.pdf](http://www.fcc.gov/Bureaus/Engineering%20Technology/Documents/fedreg/63/50184.pdf)), 01 June 2001.
- [17] Win, M. Z. Scholtz, R. A., "Impulse radio: How it works," *IEEE Communication Letter*, vol. 2, pp. 36–38, February 1998.
- [18] Win, M. Z. Scholtz, R. A. "Ultra-wide bandwidth time-hopping spread-spectrum impulse radio for wireless multiple-access communications", *IEEE Trans. Communication*, vol. 48, pp. 679–691, 2000.
- [19] Proakis, J. G., *Digital Communications*. New York: McGraw-Hill, 3rd ed., 1995
- [20] Welborn, M. McCorkle, J., "The importance of fractional bandwidth in ultra wideband pulse design," *Proc. IEEE Int. Conf. Communications*, vol. 2, pp. 753–757, 2002.
- [21] Orlik, P. Haimovich, A. M. Cimini, L. J. Jinyun Zhang, "On the Spectral and Power Requirements for Ultra-Wideband Transmission Communications", *ICC '03. IEEE International Conference on communication*, vol. 1, pp. 738 – 742, 2003.
- [22] Lottici, V, Andrea, A. D. Mengali, U., "Channel estimation for ultra wideband communications", *IEEE J. Select. Areas Communication*, vol. 20, no. 9, pp. 1638–1645, 2002
- [23] Hamalainen, M. Hovinen, Tesi, V. R., M. "On the UWB System Coexistence with GSM900, UMTS/WCDMA, and GPS," *IEEE Journal on Selected Areas of Communications*, vol. 20, no. 9, pp. 1712–1721, 2002.
- [24] Xtremespectrum White Paper, "Ultra-Wideband: Wireless Without Compromise, A Renaissance in the Making"; 5 May 2003 <http://www.xtremespectrum.inc>. 2002
- [25] Salehi, J. A., "Code division Multiple-Access Techniques in Optical Fiber Networks- Part I: Fundamental Principles", *IEEE Trans. Commun.*, vol. 37, no. 8, 1989.
- [26] Scheers, B. Acheroy, M. Vander Vorst, A., "Time-domain simulation and characterization of TEM horns using a normalized impulse response", *IEE Proc. Microwaves, Antennas and Propagation*, vol. 147, no. 6, pp. 463-468, Dec. 2000.
- [27] Liu, H., "Error Performance of a Pulse Amplitude and Position Modulated Ultra-wideband System over Lognormal Fading Channels", *IEEE transactions on communications*, vol. 7, No. 11, November 2003
- [28] Forouzan, A. R. Nasiri-Kenari, M. Salehi, J. A., "Performance analysis of ultra wideband time-hopping code division multiple access systems: uncoded and coded schemes", in *Proc. IEEE ICC 2001*, vol. 10, pp. 3017-3021, 2001.

- [29] Matthu, L. Welbom, "System consideration of Ultra Wideband wireless Networks"
XtremeSpectrum, Inc.
- [30]. Kim K. J., "Effect of Tap Spacing on the Performance of Direct-Sequence Spread Spectrum RAKE Receiver", IEEE transactions on communications, vol. 48, No. 6, 2000
- [31] Foerster, J. R., "Performance Comparisons between a RAKE Receiver and a differential detector for Ultra-Wideband Communications System", IEEE Journal on Selected Areas in Communication, 2002.
- [32] Klein, A. G., "Rake Reception for UWB Communication Systems with Intersymbol Interference", SPAWC Conference 2003.
- [33] Molisch, A. F., "Mitsubishi Electric's Time-Hopping Impulse Radio standards proposal", IEEE 802.15 Working Group for Wireless Personal Area Network (WPANs), IEEE P802.15-03112, May 2003
- [34] Pickholtz R. L., "Theory of Spread-Spectrum Communications-A Tutorial", IEEE transactions on communications, vol. Com-30, No. 5, May 1982
- [35]. Kim K. J., "Effect of Tap Spacing on the Performance of Direct-Sequence Spread Spectrum RAKE Receiver", IEEE transactions on communications, vol. 48, No. 6, 2000
- [36] Fishler, E. Poor, H. V., "On the tradeoff between two types of processing gain", proceedings of the 40th Annual Allerton Conference on Communication, Control, and Computing, Monticello, 2002.
- [37] Zang, G. Ling, C., "Performance evaluation for band-limited DS-CDMA systems based on simplified improved Gaussian approximation," IEEE Transactions on Communications, vol. 51, issue 7, pp. 1204-1213, 2003.